Report No. K-TRAN: KSU-96-8
Final Report

Development of a Low-Cost Crash Cushion Using Recycled Automobile Tires

Daniel T. Nabors
Mustaque Hossain
Kansas State University
Manhattan, Kansas

September 1998

K-TRAN

A COOPERATIVE TRANSPORTATION RESEARCH PROGRAM BETWEEN:
THE KANSAS DEPARTMENT OF TRANSPORTATION
KANSAS STATE UNIVERSITY
THE UNIVERSITY OF KANSAS

1. Report No. K-TRAN: KSU-96-8	**2. Government Accession No.**	**3. Recipient Catalog No.**
4 Title and Subtitle Development of a Low-Cost Crash Cushion Using Recycled Automobile Tires		**5 Report Date** September 1998
		6 Performing Organization Code
7. Author(s) Daniel T. Nabors and Mustaque Hossain		**8 Performing Organization Report No.**
9 Performing Organization Name and Address Kansas State University Department of Civil Engineering Manhattan, Kansas 66506		**10 Work Unit No. (TRAIS)**
		11 Contract or Grant No. C-991
12 Sponsoring Agency Name and Address Kansas Department of Transportation Docking State Office Bldg. Topeka, Kansas 66612		**13 Type of Report and Period Covered** Final Report September 1996 to September 1998
		14 Sponsoring Agency Code 106-RE-0081-01

15 Supplementary Notes

Additional funding was provided by the Mid America Transportation Center

16 Abstract

Approximately 30 percent of all vehicle related fatalities that occur each year are caused by a single vehicle leaving the road and striking a fixed object; the most common objects struck being trees, guardrails, and utility poles. In many cases current crash cushion systems are not cost effective to be installed on such obstacles. In addition to high initial costs many crash cushions require extensive maintenance or require expensive replacement parts driving costs up even more. This makes the development of a more cost-effective crash cushion a necessity.

The objective of this study was to propose *an initial design* for a low-cost, reusable crash cushion using recycled materials. Used tires and tire-derived materials were tested in both static and dynamic modes to evaluate their application in a crash cushion. Both the tires and the tire-derived materials proved to be able to sustain high loads and proved to be durable, making them good candidates for use in a crash cushion. However, the tire-derived pads had excessively high loads per unit deflection, which would prohibit their use in a crash cushion. This problem could be eliminated if voids were added to allow material to deflect more under loading. The whole used tires could be used effectively as energy absorbing elements in crash cushions or truck mounted attenuators (TMA's) if compressed horizontally or vertically.

17 Key Words Crash Cushion, Fatality, Recycle, Tires, Truck Mounted Attenuators (TMA).		**18 Distribution Statement** No restrictions. This document is available to the public through the National Technical Information Service Springfield, Virginia 22161	
19 Security Classification (of this report) Unclassified	**20 Security Classification (of this page)** Unclassified	**21 No. of pages** 94	**22 Price**

Form DOT F 1700.7 (8-72)

PREFACE

This research project was funded by the Kansas Department of Transportation K-TRAN research program and the Mid-America Transportation Center (MATC). The Kansas Transportation Research and New-Developments (K-TRAN) Research Program is an ongoing, cooperative and comprehensive research program addressing transportation needs of the State of Kansas utilizing academic and research resources from the Kansas Department of Transportation, Kansas State University and the University of Kansas. The projects included in the research program are jointly developed by transportation professionals in KDOT and the universities.

NOTICE

The authors and the State of Kansas do not endorse products or manufacturers. Trade and manufacturers names appear herein solely because they are considered essential to the object of this report.

This information is available in alternative accessible formats. To obtain an alternative format, contact the Kansas Department of Transportation, Office of Public Information, 7th Floor, Docking State Office Building, Topeka, Kansas, 66612-1568 or phone (785)296-3585 (Voice) (TDD).

DISCLAIMER

The contents of this report reflect the views of the authors who are responsible for the facts and accuracy of the data presented herein. The contents do not necessarily reflect the views or the policies of the State of Kansas. This report does not constitute a standard, specification or regulation.

ABSTRACT

Approximately 30 percent of all vehicle related fatalities that occur each year are caused by a single vehicle leaving the road and striking a fixed object; the most common objects struck being trees, guardrails, and utility poles. In many cases current crash cushion systems are not cost effective to be installed on such obstacles. In addition to high initial costs many crash cushions require extensive maintenance or require expensive replacement parts driving costs up even more. This makes the development of a more cost-effective crash cushion a necessity.

The objective of this study was to propose *an initial design* for a low-cost, reusable crash cushion using recycled materials. Used tires and tire-derived materials were tested in both static and dynamic modes to evaluate their application in a crash cushion. Both the tires and the tire-derived materials proved to be able to sustain high loads and proved to be durable, making them good candidates for use in a crash cushion. However, the tire-derived pads had excessively high loads per unit deflection which would prohibit their use in a crash cushion. This problem could be eliminated if voids were added to allow material to deflect more under loading. The whole used tires could be used effectively as energy absorbing elements in crash cushions or truck mounted attenuators (TMA's) if compressed horizontally or vertically.

TABLE CONTENTS

LIST OF TABLES

LIST OF FIGURES

ACKNOWLEDGMENTS

Funding for this study has been provided by the Mid-America Transportation Center (MATC) and the Kansas Department of Transportation (KDOT). The authors wish to acknowledge the invaluable guidance and insight provided by Dr. Dean Sicking of the University of Nebraska, Lincoln. The authors also thank John Steele and Larry Cheek of KDOT for their time and efforts in helping with the static tests and also Don Bruns of Kansas State University for helping with the dynamic tests. Finally, special thanks to John Aten of Dodge-Regupol, Inc. who provided the tire-derived samples for this experiment.

Chapter 1

INTRODUCTION

1.1 Problem Statement

The volume of solid waste in this country continues to grow at an astonishing rate of 4.6 billion tons (4.2×10^6 kg) every year. This problem is exacerbated by the increasing difficulty in finding areas to dispose of waste, leading to an increased interest in the manufacturing industry and in government to use recycled materials. This recent focus has been demonstrated by the Executive Order signed by President Bush in 1991, which required federal agencies to use recycled materials whenever possible. This trend is expected to continue with legislation requiring a certain percentage of roadside safety devices to be made from recycled materials (Bligh et al. 1995).

One of the most promising materials which can be recycled for use in roadside safety appurtenances are used tires. Each year approximately 242 million used tires are added to the already staggering stockpile of 2 to 3 billion used tires strewn throughout the United States (Epps 1994). This vast quantity of tires provides a nearly unlimited supply of material that can be used whole or used to produce recycled rubber which can then be used in crash cushions. Unfortunately, solid waste is not the only problem in this country. Over the past decade an average of more than 40,000 people were killed annually in automobile accidents. In 1996, 41,907 people died in motor vehicle accidents, 3,511,000 people were injured, and 4,548,000 crashes involved property damage only. In fact, the number of fatalities in traffic crashes has steadily increased each year since 1992, although the rate decreased due to higher

mileage being traveled. Not only do these statics relate the tremendous loss of life on our nation's roads, but they also represent economic costs exceeding $150 billion annually based on crashes in 1994 (NHTSA 1997). Approximately 30 percent of the fatalities that occur each year are the result of a single vehicle running off the road and striking a fixed object, thus making roadside safety an area where there is great potential to save lives and reduce economic losses (AASHTO 1996).

Roadsides are designed to provide a safe recoverable area (clear zone) for vehicles that depart from the traveled way. Clear zone widths are based upon traffic volume, road speeds, and roadside geometry. The ideal roadside design strategy would be to provide an adequate recovery area free from all obstacles and non-traversable features. This, however, is not always feasible. Costs associated with removal and relocation of obstacles may not be economically sound. In such cases crash cushions are a viable alternative to increasing the safety performance of the roadway. A crash cushion, also known as an impact attenuator, is defined as a device that prevents an errant vehicle from impacting fixed object hazards by gradually decelerating the vehicle to a safe stop or by redirecting the vehicle away from the hazard (AASHTO 1996). Crash cushions are most frequently used in gore areas on exit ramps, around bridge piers, and on the ends of roadside and median barriers. In these applications crash cushions have proven to be quite effective, reducing fatalities by an estimated 78 percent and reducing all injuries by an estimated 20 percent (Griffin 1984). Serious injuries were reduced by 67 percent, moderate by 8 percent, and minor injuries by 12 percent (Griffin 1984).

However, the high cost of current impact attenuation devices makes their installation in many locations prohibitive. Even sand barrels, the most widely used impact attenuator, can cost anywhere from $7,000 to $11,000 to emplace (AASHTO 1996). However, the costs of sand barrels in Kansas may vary anywhere from $3,000 to $4,500 depending upon the size of array (Seitz 1998). In addition to being expensive to install, the sand barrels are also difficult and expensive to maintain. The lids of the barrels may come off and barrels may "break open" exposing the sand to the weather and causing the sand to leach out, thus reducing the effectiveness of the cushion (Figure 1.1). For sand barrels and for many other types of crash cushions, maintenance costs may exceed installation costs. Still, one of the most serious problems with many types of crash cushions is their ability to be used only once. This not only makes replacement of the crash cushion expensive, it also leaves the obstacle unprotected until the impact attenuator can be replaced (Carney 1994).

FIGURE 1.1 Poorly Maintained Sand Barrels (Fitch System)

1.2 Objective of the Study

The primary objective of this study was to determine whether tires and recycled tire-derived rubber materials could be used as energy-absorbing elements in impact attenuator devices. The tire-derived materials used for testing were composed of shredded tires with different coarseness. The secondary objective was to develop some preliminary designs of crash cushions using the materials tested.

The crash cushions will be designed for applications such as roadside safety hardware and truck-mounted attenuators (TMAs). Roadside safety applications will emphasize dissipating a vehicle's energy and momentum by applying the conservation of kinetic energy principle and the conservation of momentum principle which will be discussed later. This type of crash cushion requires a rigid, fixed support and is ideal for protecting concrete barriers, bridge piers (Figure 1.2), or other permanent objects in the clear zone of the roadway. However, Kansas always protects the bridge piers with some kind of roadside safety hardware (Seitz 1998).

The basic idea behind this study is that by making a crash cushion from used tires and tire-derived materials, a low-cost, low-maintenance, reusable crash cushion could be developed. The potential benefits of this type of crash cushion are tremendous. Not only would it be less expensive to install and maintain due to the low cost of its attenuating or energy absorbing elements, but it would also provide continuous protection of obstacles. Also, reusable crash cushions would take shorter time to restore thereby reducing risk to the

workers and traveling public while repairs are being done.

FIGURE 1.2 Unprotected Bridge Pier in the Median of I-64 in Illinois

1.3 Scope of the Work

Tests were conducted to evaluate the following properties of the used tires and tire-derived recycled specimens (pads):

1. Strength
2. Durability
3. Energy Absorbing Ability

Static tests were conducted on each tire and tire-derived pad repeatedly to determine the strength and durability of each test material. Dynamic tests were conducted to evaluate the energy absorbing ability of the test materials.

The impacts of temperature and environment on the performance of the tires or tire-derived pads were not included in this study. This data is available from the tire manufacturers and the problem was studied previously by Sicking and Ross (1985). Their findings showed that for the rubber samples, stiffness increased anywhere from 25 percent to 100 percent at temperatures well below freezing (Sicking and Ross 1985). This study was initiated to determine the feasibility of using used tires and tire-derived rubber materials as energy absorbing elements in impact attenuators. If this could be proven feasible by conducting static and dynamic tests, a preliminary crash cushion design could be developed. Further study would be necessary to conduct reduced-scale or full-scale impact testing on the proposed design and to evaluate environmental effects.

1.4 Synopsis

This report is divided into six chapters. Chapter One is an introduction to the problem. Chapter Two reviews existing knowledge of crash cushions. The chapter discusses the principles upon which crash cushions are designed and discusses a few of the most widely used crash cushions. The chapter concludes with some examples of experimental, low-cost crash cushions and previous work done on crash cushions using tires. Chapter Three describes the materials selected for the study. Chapter Four discusses the test set up and procedures for the static and dynamic tests. Chapter Five is the analysis of the results of this study which includes a statistical analysis of the data and the development of proposed designs for crash

cushions using the materials tested. The conclusions and recommendations for further study are included in Chapter Six. Appendix A summarizes the characteristics of the materials and lists all test results. Appendix B shows sample output for selected static and dynamic tests. Appendix C contains sample output from the Statistical Analysis System (SAS) software used for the statistical analysis of data for this project.

Chapter 2

LITERATURE REVIEW

2.1 The Principles of Crash Cushion Design

The primary purpose of a crash cushion is to slow a vehicle to a safe stop when hit head-on so that injury to the occupant of the vehicle is minimized. To accomplish this task crash cushions are usually designed on one or both of the following two principles: (i) the conservation of energy or kinetic energy principle and (ii) the conservation of momentum principle (AASHTO 1996).

2.1.1 The Conservation of Energy Principle

The conservation of energy principle operates on the rule that when a vehicle impacts a crash cushion all of its kinetic energy is dissipated through the crash cushion (Figure 2.1). In other words, no energy is lost in the process, it is simply transferred from the vehicle to the crash cushion. The kinetic energy (KE) of the vehicle may be determined from the following equation:

$$KE = \frac{1}{2} mv^2$$

where m is the mass of the vehicle and v is the speed of the vehicle just before impact. The work done by the crash cushion in deforming is defined as follows:

$$W = Fd$$

where F is the stopping force of the cushion and d is the length of deformation of the cushion. By the conservation of energy principle the following expression can be obtained (AASHTO 1996):

$$KE = W = \frac{1}{2}mv^2 = Fd$$

This relationship can be used for designing crash cushions which need a rigid fixed object for supporting the deforming cushion (Carney 1994).

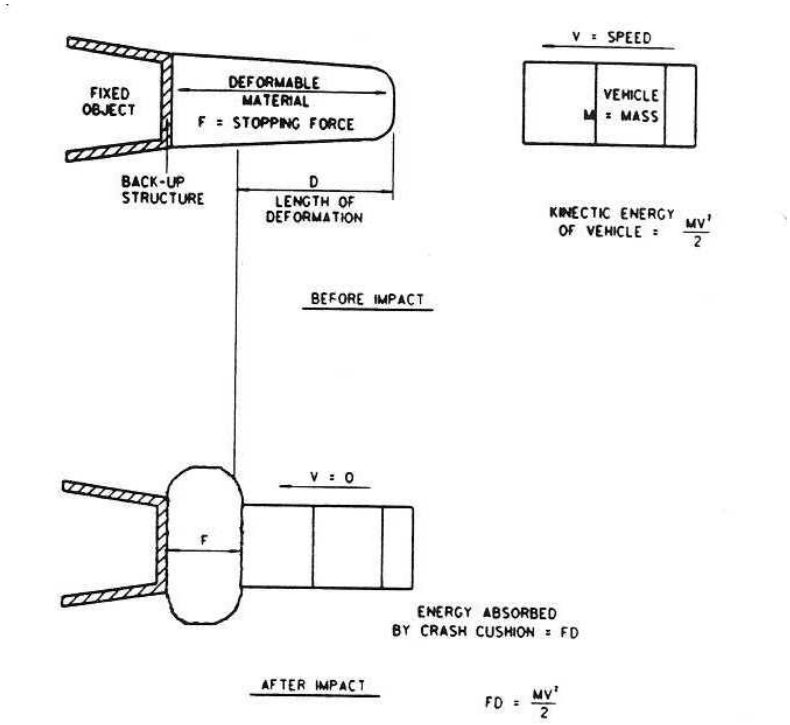

FIGURE 2.1 The Kinetic Energy Principle (after AASHTO 1996)

2.1.2 The Conservation of Momentum Principle

The conservation of momentum principle works on the principle of transferring the vehicle's momentum to an expendable mass, normally sand barrels (Figure 2.2). The momentum of the vehicle before impact must be equal to the combined momentum of the vehicle and the sandbarrel when impacted. This collision can be expressed as follows:

$$m_v v_0 = m_v v_1 + m_1 v_1$$

where

m_v is the mass of the vehicle,

v_0 is the original impact velocity,

m_1 is the mass of the sand, and

v_1 is the velocity after first impact.

Solving this equation for v_1 and generalizing the formula results in an equation for the speed of the vehicle after the nth impact :

$$v_n = \frac{v_{n-1} m_v}{(m_v + m_n)}$$

where m_n is the mass of sand in the nth container(s). This equation is solved for a velocity (v_n) of about 9 mph (15 km/h), but many manufacturers recommend placement of an additional container (or a row of containers) as an extra safety measure. The advantage of this type of system is that it does not require a rigid support (AASHTO 1996).

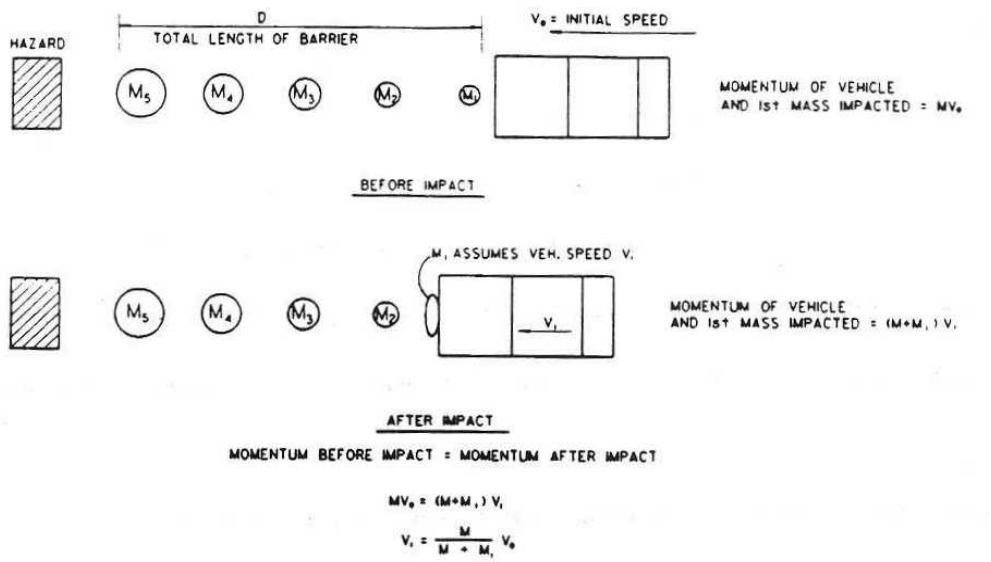

FIGURE 2.2 The Conservation of Momentum Principle (after AASHTO 1996)

2.1.3 The Conservation of Kinetic Energy and Momentum

Many crash cushions are designed based on both the principles of conservation of energy and conservation of momentum. Sicking et al. (1982) have developed a methodology for evaluating a crash cushion which uses both of these principles on a crash cushion consisting of sand-filled 55-gallon steel drums (Figure 2.3). For this type of crash cushion, the conservation of kinetic energy principle can be applied to the crushing of the drums and the conservation of momentum principle can be applied to the effects of the weight of the sand. This methodology can be expressed in general terms and applied to crash cushions

with similar design. First, the conservation of kinetic energy can be applied to find the change in velocity of the vehicle due to crushing the first component of the crash cushion when the energy required to crush the first component, KE_c, is known. This can be expressed by the following equations:

$$KE_i - KE_c = KE_f$$

$$\frac{1}{2}mv_i^2 - KE_c = \frac{1}{2}mv_f^2$$

$$v_f = \sqrt{\frac{mv_i^2 - 2KE_c}{m}}$$

where

KE_i = kinetic energy of vehicle prior to crash,

KE_f = kinetic energy of vehicle after crash,

KE_c = kinetic energy required to crush crash cushion component,

v_i = velocity of vehicle before impact,

v_f = velocity of vehicle after impact and

m = mass of the vehicle

Next, the change in velocity due to the mass of the component of the crash cushion can be found using the conservation of momentum principle (Sicking et al. 1982).

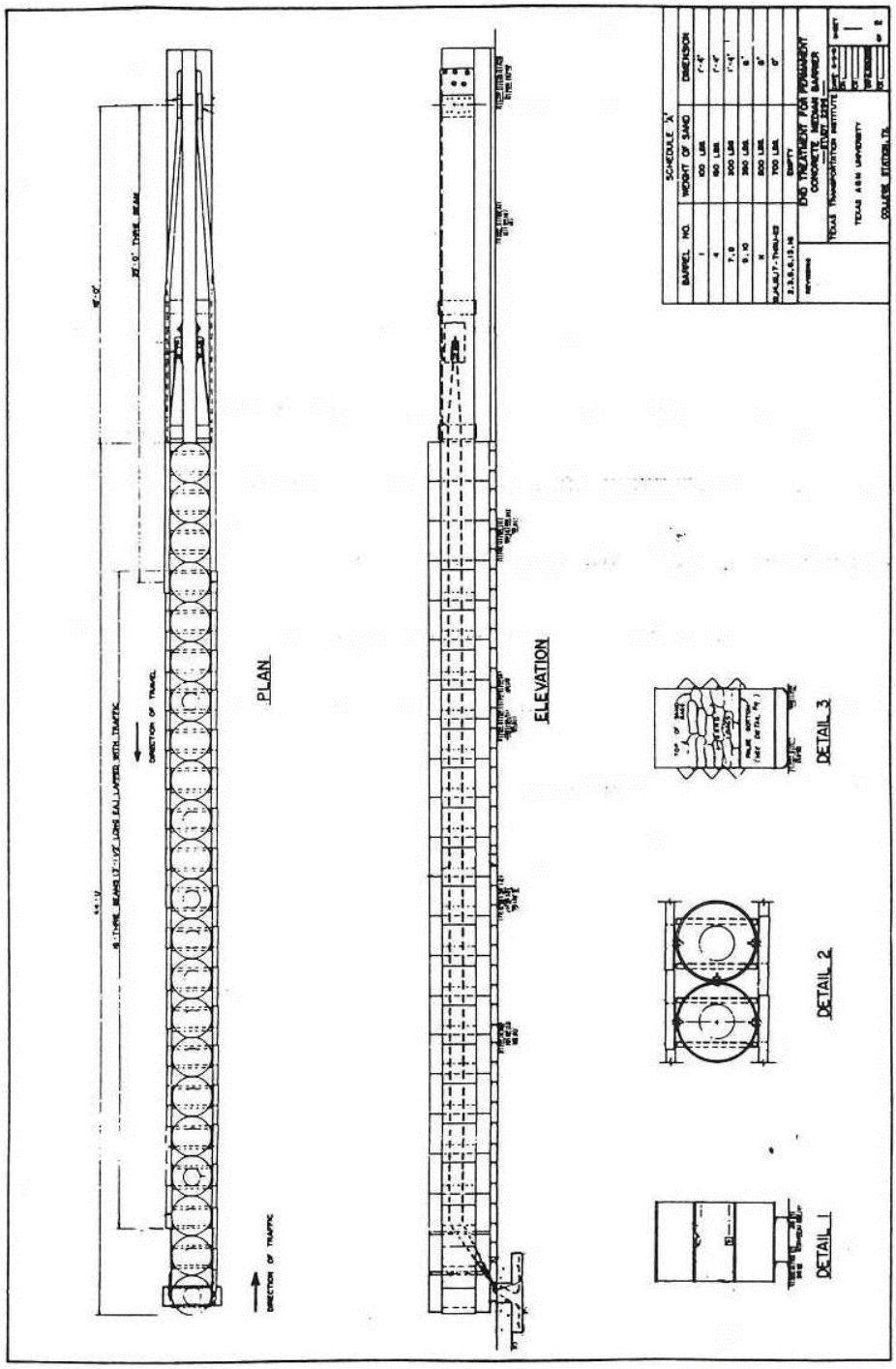

FIGURE 2.3 Construction Drawings for Crash Cushion Using 55-gallon Steel Drums.

2.1.4 Estimating Occupant Risk

One of the most important aspects of designing a crash cushion is estimating the movement of the occupant relative to the vehicle. Crash cushions are designed to protect people, therefore, this analysis should always be conducted. The movement of the occupant can be found from the initial and final velocities of the vehicle and the travel distance of the vehicle as follows (Sicking et al. 1982):

$$a_{avg} = \frac{v_i^2 - v_f^2}{2d}$$

$$v_f = a_{avg} t + v_i$$

$$t = \frac{v_f - v_i}{a_{avg}}$$

$$s_v = v_i t - \frac{1}{2} a_{avg} t^2$$

$$s_0 = v_0 t$$

$$s_r = s_0 - s_v$$

where

a_{avg} = average acceleration (deceleration) of the vehicle,

t = time,

s_v = distance traveled by the vehicle,

s_0 = movement of occupant,

v_0 = velocity of occupant (vehicle velocity upon initial impact),

s_r = movement of occupant relative to the vehicle, and

d = distance component of cushion is crushed.

When the movement of the occupant relative to the vehicle (s_r) reaches 2 ft (0.6 m) for each impact, the impact velocity of the occupant is equal to the difference in the initial and final velocities of the vehicle (Sicking et al. 1982).

The National Cooperative Highway Research Program (NCHRP) Report 350, *Recommended Procedures for the Safety Performance Evaluation of Highway Features,* contains the current recommendations for testing and evaluating the performance of crash cushions and barrier end terminals. The evaluation criteria by which the success of each test is judged requires that the impacting vehicle be gradually stopped or redirected by the crash cushion or end terminal when impact end-on. In addition to end-on impacts, barrier end terminals and redirective crash cushions must be capable of safely redirecting a vehicle impacting the side of the device. No debris may penetrate the passenger compartment or encroach on other traffic. Generally, the vehicle must remain upright during and after the collision and not be redirected into adjacent traffic lanes. Finally, the velocity with which an unrestrained passenger strikes the interior of the vehicle should not exceed12m/s and the

subsequent vehicle deceleration should not exceed 20 g's (highest 10 millisecond average). Preferred values are 9 m/s and 15 g's. The occupant risk criteria differ from earlier guidelines. These criteria specify ride-down accelerations and are not directly comparable with the average acceleration for the entire crash event which is often associated with crash cushion design. However, the acceptance levels of safety performance are approximately the same, and the various design charts prepared by the manufacturers of proprietary crash cushions and terminals may be used to select an appropriate unit. If these charts are used, the maximum average deceleration level should not exceed approximately 7.0 g's (AASHTO 1996).

The NCHRP Report 350 also specifies the criteria for evaluating the risk of a crash cushion to the occupant of the striking vehicle (AASHTO 1996). The model for evaluating occupant risk considers the worst case scenario for a vehicle collision: the occupant is assumed to be unrestrained. The occupant moves forward during the collision until he strikes the dashboard or some other interior surface of the car (assumed to be 2 ft or 0.6 m in the methodology previously discussed). Once the occupant strikes the surface he is assumed to remain in contact with the surface and therefore experiences the deceleration of the vehicle during the last phase of the collision. The severity of the impact is evaluated in terms of the velocity at which the occupant strikes the interior of the automobile and the deceleration that the occupant experiences during the final phase of deceleration or **?**ride down**?** phase. The preferred and maximum values for impact velocity of the occupant are 30 ft/s (9 m/s) and 40

ft/s (12 m/s) and the preferred and maximum values for deceleration are 15 g's and 20 g's, respectively (Michie and Bronstad 1992 and Ross et al. 1993). However, the design would be based on the highest average deceleration which is usually limited to about 7 g's .

2.1.5 Truck Mounted Attenuators (TMA's)

TMAs are designed on the kinetic energy principle and are evaluated on the basis of the risk to the occupant of the errant vehicle in the same manner as is done for the stationary crash cushions. This is because the occupants in the errant vehicle are at greater risk than the occupants in the protective vehicle, and again, the system is designed so that the ?worst case? occupant is protected. However, an additional factor must be considered when designing a TMA: the roll-ahead or skid distance of the protective vehicle to which the TMA is attenuated. This is important since the roll-ahead distance of the protective vehicle affects that amount of energy dissipated by the crash cushion and thus, the occupant risk factors. In addition, this is important in determining the necessary space between the protective vehicle and the work vehicle or workers. For a stationary protective vehicle, the roll ahead distance may be found as follows (Michie and Bronstad 1994):

$$S = v_I^2 \frac{(M_I)^2}{2M_p(M_I + M_p)gD}$$

where

S = roll ahead distance,

M_I = mass of impacting vehicle,

M_p = mass of protective vehicle,

g = gravitational constant, (32.2 ft/s^2),

D = drag factor of protective vehicle, and

v_I = impact speed of impacting vehicle.

The drag factor is simply the ratio of the force required for acceleration or deceleration in the direction of acceleration or deceleration over the vehicle's weight. It also can be described as the ratio of the acceleration or deceleration of the vehicle over the acceleration due to gravity. This can be written as follows:

$$D = a/g$$

From this it is clear that the drag factor is also a decimal percentage of the acceleration due to gravity or "g-force." Drag factor is maximum and equal to the coefficient of friction when all wheels are locked and skidding (Fricke 1990).

The roll-ahead distance for a moving vehicle can be determined from the following equation (Michie and Bronstad 1992):

$$S = \frac{[M_I(v_I - v_p)]^2}{2M_p(M_I + M_p)gD}$$

where v_p = velocity of the protective vehicle and v_I-v_p represents the closing velocity of the protective vehicle and impacting vehicle (Michie and Bronstad 1992).

2.2 Crash Test Guidelines

Although the basic design principles of a crash cushion are quite simple, the actual crash testing requirements are quite rigorous and are the determining factor in evaluating the effectiveness of the crash cushion. NCHRP Report 350 contains the guidelines for conducting full-scale crash testing on crash cushions and specifies the requirements which must be met (AASHTO 1996). The crash cushion's performance is evaluated on the basis of its structural adequacy, the risk to the occupant, and the vehicle's trajectory after the collision. The structural adequacy of an impact attenuator is evaluated on how it holds up in collisions with vehicles of different sizes traveling at different speeds and approaching from different angles. An important quality of the attenuator is whether it scatters debris which could strike other vehicles or land in the driving lanes. The risk to the occupant is evaluated by the crash cushion's ability to keep an impacting vehicle upright and maintain the integrity of the impacting vehicle's passenger compartment. The vehicle trajectory is evaluated on the basis of whether the attenuation system deflects an impacting vehicle back into traffic or not (Ross et al. 1993 and Carney 1994). NCHRP Report 350 also defines several types of crash cushions by their performance characteristics. Crash cushions can be termed "gating" or "non-gating," the former is a crash cushion which allows controlled penetration along part of its length and the latter is a crash cushion which has redirection capabilities along its whole length. A redirective crash cushion is one which can redirect a vehicle impacting its side while

a nonredirective crash cushion brings a vehicle to a stop when impacted from the side (Ross et al. 1993).

2.3 Analysis of Current Systems

2.3.1 Sand Barrels

There are over a dozen crash cushion systems that are widely used today. The most common types are the sand-filled barrels (Figure 2.4). In 1992, there were approximately 3,992 sand-filled barrel crash cushion systems in place in the United States (Carney 1994). A system of over a dozen barrels would cost from $3,000 to $4,500 in Kansas (Seitz 1998). As already mentioned, sand barrels work by dissipating a vehicle's momentum, however, the array of barrels performs best when hit head-on. It is a non-redirective system. This should be carefully considered when determining the type of crash cushion for a particular location. Significant maintenance problems may include sand within the barrels freezing (this, however, can be avoided by mixing $CaCl_2$ with sand and most cold weather states do practice this) and becoming an obstacle, the long set up time due to having to fill the barrels with sand, measuring the amount of sand needed in each barrel in the field, barrels moving out of place due to vibrations on the road, the cracking of the barrels, minor hits requiring replacement of the system, and the clean up required after a collision (Carney 1994). In fact cleanup takes some agencies up to 22 man-hours even with special equipment (Kircher 1985). This is a

problem in that the obstacle is left unshielded for an extended period of time, repair crews are exposed to traffic while repairing or replacing the cushion, and the traffic may be delayed.

FIGURE 2.4 Sand Barrels Protecting a Concrete Barrier

2.3.2 The GREAT System

The GREAT System is used to shield narrow hazards and costs anywhere from $15,000 to $30,000 (Figure 2.5). It operates by dissipating the kinetic energy of a colliding vehicle by crushing cartridges held in place by triple-corrugated steel rails; during a collision usually only the cartridges and the nose are expended. The attenuator is capable of redirecting vehicles that impact it from the side with little damage to the system (AASHTO 1996). The main problems encountered with the 1,877 units in place in the United States are the high cost of the replacement parts and the large amount of time required to repair the system. The latter problem is especially critical because these systems may be located in narrow median areas making the exposure of the repair crew to traffic and causing long traffic delays. The GREAT System also requires a substantial amount of maintenance; cartridges deteriorate and need replacement, the nose needs replacement due to sideswipes, and the hardware rusts easily (Carney 1994). Kansas experienced no excessive rust problems, but the anchor cables need to be checked and may need tightening time to time (Seitz 1998). However, GREAT does not meet the NCHRP 350 requirements and has been replaced with QuadGuard (Seitz 1998).

Although there are high maintenance costs associated with these widely used crash cushions, their benefits are indisputable. However, the high initial costs, maintenance costs, and replacement costs of these systems merit further research and development of a more

economical crash cushion. The ability to make a crash cushion that would reduce any of these costs has the potential to create savings to the highway agencies. The resulting savings could be used for other needed highway improvements.

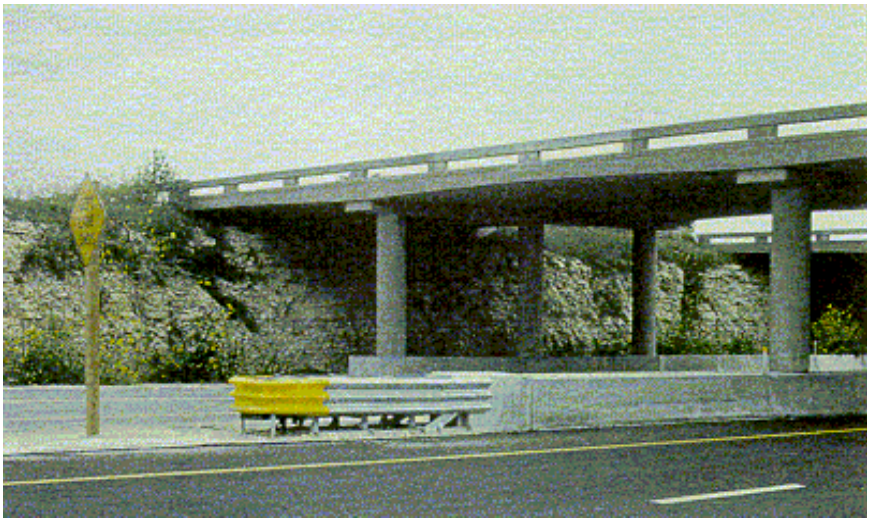

FIGURE 2.5 The GREAT System Protecting Bridge Piers in a Narrow Median

2.4 Low Cost Crash Cushion Studies

2.4.1 Aluminum Can Crash Cushion

The high-cost and non-reusability of most commercial crash cushions has led to the testing and development of less expensive crash cushions, some of which contain non-expendable elements. One low-cost system made use of empty aluminum cans by enclosing the cans in a bag which was held together by a steel frame. This system was designed to be

used on trees and utility poles, both of which have been found to be obstacles to the motorists. The crash cushion tested was made of five rows of cans placed with their long axis facing the front of the cushion and a bay with cans placed randomly (Figure 2.6). This crash cushion was found to be effective in head-on and off angle collisions of automobiles at speeds up to 40 mph (64 km/h). Naturally, once struck the cushion could not be reused; its primary advantage lies in its cost, approximately $500 in 1983, dollars including installation (Public Works 1983).

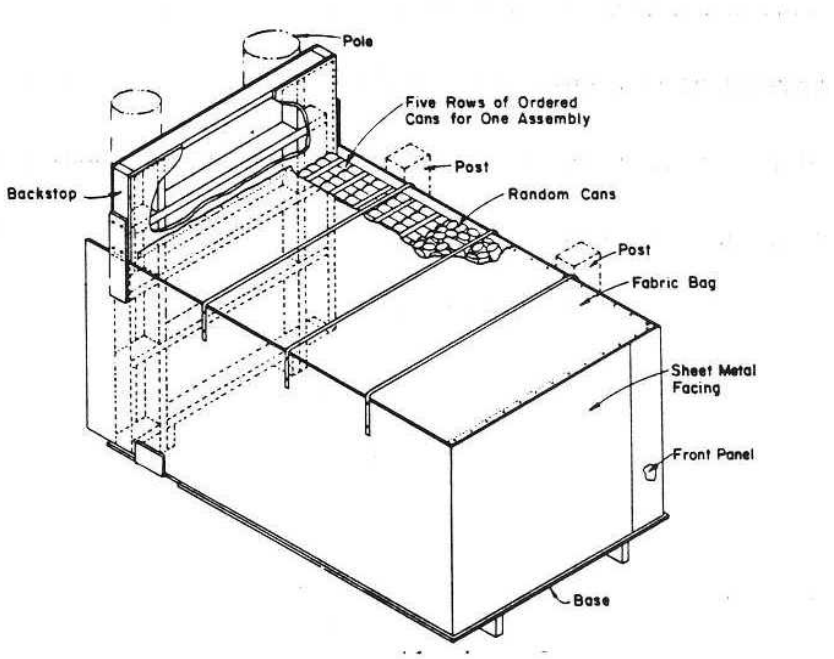

FIGURE 2.6 A Low-Cost Cushion Made from Aluminum Cans (after Public Works 1983)

2.4.2 The Low Maintenance Attenuator (LMA)

LMA is a proprietary crash cushion marketed by Energy Absorption, Inc., which is designed to protect narrow obstacles in locations where a high frequency of impacts is anticipated (AASHTO 1996). Repair costs for end-on impacts of this system are low due to the use of highly reusable parts. For most design impacts the main structural elements and energy absorbing materials do not require replacement and can be placed back into service in a short time. Figure 2.7 shows an LMA. The LMA shown is composed of 12 modular bays, which consist of elastomeric cylinders surrounded by a framework of triple corrugated steel diaphragms and three-beam guardrail. A flexible, reusable nose section is fastened to the end. When impacted head-on, the kinetic energy is absorbed by the telescoping movements of the guardrail and compression of the elastomeric cylinders. Longitudinal stiffness for side impact resistance is attained by use of restraining chains and a restraining cable (AASHTO 1996). The LMA has been fully tested and found to stop passenger cars in the 1,800 to 4,400 lb (820 to 2000 kg) range at speeds up to 62 mph (100 km/h) within the guidelines of NCHRP Report 350. Side angle impact can result in damage to the unit, which can result in high-maintenance cost (AASHTO 1996).

FIGURE 2.7 Low Maintenance Attenuator (LMA) (after AASHTO 1996)

2.4.3 HMW/HDPE Crash Cushion

The materials which show the most promise in developing low-cost, non-expendable crash cushions are high molecular weight/high density polyethylene (HMW/HDPE), rubber, and other rubber-based materials such as tires. The characteristics of HMW/HDPE which makes it useful in a crash cushion are its high stiffness, high ductility, high toughness, high tensile strength, and high impact resistance. Carney and Faramawl (1995) developed a crash cushion using HMW/HDPE cylinders. The device contained nine HMW/HDPE cylinders which varied in thickness from 0.796 in. (20.2 mm) for the front

cylinder to 1.39 in. (35.2 mm) for the back or last cylinder. The cushion was also designed to redirect vehicles impacting the side of the cushion by installing two 1 in. (25.4 mm) thick cables on each side of the cushion. The results of full scale testing of this experimental device in accordance with NCHRP 350 with a 4,500 lb (2,000 kg) pickup truck showed that the crash cushion was capable of bringing the vehicle to a stable, controlled stop. Furthermore, when the load was removed from the cushion, it restored itself to its original shape and could continue to serve its designed purpose (Carney and Faramawl 1995).

Carney (1997) also used HMW/HDPE cylinders to develop a TMA. This TMA, called Vanderbilt Truck Mounted Attenuator (VTMA), demonstrated that it was capable of safely decelerating a vehicle traveling 62 mph (100 km/h) and restoring itself to its original shape upon removal of the load. The VTMA also met the testing requirements in NCHRP Report 350 with an 1,800 lb (820 kg) Ford Festiva and a 4,500 lb (1,000 kg) Chevy pickup truck and was approved for use by the Federal Highway Administration (FHWA). The attenuator (Figure 2.8) is made of four HMW/HDPE cylinders, the largest of which is 10 ft (3.048 m) long and has a 1 in. (25 mm) galvanized steel cable threaded inside to pull the width to 7.08 ft (2.16 m). The three remaining cylinders are fastened to the inside of this cylinder to provide additional cushioning (Carney 1997).

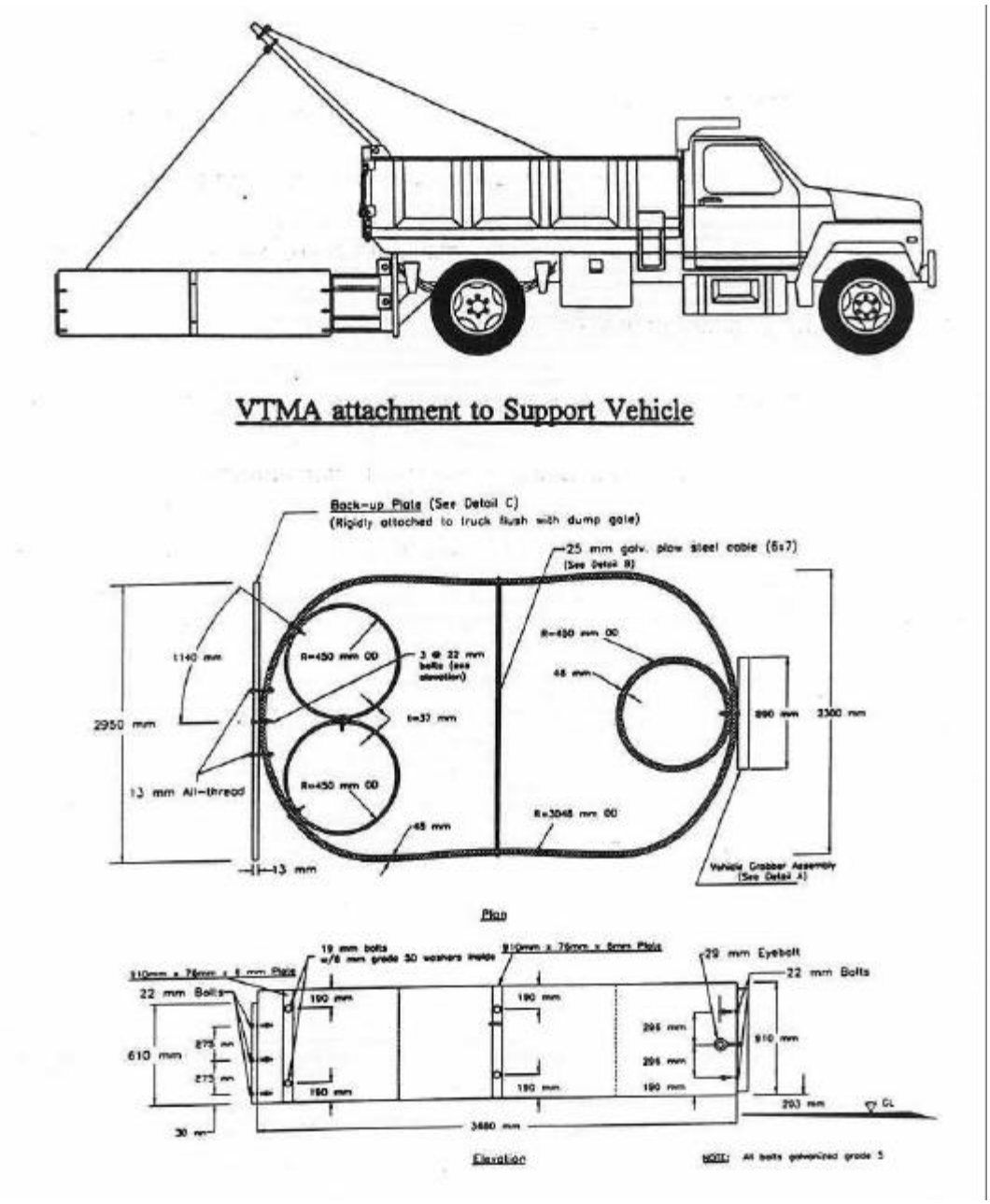

FIGURE 2.8 Details of the VTMA (after Carney 1997)

2.4.4 Rubber Crash Cushion

Sicking and Ross (1985) tested several materials for use in a low-cost, reusable crash cushion. Their testing concluded that polyurethane and polyethylene foams were not suitable due to the extensive damage they sustained in a single compression test. Rubber, however, was found to be a good candidate material for use in a reusable crash cushion. They also found that cylindrical shapes of rubber seem to be the most efficient of many different shapes tested. The cylinders have the ability to absorb the highest amount of energy per pound of rubber (Sicking and Ross 1985).

Sicking and Ross (1985) designed a crash cushion using data from the initial material tests by using the principles of conservation of energy and momentum discussed earlier in this report. The final design included 13 rubber cylinders. One cylinder was placed vertically at the front of the crash cushion to "capture" an impacting vehicle while the remaining 12 were all placed horizontally (Figure 2.9). The first six cylinders were thin-walled to reduce the weight of the front of the crash cushion thereby reducing the momentum transfer when the vehicle first impacts the attenuator. Heavier elements would transfer more weight in the impact and, therefore, decelerate the vehicle too quickly. The cylinders were supported by steel diaphragms that were connected to three beam fender panels which would help provide redirectional capabilities along with four 5/8 in. (1.59 cm) cables. All components of the crash cushion were intended to be reusable (Sicking and Ross 1985).

Crash tests revealed that this crash cushion meets NCHRP 230 standards using 1,800 lb (820 kg) and 4,500 lb (2,000 kg) vehicles. However, the crash cushion is not self-restoring but can be restored in less than one hour for under $100 (estimated). The total cost for the crash cushion was initially $20,000 but could be reduced to $13,000 for subsequent systems (Sicking and Ross 1985).

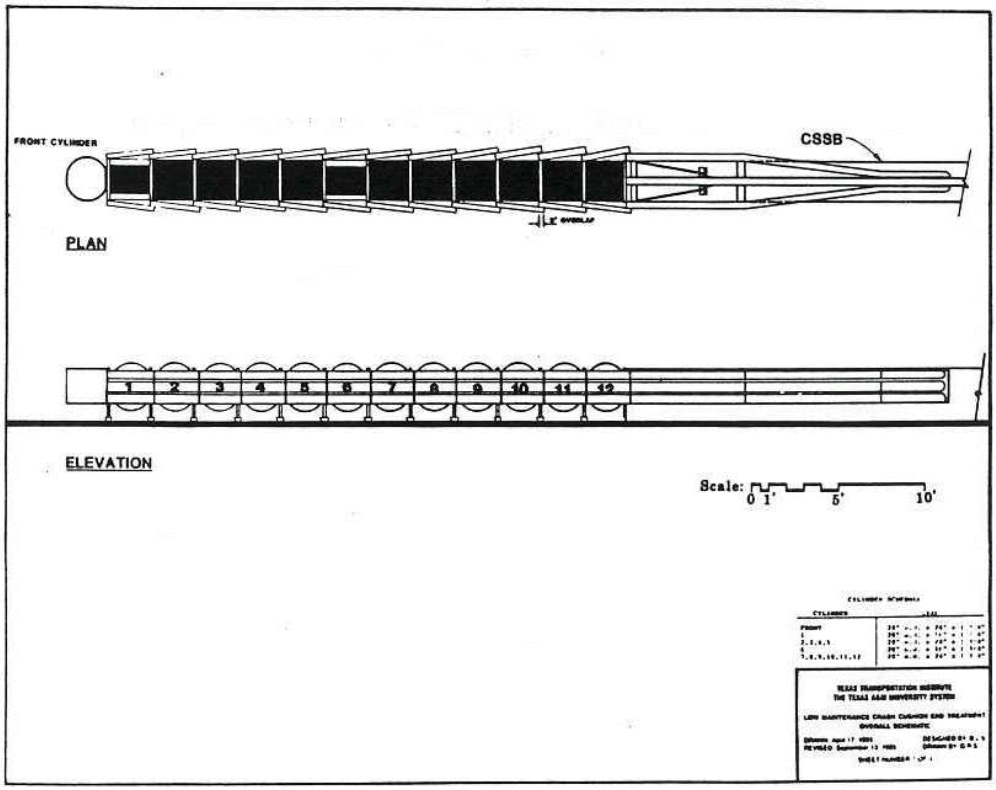

FIGURE 2.9 Rubber Cylinder Crash Cushion (after Sicking and Ross 1985)

2.4.5 Crash Cushion From Tires

Marquis et al. (1975) were the first to study used tires in crash cushion applications. They developed a tire-sand inertial crash cushion by using the conservation of momentum principle. The system consisted of tires filled with sand placed on collapsible bases and placed in rows very similar to the sand barrel systems used today. The sand filled tires were placed on bases so that the center of gravity of the tire-sand modules would be raised to help prevent vehicle ramping. Each module was covered with a 4 mil thick polyethylene sleeve to protect it from environmental effects and to make the system appear more aesthetically pleasing. Figure 2.9 shows how the modules would be arranged typically to protect motorists from a potential hazard. Full scale crash testing demonstrated that the system could stop a 4,000 lb (1,810 kg) vehicle (1968 Chevrolet) traveling 60 mph (96.6 km/h) within tolerable limits for unrestrained occupants. The primary disadvantage of the system is the possibility of the scattering of debris (i.e., sand and tires) when impacted. Therefore, this system should be used in areas where debris would not cause a secondary obstacle. Still, after impact all of the tires and most of the sand was reusable, thus virtually eliminating replacement costs of materials. The estimated installation cost of the system was $850 in 1975 dollars (Marquis et al. 1975).

Marquis and Hirsch (1973) also tested used tires in a crash cushion based on a design created by the Goodyear Tire and Rubber Company. The Goodyear design was 70 ft (21.3

m) long and used 250 tires. Marquis and Hirsch (1973) deemed that this length was not practical for use at most roadside locations and therefore reduced the crash cushion to 35 ft (10.7 m) long while keeping the same modular design (see Figure 2.11) used by Goodyear. Two 0.75 in. (1.91 cm) cables were threaded through the outside row of the tires on each side and fish scales were later added to work with the cables in providing redirectional capabilities (Figure 2.11). The crash cushion proved to be effective in decelerating vehicles to a safe stop and resulted in average decelerations of under 12 g's. Once impacted, the crash cushion almost rebounded to its original shape so that it could still provide most of its attenuation capabilities. It was estimated that the cushion could be restored to its original shape in a matter of minutes (Marquis and Hirsch 1973).

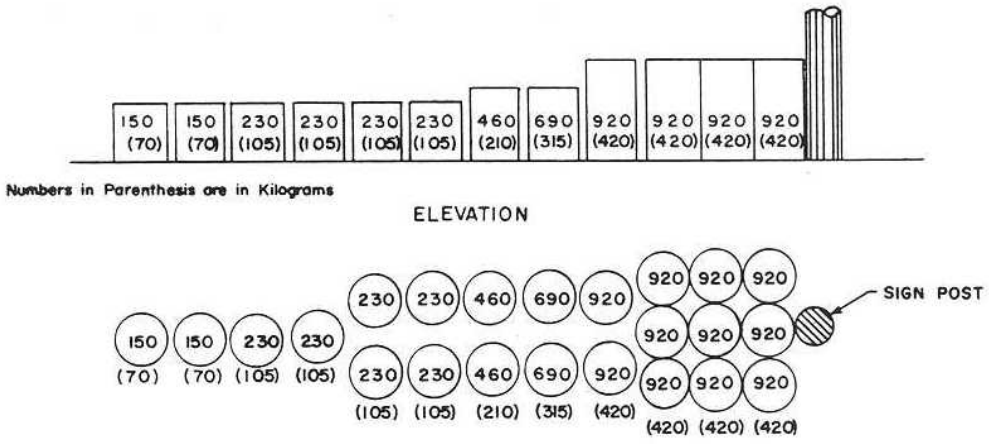

FIGURE 2.10 Typical Layout for the Tire-Sand Crash Cushion (after Marquis et al. 1975)

Another problem discovered during crash testing was that the vehicle rebound was significant for vehicles not in gear. Therefore, this cushion should not be used in areas with high traffic or when vehicle rebound may have high potential for secondary crashes. Finally, the front of the crash cushion caused high deceleration rates especially in small vehicles. Therefore, the front should be reduced in weight or stiffness to lessen initial deceleration of the impacting vehicle. Still, this crash cushion showed much promise for application on roadsides. One of the greatest aspects about it was that it was totally reusable and its total cost ranged from $2,100 to $4,100 in 1973 dollars (Marquis and Hirsch 1973).

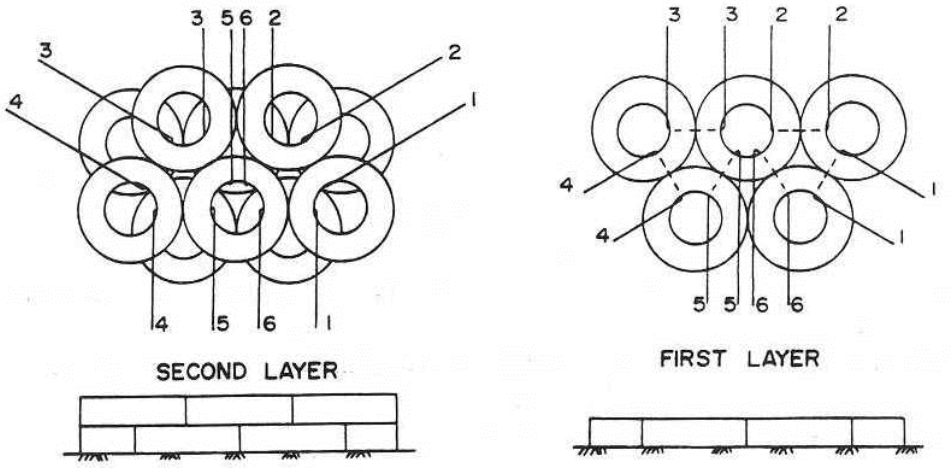

FIGURE 2.11 Modular Design of the Goodyear Crash Cushion (after Marquis and Hirsch 1973)

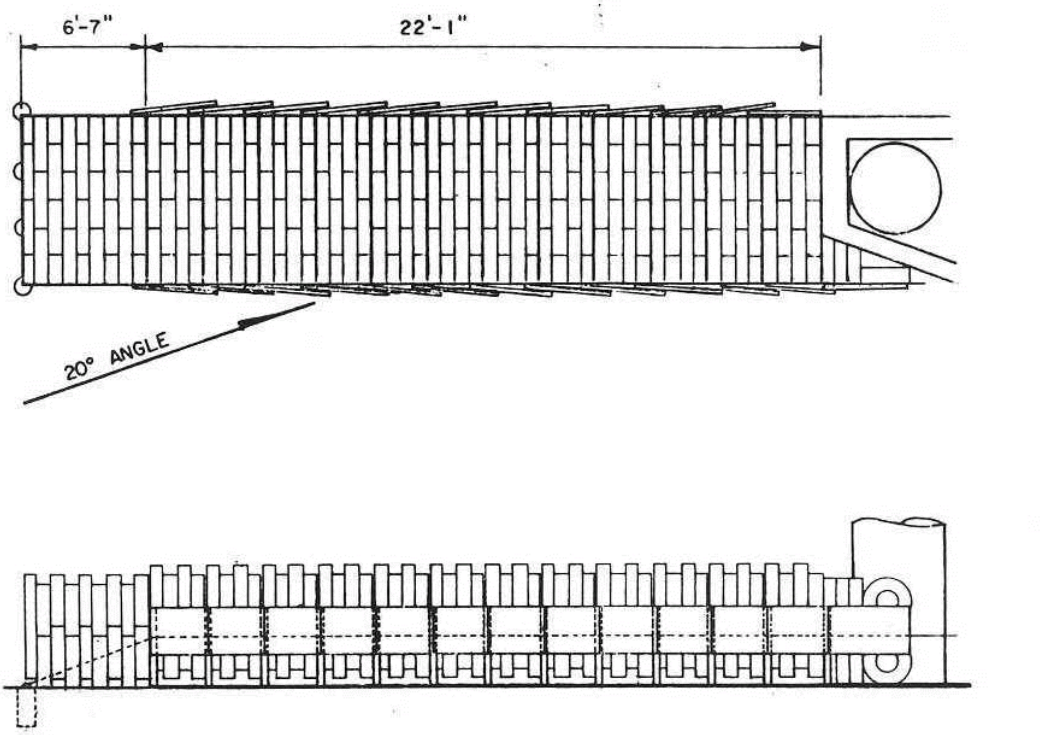

FIGURE 2.12 Goodyear Crash Cushion as Modified by Marquis and Hirsch (1973)

Chapter 3

MATERIAL PROPERTIES

3.1 Tires

More than 30 used tires were used for this study. Tires were obtained from tire sales stores located in Manhattan and Topeka, Kansas. The only criteria for selecting a tire was that it had to have an outside diameter of 24 in. (60.96 cm) or less so that it would fit in the testing apparatus and the tire had to be an automobile (pickup trucks and mini-vans included) tire. Tires were not selected on a basis of weight, thickness, apparent wear, manufacturer, brand, function, or style. The tires sampled were probably relatively new due to the fact that they were still in the tire sales shop and had not been sent to a landfill, junkyard, or other type of disposal facility. Some tires exhibited significant tread while others had little tread left. Only two tires were worn to the point where the steel belts were visible.

Two tires were used to test the experimental set-up. The remaining 30 tires were used as the experimental units of this study. The type and manufacturer, size, height (or width of the tire measured from sidewall to sidewall), inner diameter, outer diameter, and sidewall area (outer diameter-inner diameter) were all recorded and shown in Table 3.1. The widths of the tires ranged from 6.3 in. (16.0 cm) to 8.8 in. (22.35 cm). Weights ranged from 12.20 lbs (5.53 kg) to 21.76 lbs (9.87 kg).

Table 3.1 Whole tire characteristics

TIRE	TYPE	SIZE	WIDTH (in)	WEIGHT (lbs)	OUT.DIA (in)	IN.DIA (in)	AREA (in^2)
1	Firestone FR22	P195/75 R14	7.35	17.08	23.75	15.50	254.32
2	Dayton Quadra XT2	P195/75 R14	6.30	16.83	24.00	15.50	263.70
3	Copper Lifeliner	P185/70 R14	6.92	17.50	22.50	15.50	208.92
4	Toyo 800 Plus Touring Radial	P185/70 R13	6.60	15.54	21.75	14.50	206.41
5	Ultra Supreme 770	P185/70 R14	6.50	16.17	22.50	15.50	208.92
6	Firestone FR480	P175/70 R14	6.50	14.60	22.25	15.50	200.13
7	Classic Premium Steel Belted Radial	P175/70 R13	6.56	13.13	20.50	14.50	164.93
8	Dean Celestial Metric	P195/65 R14	7.92	16.76	21.50	15.50	174.36
9	Goodyear F32-S	P195/70 R14	7.55	14.35	22.50	15.50	208.92
10	Supreme 700 Ultra Patriot	P185/70 R14	6.84	17.34	23.00	15.50	226.78
11	Pirelli Response	P195/60 R14	7.70	16.33	22.00	15.00	203.42
12	Firestone FR22	P195/75 R14	7.41	16.33	24.00	15.50	263.70
13	Ultra Supreme 770 Patriot	P195/70 R14	7.50	16.75	23.00	15.50	226.78
14	Falken Fk-06U	P195/60 R14	8.55	17.20	21.00	15.50	157.67
15	Goodyear Aquatread	P175/70 R13	6.65	15.22	20.50	14.50	164.93
16	Michelin X Metric	P175/70 R13	7.00	14.38	21.25	14.25	195.17
17	American Turbo Metric	P175/70 R13	6.87	12.20	20.50	14.50	164.93
18	Goodyear Conquest	P195/70 R14	7.40	15.28	23.00	15.50	226.78
19	Michelin Radial X	P175/70 R14	6.95	14.10	22.25	15.50	200.13
20	Michelin Radial X	P175/70 R14	6.90	13.27	22.00	15.50	191.44
21	Defender HRX Radial	P205/55 R15	8.80	21.66	23.25	17.50	184.03
22	Goodyear Regatta	P205/65 R15	7.78	18.28	24.00	16.50	238.57
23	General Ameri* G45	P195/70 R14	7.64	15.64	22.75	15.50	217.80
24	Ultra STRSport	P185/70 R14	6.92	14.38	22.25	15.50	200.13
25	General Ameri* G45	P195/70 R14	7.55	15.25	22.50	15.50	208.92
26	Goodyear Invicta Gl	P175/70 R13	6.86	13.32	21.00	14.50	181.23
27	Michelin Radial X	P175/70 R14	6.85	14.04	22.50	15.50	208.92
28	Goodyear Conquest	P195/70 R14	7.22	15.04	23.00	15.50	226.78
29	Michelin X Metric	P175/70 R13	6.85	14.24	21.25	14.25	195.17
30	Defender HRX Radia	P205/55 R16	8.80	21.76	23.00	17.50	174.95
		Average	7.24	15.80	22.31	15.40	204.96
		Std. Deviation	0.655011	2.186732	1.03325	0.767329	28.12808

3.2 Tire-Derived Rubber Samples

The tire-derived rubber samples were provided by Dodge-Regupol, Inc. in Lancaster, Pennsylvania. The samples were made from shredded used tires and a resinous binder. There are two methods of shredding used tires: tires can be cryogenically frozen to a temperature where the rubber can be easily removed from the steel belts and chords inside the tire or the tires can be shredded whole and the steel is removed by passing magnets over the shredded product. Since the major component of these samples are shredded used tires, they can be produced at a reasonable cost.

Three different types (four samples of each type) of the shredded tire-derived material were tested for this project as shown in Figures 3.1 and 3.2. Table 3.2 lists the characteristics of each sample type. The SPAV paver tile is composed of finely shredded, densely-packed used tires and will be referred to as the "fine" pad for the purposes of this study. The second sample is a SPX50 tile which does not contain the dense component. It is composed of shredded tire pieces larger than those in the fine pad and the shreddings are more loosely packed. This pad will be referred to as the "coarse" pad in this study. The last sample is a SPX50 tile. One of its square faces is composed of fine tire shreddings similar to that of the fine sample pad and measuring 0.5 inch (1.27 cm) in thickness. The remainder of the pad is composed of a coarse material similar to the coarse sample pad. In this study this pad will be referred to as the "composite" pad because it is made from both fine and coarse tire shreddings.

Table 3.2 Recycled Tire-Derived Pad Characteristics

Type	Weight		Size		Cost	
	lbs	kg	in	mm	$/ft^2	$/m^2
SPAV Paver tile (Fine)	6.60	2.99	12x12x 1 3/4	305 x 305 x 44.5	7.00	75.35
SPX50 Tile Minus (Coarse)	5.68	2.58	12 x 12 x 2	305 x 305 x 50.8	6.75	72.66
SPX50 Tile (Composite)	8.16	3.70	12 x 12 x 3 1/4	305 x 305 x 82.6	5.50	59.20

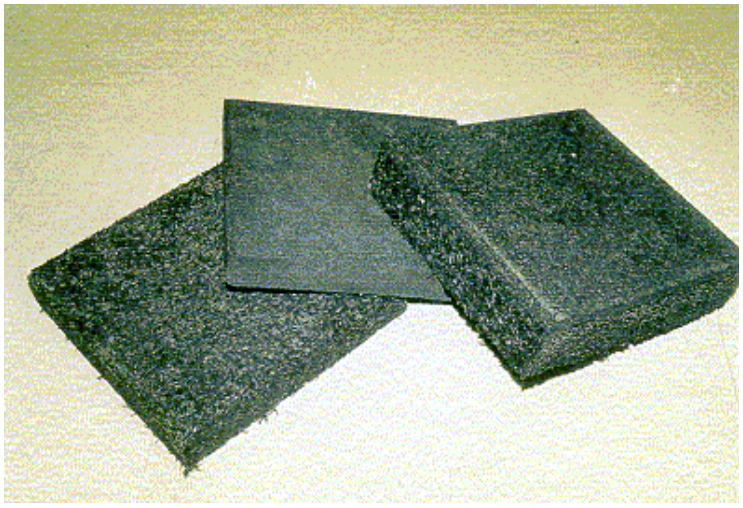

FIGURE 3.1 Tire-Derived Pads (from left to right: coarse, fine, and composite)

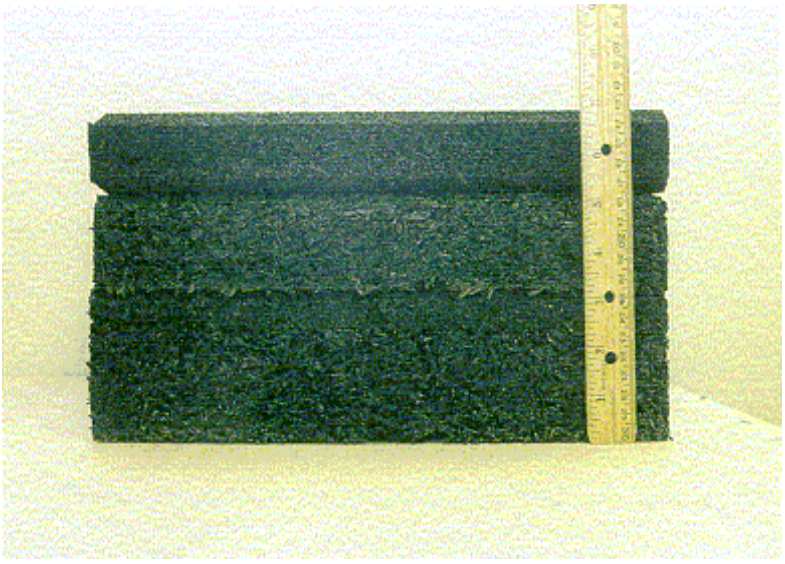

FIGURE 3.2 Tire-Derived Pads (from top to bottom: fine, coarse, and composite)

Chapter 4

SAMPLE TESTING

4.1 Introduction

The tires and the tire-derived pads were tested both statically and dynamically to determine whether they could be used in a low-cost, reusable crash cushion. The effect of temperature and environment on the samples were beyond the scope of this study. As discussed earlier in this report much of this data can be obtained from the manufacturer and these effects have been the subject of other studies. All materials were tested indoors at temperatures ranging from 68°F to 78°F (20°C to 26°C).

4.2 Static Tests

Static Compression tests were conducted on all materials to determine durability, load versus deflection relationship, and maximum loads. Testing was conducted at the Kansas Department of Transportation (KDOT) Materials Testing Lab on a 120,000-lb capacity SATEC Systems Universal Testing Machine (Figure 4.1) and a 440,000-lb capacity SATEC Systems Universal Testing Machine. Each machine was controlled by a 486-computer using the MATS-II Universal Materials Automated Test System Program. This program also stored test results on computer disks and printed the specified output.

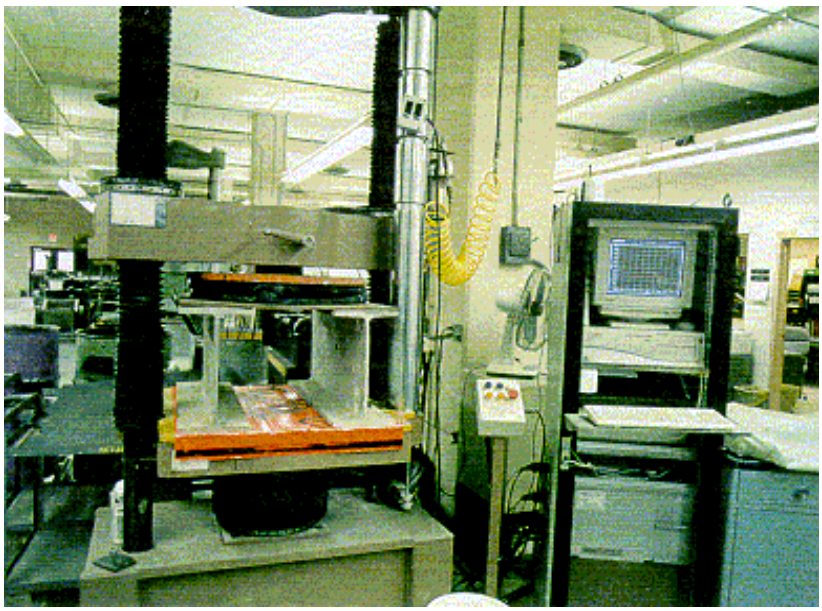

FIGURE 4.1 SATEC Systems 120,000-lb Capacity Universal Testing Machine with 486-Computer Crushing Tire in Horizontal Compression

4.2.1 Whole Tires

All whole, single tire tests were conducted on the 120,000-lb capacity Universal Testing Machine. Tires were placed on their side (longitudinal axes oriented horizontally) on a 1/4 in. (6.4 mm) steel sheet placed on steel I-beams to bring them up to where they could be compressed under the head of the testing machine. A one-inch (25 mm) thick steel plate with a diameter of 24 in. (610 mm) was fixed to the head to compress the entire sidewall area of the tire as shown in Figure 4.2. Three of these tests, hereafter called horizontal tests, were conducted on each tire to determine the durability and peak load of the tire. The initial loading for these tests was 500 lbs/min, which was determined to be an adequate loading rate from the two initial set-up tires. However, subsequent tires

proved to be much tougher and the loading rate was increased to 2,500 lbs/min. Tests on earlier samples were repeated so that correlation could be drawn between the tire tests at the same rate. A total of 112 single-tire horizontal compression tests were performed.

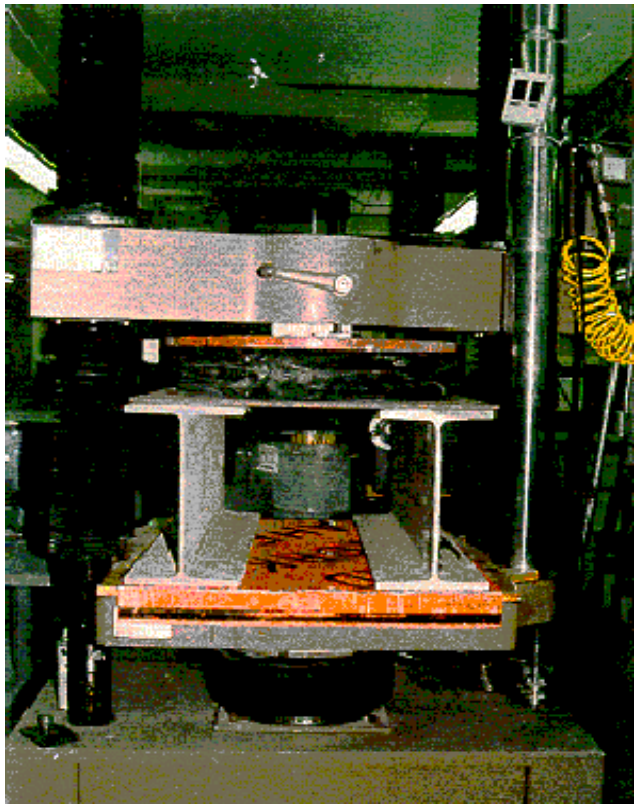

FIGURE 4.2 Setup for Horizontal Tire Static Compression Test

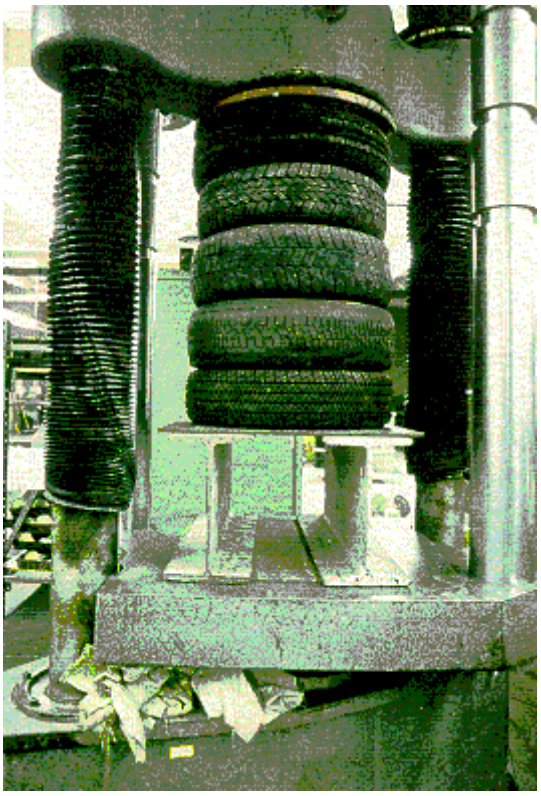

FIGURE 4.3 Setup for Horizontal Multiple-Tire Static Compression Test

Horizontal compression tests on multiple tires were conducted on the 440,000-lb capacity Universal Testing Machine. The set-up for the test was similar to that of the single tire tests. Tires were stacked horizontally so that their sidewalls were in contact as depicted in Figure 4.3. Thirteen tests using two tires, 12 tests using three tires, and 12 tests using five tires were conducted for a total of 37 multiple-tire horizontal compression tests.

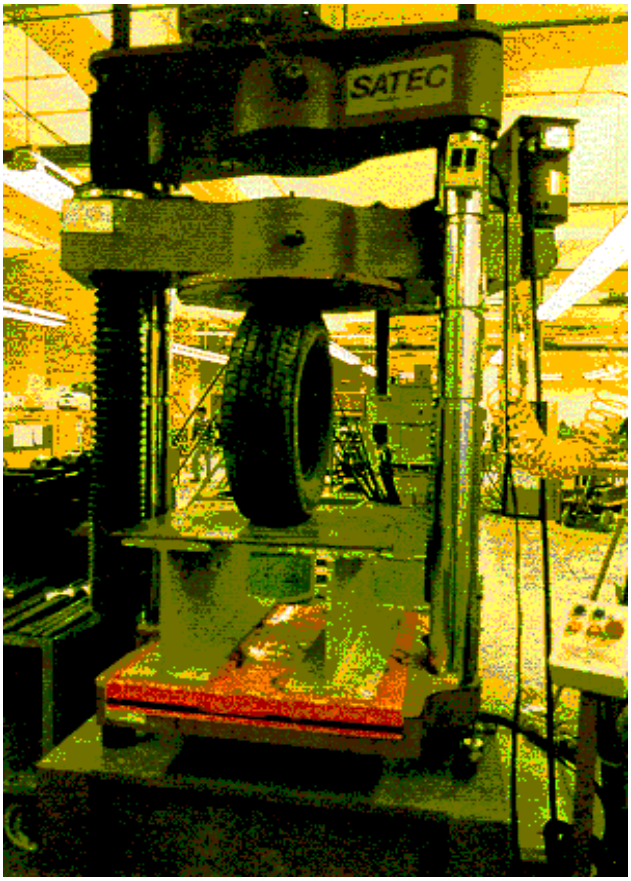

FIGURE 4.4 Setup for Vertical Tire Static Compression Test

Individual tires were also tested vertically (longitudinal axes vertical) on the 120,000-lb testing machine shown in Figure 4.4. Tires tested in this manner had already been tested horizontally. Tires were damaged when tested in this manner, therefore, only 11 single-tire vertical compression tests were conducted.

Output data of the tests was stored by the MATS-II program on computer disk. The output specified for these tests was a plot of the load verses deflection.

4.2.2 Recycled Tire-Derived Pads

Each of the three different types of tire-derived pads were marked as samples one through four. The first sample for each type of pad was used to determine the loading rate for the static compression tests. Since pads were solid it was concluded that they would be able to take a larger load per unit of deflection. Therefore, the first four tests were conducted at loading rates ranging from 2,500 lbs/min to 5,000 lbs/min on the 120,000-lb capacity testing machine. It was quickly discovered that the pads would be capable of sustaining much higher compressive loads than the tires. Therefore, all subsequent testing was conducted on the 440,000-lb capacity testing machine. A range of loading rates were tested for each sample type until a loading rate of 60,000 lbs/min was decided upon for the remainder of the tests.

The initial 27 tests were conducted by placing a steel cylindrical pedestal on the testing machine. A one inch (25 mm) thick steel plate the same size as the pads (one square foot) was placed on top of the cylindrical pedestal as illustrated in Figure 4.5. This portion of the setup was designed to move the specimen closer to the head of the testing machine so it could be compressed. A 3/8 in. (9.5 mm) thick reinforced steel plate was attached to the head of the testing machine. Each pad was placed between these plates and tested in compression. During compression tests, the pads would deform laterally in all directions so that when the load was released and the pads returned to their original shape, they would snag on the corners of the plate. These plates were then placed with one inch (25 mm) thick circular plates with a 24 in. (610 mm) diameter and the tests were completed.

A total of 59 static compression tests were performed on the tire derived samples. Tests were repeated on single pads and tests were conducted stacking two and three pads on top of each other. A complete record of the tests conducted can be found in Appendix A.

FIGURE 4.5 Initial Setup for Static Compression Tests on Tire Derived Pads.

4.3 Dynamic Tests

Dynamic tests were conducted on a high response, closed loop, electrohydraulic Minnesota Testing System (MTS) with a 5,500 lb (25 kN) load cell (Figure 4.6) at Kansas State University. Materials were loaded using a haversine function since this seemed to most closely model loading during an impact. The data output for these tests were load-deflection curves showing both the loading and the unloading phases of the test.

4.3.1 Whole Tires

Tests on whole tires were performed by placing the tires horizontally between two one inch (25 mm) thick steel plates 24 in. (610 mm) in diameter. A total of ten tires were tested, each at two different frequencies (0.1 Hz and 0.08 Hz) and three different loads

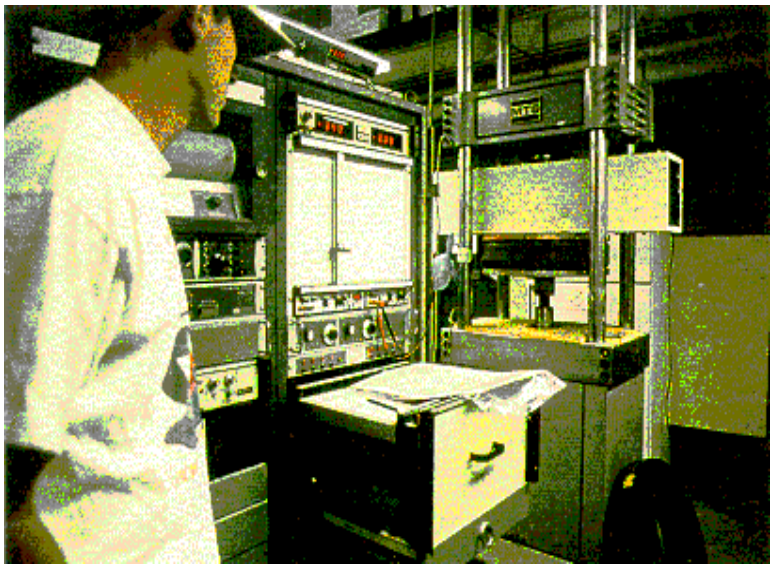

FIGURE 4.6 Dynamic Test on Tires using the MTS Machine at Kansas State University

(1,000 lbs, 2,500 lbs, and 5,000 lbs) for a total of 60 tests. Tires were tested at different frequencies and loads to determine the effects of each factor. The 5,000 lb (22.3 kN) load was almost to the point on the load-deflection curve where the slope changes from horizontal to vertical. This point is a critical point because it is the point where the tire begins taking on load quickly while deforming very little. The work done in crushing each specimen and in returning each specimen to its unloaded state was found by measuring the areas under the load-deflection curves with a planimeter. A complete listing of the dynamic tire tests conducted can be found in Appendix A.

4.3.2 Recycled Tire-Derived Pads

Testing of the pads utilized the same set-up as the whole tires. Each of the three pads was tested at the same frequencies and loads as the tires for a total of 18 tests. Data for each dynamic test on the pads can be found in Appendix A.

CHAPTER 5

CALCULATIONS AND RESULTS

5.1 Results and Discussions

Tires in the horizontal static tests were loaded until the load versus displacement curve was nearly vertical (or, slope of infinity). In other words, samples were loaded until the load was increasing rapidly but deflection was increasing very little. This usually occurred after the tires had been compressed to about 75% of their width. Since this criterion for terminating the test is somewhat subjective, tests were conducted for the same length of time as frequently as possible to minimize any variation in the results. The resultant loads for the 500 lbs/min tests had a mean load of 8,415 lbs (37.4 kN) and a standard deviation of 2,442 lbs (10.9 kN). Figure 5.1 shows the average loads for each tire under the 500 lbs/min loading along with the quartile ranges.

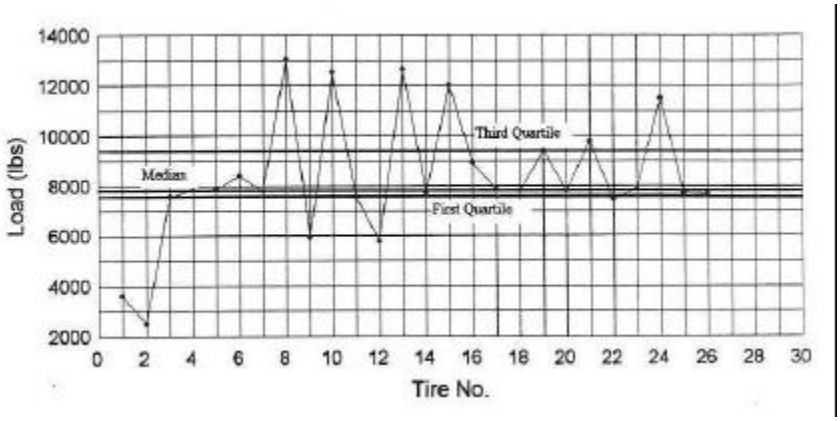

FIGURE 5.1 Average Peak Loads for Each Tire Under 500 lbs/min Loading

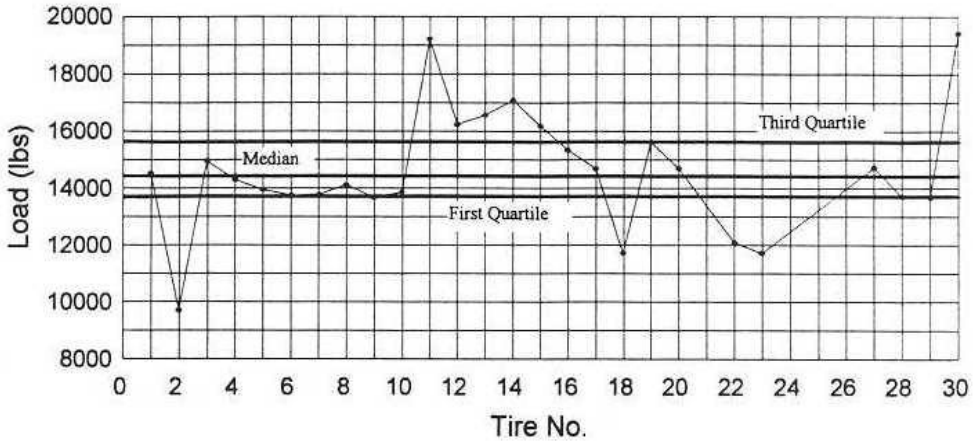

FIGURE 5.2 Average Peak Loads for Each Tire Under 2,500 lbs/min Loading

It is to be noted that there are five outliers, two lower and three upper or higher outliers presumably due to the variabilities of the used tires studied. The 2,500 lbs/min tests had an average load of 14,786 lbs (65.8 kN) and a standard deviation of 2,236 lbs (9.95 kN). Figure 5.2 shows the average loads for each tire for these tests. For this set of tests there were fewer outliers, there is one lower and two upper outliers.

The tires proved to be extremely durable. After the first compression test, the tires rebounded to an average 97% of their original width and after the second test, rebounded to an average 99.6% of their previous width. The peak loads for the tires also support their durability. Loads from the first to the second test decreased by approximately two percent while loads from second to third tests decreased by less than two percent. To summarize, tires nearly returned to their original shape and retained most of their strength after multiple

horizontal compression tests.

The shape of the load-deflection curve for the horizontal state tests shows that these two parameters have an exponential relationship (Figure 5.3). This is desirable, but not optimal. According to Sicking (1997), an optimal design would be characterized by the cushion=s ability to deflect (or crush) reasonable distances while experiencing several small increases in load (see Figure 5.4). The problem with the exponential curve is that while initially the cushion (or tire in this case) experiences a large degree of deflection compared to increase in load, this relationship is eventually reversed, load increases rapidly while deflection is small. In terms of a crash cushion, this would cause a vehicle striking the crash cushion to experience high decelerations during the final phase of stopping the vehicle. While this does not prohibit the use of tires in a crash cushion, it is an important factor which must be considered when designing a crash cushion with tires. A crash cushion should be designed so that only the flat or horizontal portion of the curve is used.

Tires subjected to vertical compression testing had a similar load-deflection relationship. Peak loads for tires in vertical compression testing were only slightly lower than they were for horizontal testing. The most important difference is that tires in vertical compression (again, in compression along their longitudinal axes) experienced greater deflections. Therefore, in terms of crash cushion design, this would allow the impacting vehicle to decelerate over a greater distance before reaching the point where the load-deflection curve turns upward sharply. From this standpoint it seems that a crash cushion

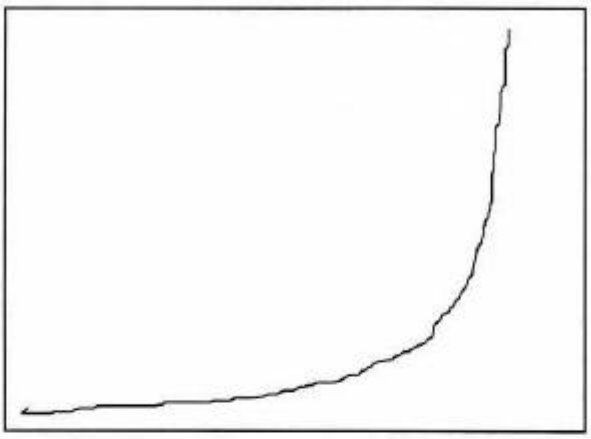

FIGURE 5.3 Typical Load-Deflection Curve for Static Tire

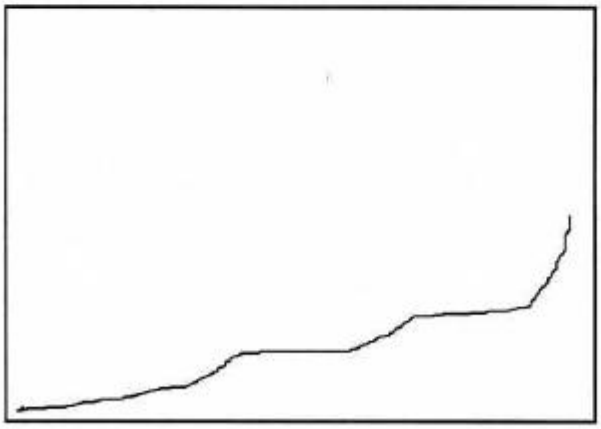

FIGURE 5.4 Ideal Load-Deflection Curve for Crash Cushions (after Sicking 1997)

design would favor tires oriented for compression on their long axes over tires oriented for sidewall compression. However, there was one problem with the vertical compression tests Tires in vertical compression were subject to loads over five minutes in duration and were compressed until they were three to four inches thick as shown in Figure 5.5. This produced a large amount of strain on the tire causing it to tear in places which were bent or folded. Since this occurred on all five tires tested in this manner, the vertical compression tests were discontinued. It is reasonable to conclude that tires during impact loading would not be subjected to the same type of compressive force and that they would have more freedom to move or rebound, in essence, preventing or reducing the likelihood of this type of damage from occurring. This hypothesis is supported by the research conducted by Marquis et al. (1975) on the tire-sand inertial barrier. In that study, the tires were struck by a vehicle along their longitudinal axis and all tires were reusable.

The tire-derived pads proved to be equally durable under static testing. Furthermore, the fine and coarse samples exhibited almost no reduction in their peak loads after three tests while the composite sample exhibited a six percent reduction of peak loading capacity from first to third loadings. The loads sustained by the individual pads were about seven times greater than that of the tires under the same loading rate of 2,500 lbs/min and were over 13 times greater at their tested loading rate of 60,000 lbs/min. Figure 5.6 shows the resultant loads of three different samples for each type of pad.

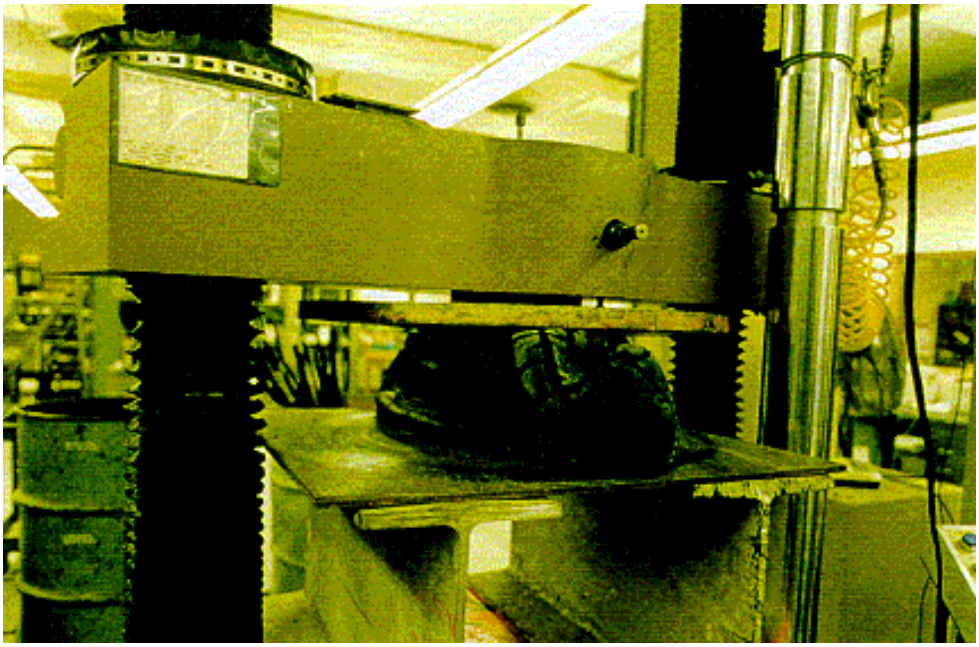

FIGURE 5.5 Static Test with Tire in Vertical Compression

The load-deflection curves for the pads followed the basic exponential curve that the tires did with the primary differences being that the loads were much greater and the deflections were much smaller. The reason for this significant difference is that when a tire is crushed in either direction, part of the deflection is due to collapsing the tire during which time the load increases very gradually. However, since the tire-derived pads are solid there are no "void" spaces, which would allow the material to undergo large deflections while only gradually increasing the load. As a result the pads have a much greater load per unit length. In terms of crash cushion performance, the tire-derived pads would cause a striking vehicle to come to an abrupt stop as if it had struck a wall. Therefore, use of these materials in a crash cushion must include "void" space

that would increase the deflection of the material upon impact so as to cause decelerations within tolerable limits. This will be discussed further later in this chapter.

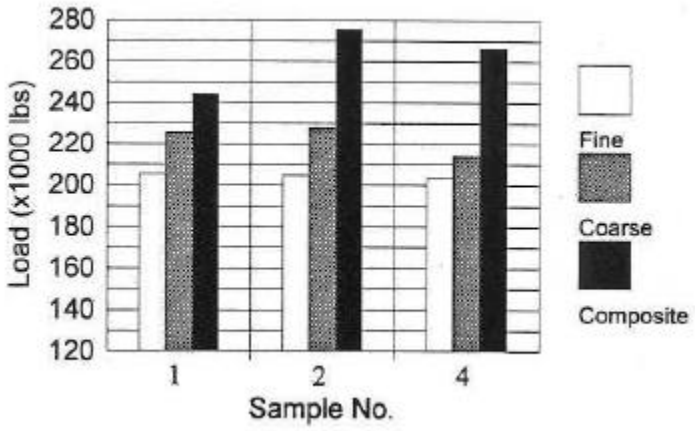

FIGURE 5.6 Peak Loads for Pads for 60,000 lb/min Static Tests

Although all the pads had higher loads than the tires, there were also significant differences among the pads. The fine pad carried much higher loads per unit length when compared to the coarse and composite samples (see Appendix B for sample load-deflection curves). The most important difference between the whole tire dynamic tests and the pad dynamic tests is the work done in crushing the pads. The work done in crushing the pads was much lower than that of the whole tires..

The output for the dynamic tests on the tires was a load-deflection curve showing both the loading and unloading phases of the test. This allowed the area under the loading and unloading curves, or work, to be compared to each other in the form of a tire rebound/tire crush (R/C) ratio. R/C ratios for the 10 tires tested ranged from 0.37 to 0.57 with one extreme outlier at 0.74 (Figure 5.9). Therefore, when a tire is crushed to a certain degree, about half of the energy that was used to crush it is regained as the tire returns to its original shape. While these values are not extremely high, they are high enough that the possibility of a tire crash cushion pushing a striking vehicle back into traffic should be considered.

The work done in crushing the tires for the 5,000 lb (22.3 kN) loads ranged from 476 ft-lbs (645 joules) to 738 ft-lbs (1,000 joules). Figure 5.10 shows the work done in crushing the tire for each test. The higher loads produced higher deflections which increased the area under the load-deflection curve and thus, resulted in more work.

Table 5.1 Tire and Pad Dynamic Test Comparison[1]

	Deflection (in.)	Work (ft-lbs)	R/C Ratio
Tire	4.07	603	0.46
Fine Pad	0.28	49.4	0.63
Coarse Pad	0.70	118	0.61
Composite Pad	1.24	193	0.54

[1] Test data for load of 5000 lbs (22.3 kN) and frequency of 0.1 Hz

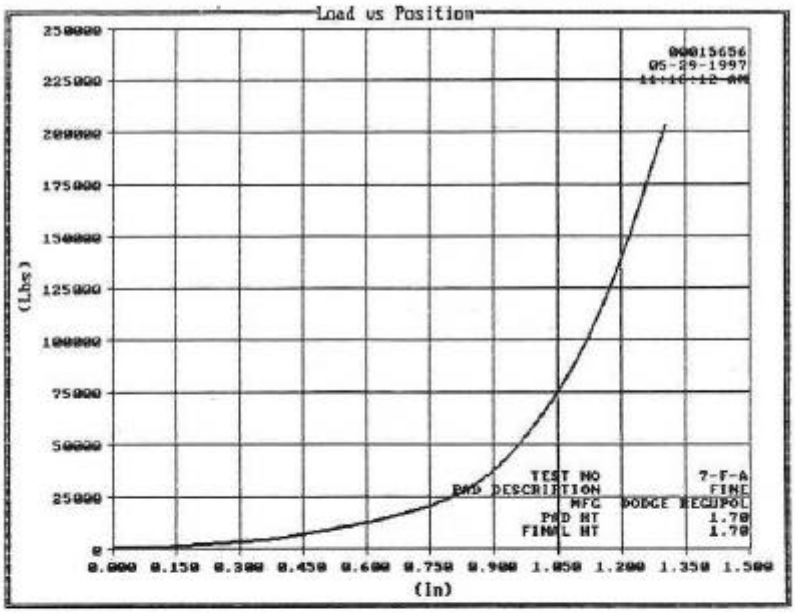

FIGURE 5.7 Static Test Load-Deflection Curve for Coarse Pad

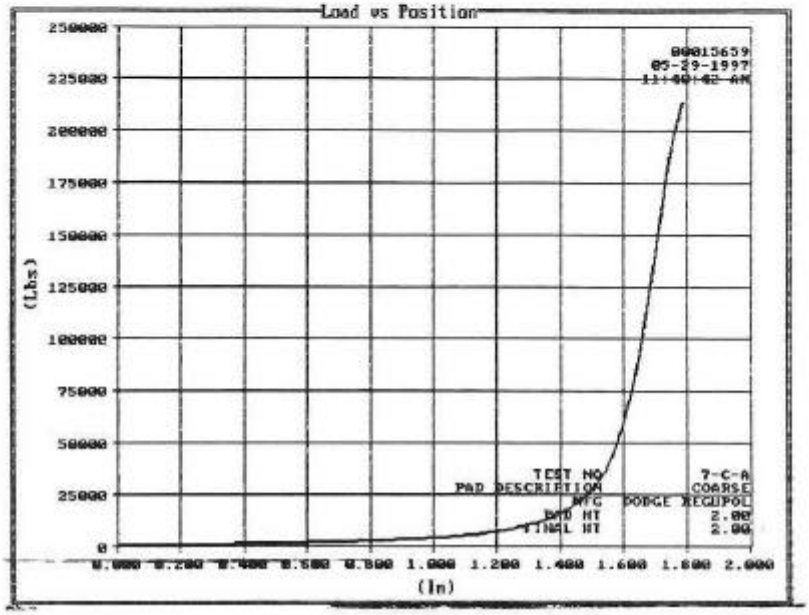

FIGURE 5.8 Static Test Load-Deflection Curve for Coarse Pad

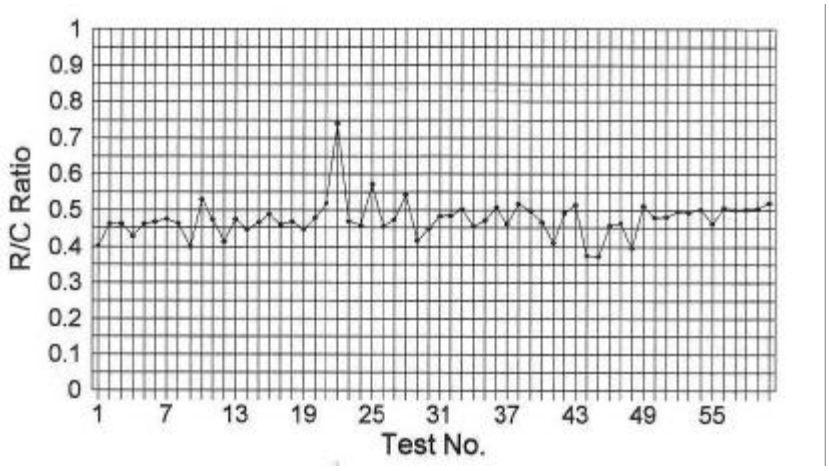

FIGURE 5.9 Rebound/Crush Ratios for Tires

R/C ratios for the tire-derived pads ranged from 0.48 to 0.63 (Figure 5.11). This was generally higher than the R/C ratios for the whole tires which is an undesirable characteristic. The pads were significantly most important difference between the whole tire dynamic tests and the pad dynamic tests is the work done in crushing the pads. (The work done in crushing the ower than that of the tires.) This is because of the fact that for the specified loads, the sample pads experienced much smaller deflections. Table 5.1 compares the differences in the deflections and the work between the whole tires and the pads. Since the loads for the specific tests were the same, the difference in the work done is due only to the deflection. The area under the load-deflection curve for the pads was smaller because they deflected less under the same load. This property was especially evident in the fine pad which resulted in peak work values of 49.4 ft-lbs (67.0 joules) and 44.9 ft-lbs (60.9 joules). This characteristic reaffirms the fact that the tire-derived pads would be unsuitable for use in a crash cushion in any solid form. To make them practical,

"void" space must be added which would allow the material to deflect more as they take on greater loads, thus resulting in smaller vehicle decelerations when impacted by a vehicle.

Figures 5.12 and 5.13 summarize the results of the dynamic tests conducted on the pads. Note that for changes in load, the resulting changes in deflection and work are significant, whereas, for the changes in frequency, the resulting changes in deflection and work appear insignificant. Also, the composite sample had the highest deflection and work, much as it had the highest peak load for the static tests. In fact, the order of magnitude for the test results of the dynamic tests seems to parallel the results of the static tests. This observation strongly suggests that the output for the static and dynamic tests is influenced by a common factor. This factor appears to be thickness. It seems that as the thickness of the pad increases, the magnitude of the output, whether it is peak load or work, also increases. This relationship will be discussed in more detail in the next section.

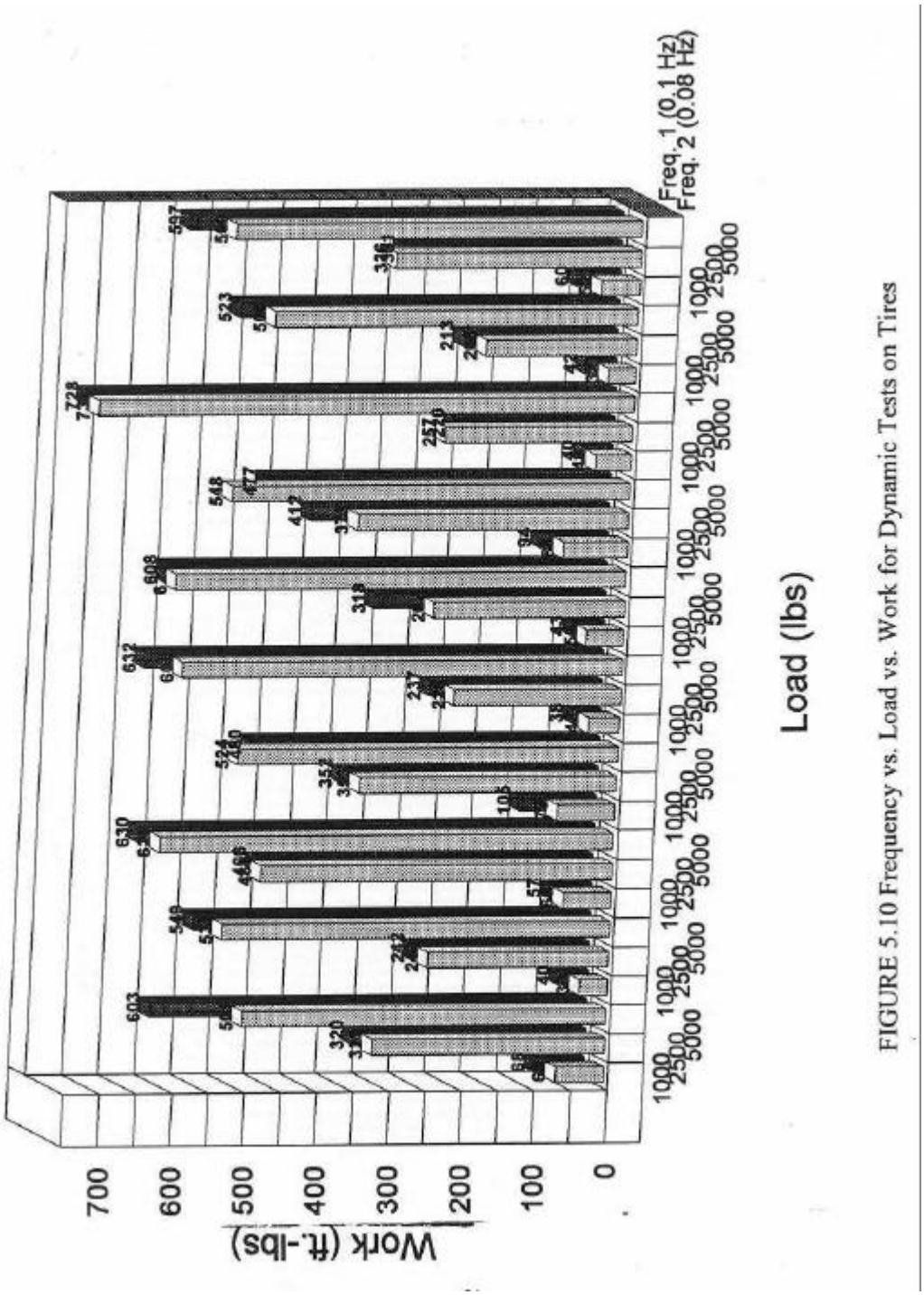

FIGURE 5.10 Frequency vs. Load vs. Work for Dynamic Tests on Tires

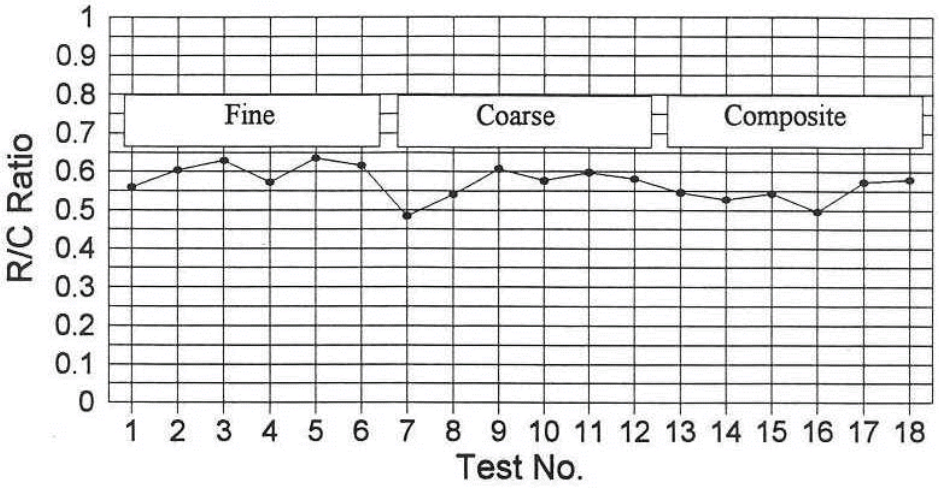

FIGURE 5.11 Rebound/Crush Ratios for Tire-Derived Pads

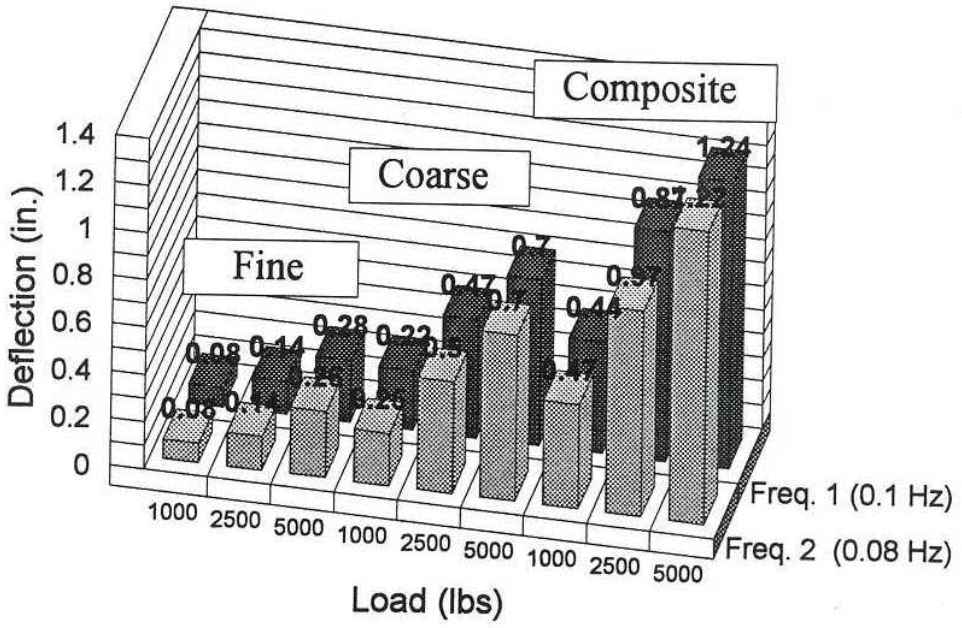

FIGURE 5.12 Frequency vs. Load vs. Deflection for Dynamic Tests on Tire-Derived Pads

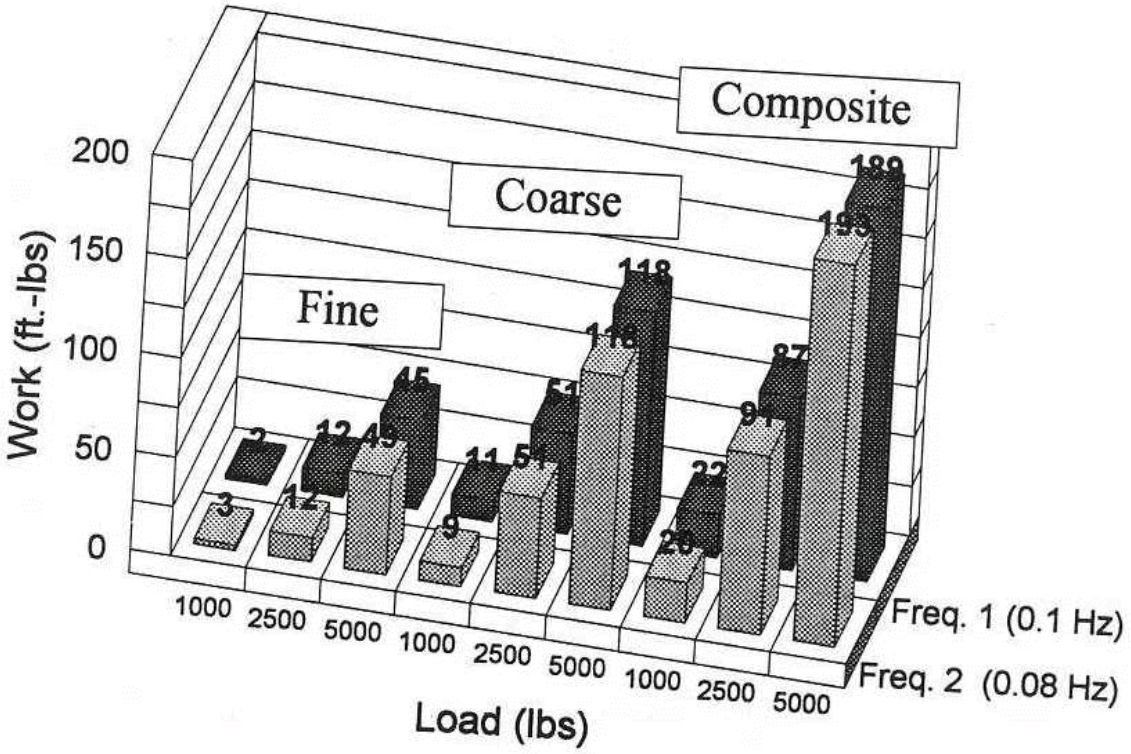

FIGURE 5.13 Frequency vs. Load vs. Work for Dynamic Tests on Tire-Derived Pads

5.2 Statistical Analysis

The results of a correlation analysis of the characteristics of each tire and the resultant peak load during horizontal static tests are tabulated in Table 5.2. From these calculations, it can be concluded that there is little correlation between a tire=s weight, area, deflection at peak load, or resultant peak load. In other words, the weight and area of a tire are not linearly related to deflection or peak load and are poor predictors of the load-deflection relationship. Deflection and load may be related to some other characteristic of the tire, such as chord strength, cross-sectional area, or age of the tire. Although a linear relationship does not exist between any of the parameters under consideration, several basic trends can be identified, but with very little confidence. For example, the heavier the tire, the less it deflects, but the more load it can take.

Table 5.2 Correlation Coefficients and p-values of Tire Properties

	Tire	Weight	Area	Deflection	Load
Tire	1.000 0.0	-0.0367 0.847	-0.2366 0.208	0.2352 0.211	0.1087 0.597
Weight		1.000 0.0	0.1541 0.416	-0.1170 0.538	0.2729 0.178
Area			1.000 0.0	0.1531 0.419	-0.4181 0.0335
Deflection				1.000 0.0	-0.1545 0.451
Load					1.000 0.0

A relationship can be drawn between the number of tires in horizontal static compression and the peak load and likewise, the total deflection due to static compression and the peak load. The equation for the relationship between the number of tires and the resultant peak static load is as follows:

$P=12{,}437+891t^3$ ($R^2 = 0.951$, MSE = 6,670 lbs)

where

P = peak static load (lbs) and

t = number of tires.

Figure 5.14 shows the plot of this equation along with the observed values used to develop the equation. This equation can be used to predict the peak load for any number of tires. Appendix C shows the peak load values predicted by the equation along with the 95% confidence interval on the mean (the range of where the mean of all observations would lie) and on the predicted value (the range of where the next observation may lie).

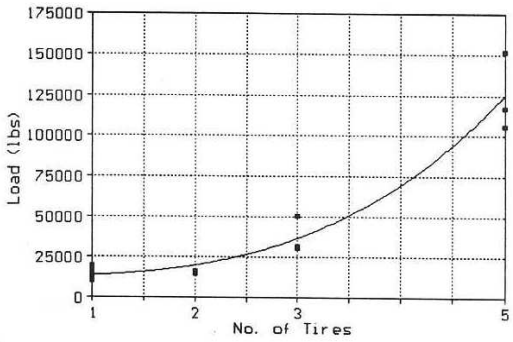

FIGURE 5.14 Number of Tires vs. Peak Load Curve for Static Tire Tests

Another useful and very similar relationship which can be modeled is the relationship between peak load and deflection as shown in Equation (5.2). Peak load and deflection cubed have a very high correlation coefficient (0.98) with a very high level of significance indicating that they would be easy to model. The equation for this relationship is:

$$P = 13{,}333 + 3.93d^3 \qquad (R^2 = 0.961, \text{MSE} = 6.048 \text{ lbs})$$

where

P = peak loads (lbs) and

d = deflection or distance compressed (in.)

A plot of Equation (5.2) along with the observed values can be found in Figure 5.15. This model is especially useful since for any given peak load and deflection the curve can be predicted fairly accurately, which is important in developing a crash cushion. The major disadvantage of this model is that it is only good for a load rate of 2,500 lb/min which makes it difficult to correlate with impact loading. These issues will be discussed further later. Appendix C contains the SAS output specifying the details of this model.

An analysis of variance of the dynamic tire tests revealed that the interaction between load and frequency was not significant in determining the deflection or work done in crushing the tires, the analysis for each yielding p-values of 0.7492 and 0.9867, respectively. In addition, the frequency was found to be not significant, resulting in a p-value of 0.7215 for deflection and 0.8328 for work. Only the tires and load were significant in determining the deflection and the work done. This seems reasonable since the differences caused by the tires can be attributed to

the random variation among the tires and the differences caused by the loads can be explained by the increased area under the curve (more work) for higher loads.

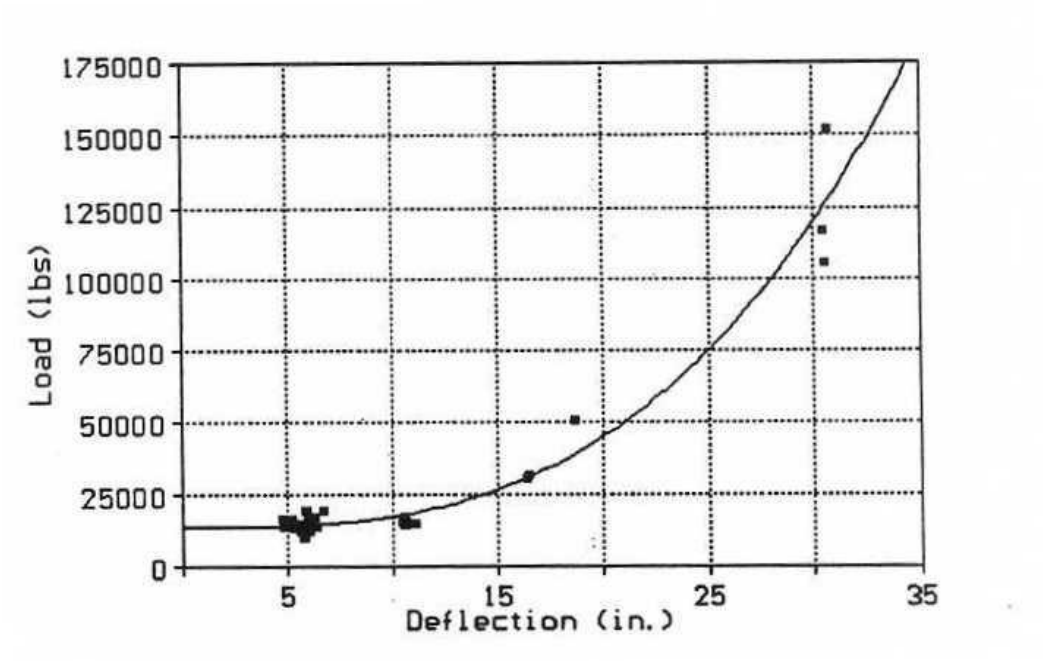

FIGURE 5.15 Deflection vs. Peak Load Curve for Static Tire Tests

The relationship between the loading rate and the peak load was explored further with the tire-derived pads. Analysis of this relationship using SAS revealed that all models of peak load versus loading rate for each type of sample had a common intercept, but the composite sample had a much steeper slope than the fine and coarse samples. This is probably due to its greater thickness since this is the only factor that is different from the other two samples.

The relationship between peak load and loading rate for each type of sample is shown below:

Fine Pad:

P=146650 + 946.2r (R^2 = 0.9446, MSE = 6034 lbs)

Course Pad:

P = 143810+ 1170 r (R^2 = 0.9745, MSE = 4988 lbs)

Composite:

P = 1315610 + 2143r (R^2 = 0.9942, MSE = 4308 lbs)

where

P = peak load (lbs) and

r= loading rate (lbs/min).

Figure 5.16 shows the plots of the relationships described. These plots show that higher loading rates produced higher peak loads in the tire-derived pads much as it did with the whole tires.

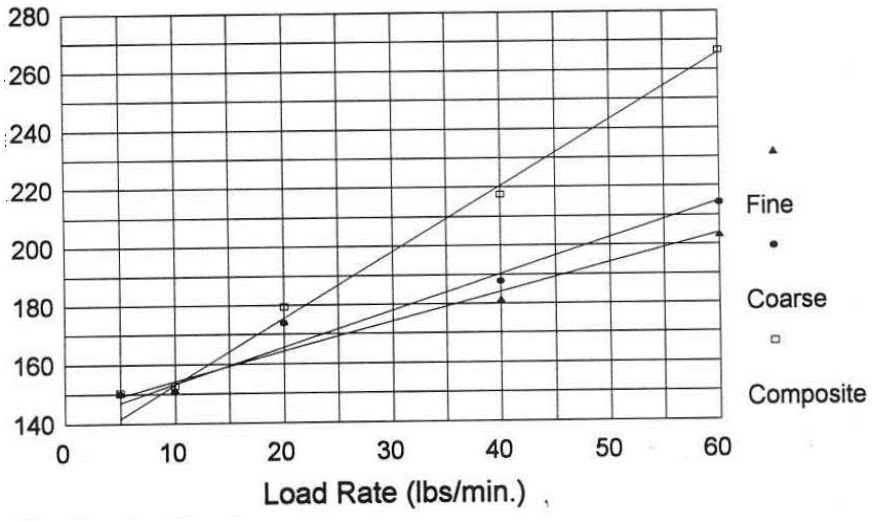

FIGURE 5.16 Load vs. Load Rate Data with Predicted Relationships for Tire-Derived Pads

As already discussed, whole tires were tested at a loading rate of 2,500 lbs/min which is at the lower end of the graph in Figure 5.16 and the tire-derived pads were tested at a loading rate of 60,000 lbs/min which is at the higher end of the graph. Therefore, whole tire tests will yield lower peak loads per unit deflection when compared to the tests conducted on the pads. The difficulty in having peak load so dependent upon loading rate is that it makes selection of a loading rate to conduct the tests at a critical factor.

Therefore, since 60,000 lbs/min loading rate seemed to best approximate impact loading, this was used to conduct the pad tests. The relationship developed between peak load and loading rate can be used to make inferences on the whole tire tests.

An equation can be developed to show the relationship between deflection and peak loads by pad type. The equations may be expressed as follows:

Fine:

$P = 149192 + 42980d$ ($R^2 = 0.9949$, MSE + 7,261 lbs)

Coarse:

$P= 185464 + 18922d$ ($R^2 = 0.8580$, MSE = 6,275 lbs)

Composite:

$P = 214186+15957d$ ($R^2 = 0.8205$, MSE = 10,713 lbs)

Single Line for all pads:

$P = 174413 + 27844d$ ($R^2 = 0.8022$,MSE = 17,208 lbs)

where P = peak load (lbs) and

d = deflection or height compressed (in.).

Figure 5.17 shows a plot of the equations for each type of pad along with the recorded observations. A notable trend can be seen on the load-deflection curve in Figure 5.17 and from Equation (5.9). Although the pads can be modeled more accurately when modeled by type, an equation for all pads can represent this relationship with a fair degree of accuracy. This relationship is made clearer by inspection of the data points and supports hypothesis made earlier in this report: the thickness of the pad has an effect on the peak load. The fact that these points can be modeled by one line shows that although the composite pad had the highest peak loads this can be accounted for by its greater thickness.

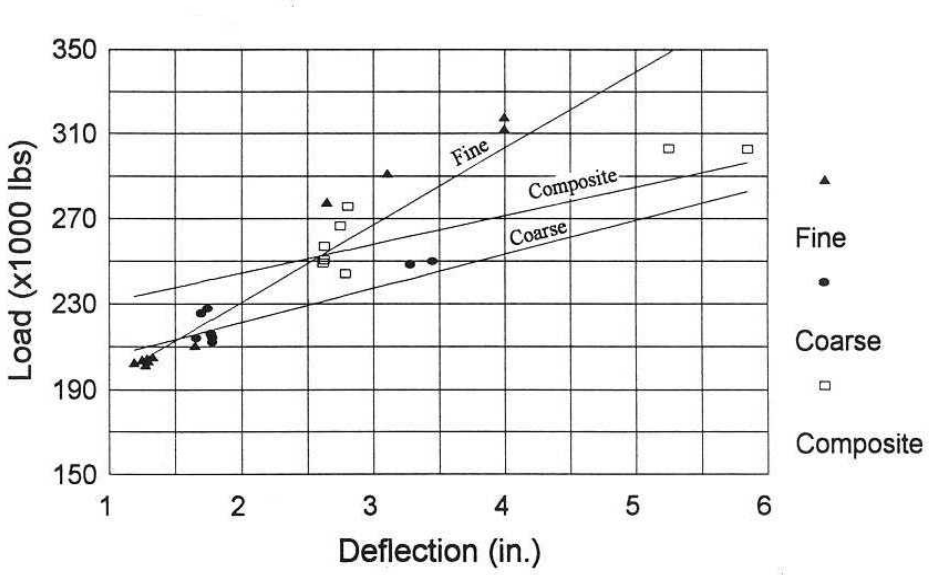

FIGURE 5.17 Load vs. Deflection Data and Lines for Tire-Derived Pads

An analysis of variance of the dynamic pad tests revealed the same basic conclusions found for the whole tires. First, interaction between the load and the frequency was not significant in determining deflection or work, and frequency, by itself, was not significant. Only load and pad type were found to be significant. This is reaffirmed by the study of the load versus deflection curves (see Appendix B).

5.3 Crash Cushion Design

There are several approaches which can be taken in designing a crash cushion as mentioned earlier in this report. The most useful method for many crash cushions with a fixed, rigid support is the design based on both the conservation of energy and the conservation of momentum. First, however, certain design criteria and guidelines must be established and defined. Crash cushion performance standards are published in NCHRP 350 (Ross et al. 1993). Table 5.3 lists the standard test vehicle types, the required mass for each (with the value converted to pounds for purposes of calculation), the required impact speed for each test, and the calculated energy for that given test. The 2000P pickup truck test vehicle impacting the crash cushion head-on at a speed of 62 mph (100 km/h) will be used as the design vehicle for a crash cushion. This is the highest energy test set by NCHRP 350 for head-on impacts. Guidelines for conducting tests with the 8000S, 36000V, and 36000T vehicles are established only if a higher performance crash cushion is desired. The 2000P pickup truck is usually the standard test vehicle (Ross et al. 1993).

Table 5.3 NCHRP 350 Test Requirements and Resulting Energy

Vehicle Type	Max. Weight (kg)	(Lbs)	Impact Speed (km/h)	Impact Speed (mph)	Energy (ft/lbs)	Energy (Joules)
700C Small Car	800	1764	100	62	226,330	306,900
820C Small Car	920	2028	100	62	260,200	352,830
2000P Pickup Truck	2200	4508	100	62	578,400	784,310
8000S Single-Unit Van Truck	8200	18080				
36000V Tractor/van Trailer	26500	80470				
36000T Tractor /Tank Trailer	26500	80470				

Since used tires are not uniform, the data in Table 3.1 describing the average characteristics of the tires will be needed to describe the average tire used in designing the crash cushion. The average work done in crushing the tires for the 5000 lb (22.3 kN) tests is 579.28 ft-lbs (785.5 joules) with a standard deviation of 73.3 ft-lbs (99.4 joules).

Another requirement which must be established is the minimum length of a crash cushion to ensure that the deceleration forces experienced by the occupant is within prescribed tolerances. Marquis and Hirsch (1975) used an average deceleration force of six g=s based on Federal Highway Administration (FHWA) guidelines. This is well below half of the preferred maximum deceleration of 15 g=s as established by NCHRP 350 (Ross et al. 1993).

Recalling the following equations of acceleration and acceleration in g=s, a relationship for finding the minimum deceleration distance can be found: $G = a/g$

$$a_{avg} = \frac{v_i^2 - v_f^2}{2d}$$

$$G = \frac{v_i^2 - v_f^2}{2gd}$$

$$d = \frac{v_i^2 - v_f^2}{2gG}$$

Converting mph to ft/s yields 62 mph (1.47) = 90.9 ft/s and replacing in the above equation gives us:

$$d = \frac{(90.9)^2 - (0)^2}{2(32.2)6} = 21.38\,ft$$

Converting mph to ft/s yields 62 mph (1.47) = 90.9 ft/s and replacing in the above equation gives us:

$$d \quad \frac{(90.9)^2 \quad (0)^2}{2(32.2)6} \quad 21.38ft$$

This number represents the deformation length, therefore, the actual length of the crash cushion must be greater than this length. Assuming that the crash cushion deforms 75% of its total length as was found during static testing, we will have a total crash cushion length of 28.5ft (8.69 m).

Since the weight and speed of the test vehicle for the crash cushion developed by Marquis and Hirsch (1975) are almost the same as our test vehicle, their test can be used to check and calibrate the data collected for this study using the principles of the conservation of energy and the conservation of momentum.

The number of tires in the Marquis and Hirsch (1975) cushion can be verified as follows:

29.67 ft = 356 in.

$$\frac{356}{7.24} = 49.17 or 50 \text{ tires long}$$

50(5 tires/module) = 250 tires in whole crash cushion

Therefore, the mass of the crash cushion is:

$$m = \frac{w}{g} = \frac{(15.8)(250)}{32.2} = 122.7 slugs$$

The kinetic energy absorbed by the crash cushion as predicted by dynamic testing is:

$$KE_c = (250)(579.28) = 144{,}820\, ft - lbs$$

The reduction in speed of the vehicle due to momentum transfer can be found as follows:

$$v_f = \frac{v_{n-1} m_v}{m_v + m_n} = \frac{(90.0)(140)}{(140 + 122.7)} = 48.4\, ft/s$$

The kinetic energy required to stop the vehicle can be found by:

$$KE_i - KE_f = KE_c$$

$$\frac{1}{2} m v_i^2 - \frac{1}{2} m v_f^2 = KE_c$$

$$KE_c = \frac{1}{2}(140)(48.4)^2 - \frac{1}{2}(140)(0)^2 = 164{,}250\, ft - lbs$$

By using the energy data collected for the dynamic tests, it is clear that the kinetic energy absorbed by the crash cushion is 19,430 ft-lbs greater than that determined by dynamic testing. This equates

to an additional 77.7 ft-lbs of energy absorbed per tire which is just outside of the standard deviation for the observed values. This agrees with what was suspected earlier. The work resulting from the 5,000 lb dynamic loads was low because 5,000 lbs was not enough load to adequately compress the tire. This can be confirmed graphically on the load versus deflection curve. The maximum dynamic load of 5,000 lbs was selected based on the limitations of the testing machine.

From these observations and calculations, we can find the adjusted average for work required to crush a tire as follows:

579.28 + 77.7 = 657 ft-lbs

This value can be used in developing prototype crash cushions. One possible useful design would be a tire crash cushion that is narrower than the Marquis and Hirsch design. A crash cushion with a three-tire form (Figure 5.18, item a) would be able to be used in narrower locations. By designing the crash cushion on the principles of conservation of energy and conservation of momentum as was done for the calibrated cushion, we should have a crash cushion with the same or greater number of tires to adequately stop the design vehicle. This would require that the crash cushion contain the following number of tires:

250/3 = 83.3 tires or 84(3) = 252 total tires or be

84(7.24) = 608.2 in. = 50.7 ft (15.46 m) in length.

The performance of this crash cushion can be checked by performing the following calculations:

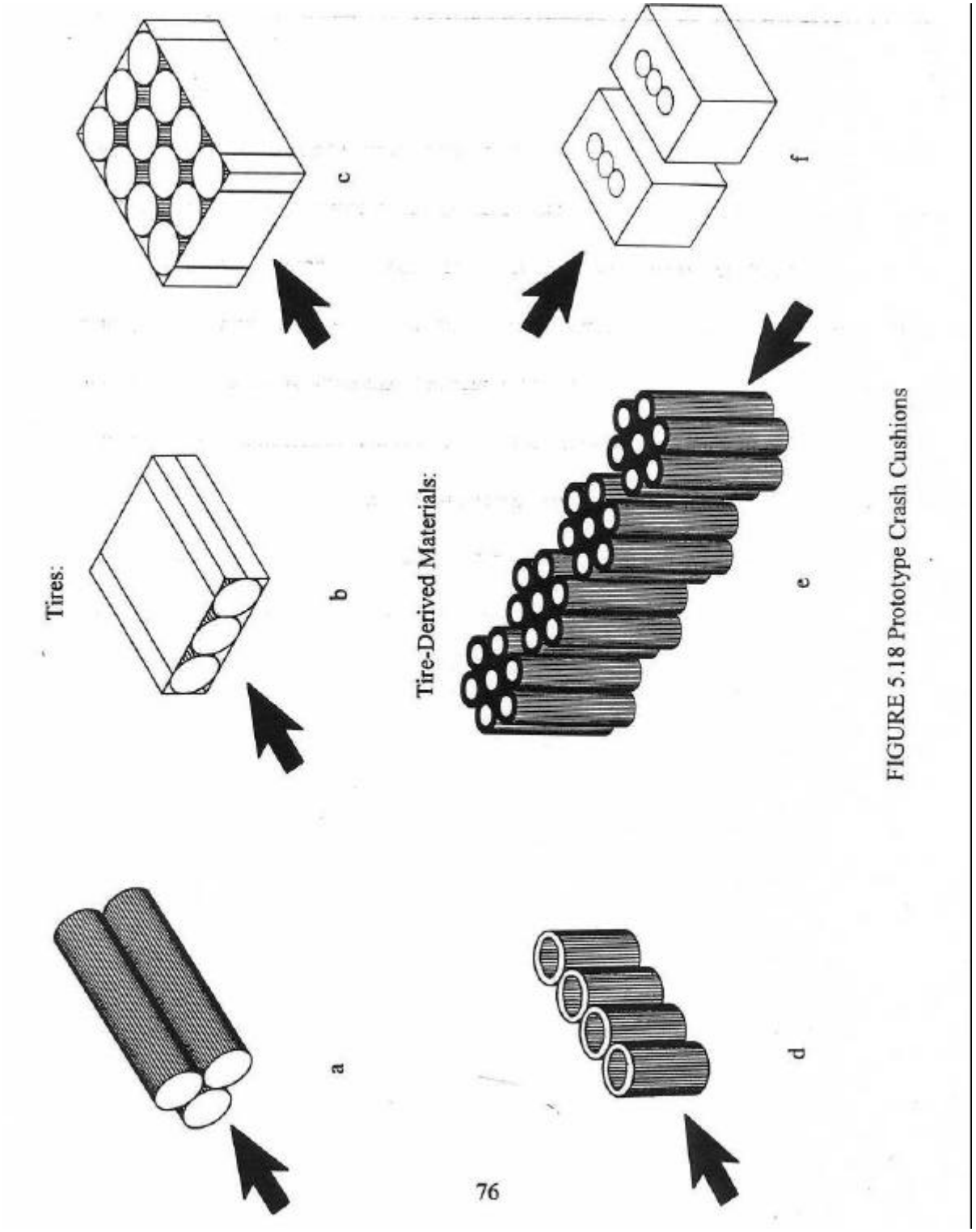

FIGURE 5.18 Prototype Crash Cushions

m = w/g = (252)(15.8)/32.2 = 124 slugs

KE = (252)(657) = 165.564 ft-lbs

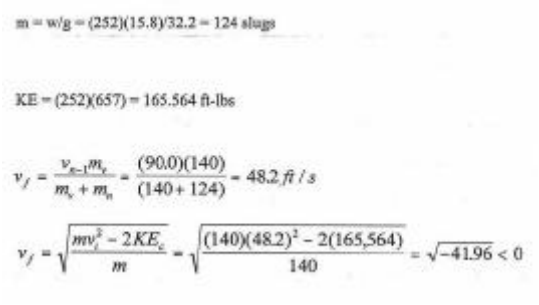

Therefore, the crash cushion will stop the vehicle.

The collision mechanics of a TMA are more complicated than that of a stationary crash cushion. However, if several assumptions are made, a TMA made from used tires can also be designed using the principles of the conservation of energy and the conservation of momentum. First, however, the design criteria need to be established. Most TMAs are designed for a capacity of 305,000 ft-lbs instead of the 578,397 ft-lbs used for a fixed, stationary crash cushion (Michie and Bronstad 1992). This is equivalent to the 2000P pickup truck traveling at an impact speed of 66 ft/s or 45 mph (72 km/h).

The protective vehicle carrying the TMA also helps “cushion”the impact of an errant vehicle by rolling forward. Therefore, the TMA does not typically absorb all of the energy in a collision nor is it intended to do so. If the roll-ahead distance is known, then the velocity of the protective vehicle and the impacting vehicle, which will be assumed to move off together in the

same direction and at the same velocity after impact, can be found. To determine this we will also have to assume a drag factor for the truck. Michie uses a drag factor of 0.30 for calculating roll-ahead distance (Michie and Bronstad 1992). This value is obtained when the truck is in gear and there is only partial braking. Assuming a roll-ahead distance of 25 ft, the velocity after impact can be found as follows:

$$a = fg = (0.30)(32.2) = -9.66 \text{ ft/s}^2$$

$$v_i = \sqrt{v_e^2 - 2ad} = \sqrt{0^2 - 2(-9.66)(25)} = 22.0\, ft/s$$

Therefore, the truck and the impacting vehicle can be moving together at a velocity of 22.0/1.47 = 15 mph. From this point on the problem becomes more complicated. The interaction between the energy dissipating characteristics of the truck and the TMA are quite complex. However, the conservation of kinetic energy and the conservation of momentum principles will be used to make a judgement as to whether a TMA design will work. Figure 5.18, item b depicts a used-tire crash cushion which will be used in this analysis. The crash cushion is three tires in width and 25 ft long. Performing the same methodology as before we arrive at a final velocity of 30 ft/s for the design vehicle. Whereas this does not meet the 22.0 ft/s requirement, it is feasible that the additional energy will be dissipated through the TMA. This design merits further testing.

Another design which should be considered is the TMA depicted in Figure 5.18, item c.

This TMA uses tires in compression along their longitudinal axes. The disadvantage of used tire TMAs is that the weights are excessive and may make the crash cushion impractical.

As already discussed, the tire-derived pads proved to have load per unit length values too high for use in a crash cushion. If this material is to be used in a crash cushion, collapsible spaces need to be added. Figure 5.18 items d, e, and f show some possible designs which would allow greater deflections of the tire-derived material. Item d (the cylinder) would be the most efficient, that is, would provide the greatest force per unit pound of material (Sicking and Ross 1985). This shape, however, would probably not work for the tire-derived material tested in this study. The cylinder, when compressed laterally, would experience a high amount of tension around it's circumference. The tire-derived material in this study, while strong in compression, would probably not be able to withstand the tension forces caused by a significant impact. Therefore, a more rigid design like items e and f may be in order.

Chapter 6

CONCLUSIONS

6.1 Overview

In this study static and dynamic tests were conducted on used tires and recycled tire-derived materials to determine whether these materials could be used in a low cost, low-maintenance crash cushion. The load versus deflection characteristics, peak loads, energy absorbed in compression (or crushing) were observed and recorded to make this determination. Also correlation analyses, regression analyses, and analyses of variance were conducted on data collected to better understand the behavior of the materials. The following conclusions and recommendations were made based on the data collected, statistical analysis, and the review of previous studies, analyses, regression analyses, and analyses of variance were conducted on data collected to better understand the behavior of the materials.

6.2 Conclusions

Both used tires and tire-derived pads are durable materials which retain most of their load-absorbing capacity and retain their shape after successive loading. In addition, they are fairly inexpensive and the raw materials (used tires) are readily available. These properties make them good candidates for use in a low-cost, low-maintenance crash cushion. However, the tires and the tire-derived pads exhibited properties which merit special attention or were deemed to be unacceptable for use in a crash cushion. These properties are:

- R/C ratios for the tires and the tire derived pads were fairly high, each having an average value of 0.48 and 0.57, respectively. By themselves these values are not high enough to preclude either material from being used in a crash cushion, but do alert us to the possibility of excessive vehicle rebound for which special design considerations must be made.
- The load-deflection curve for the tires and the tire-derived samples resembles an exponential curve. Although this is not an ideal relationship it can be effective if incorporated properly into the design of a crash cushion. Only the horizontal portion of the curve should be used when considering the deflection or distance of crush for a crash. A crash cushion that deflects beyond the horizontal portion of the load deflection curve will cause excessive decelerations to an impacting vehicle.
- The tire-derived pads had excessively high loads per unit deflection. This characteristic does prohibit the use of pads in a crash cushion. This material could possibly be used in a crash cushion if "voids" were added to make the material more "crush able" or allow it to deflect more under loading. Several possible designs that would allow this to occur were presented. The problem that may be encountered in developing a crash cushion component from the pad material is the material's inability to take very high tension loads.

Considering the factors mentioned above, used tires in horizontal compression make

effective low-cost, reusable crash cushions. This study determined that approximately 657 ft-lbs (891 joules) of energy is needed to crush a typical automobile tire. This value can be used to design many different types of crash cushions including TMAs. The limiting factors for a tire crash cushion or TMA is the excessive number of tires required (or, size of the crash cushion) and the resulting heavy weight.

Tires in vertical compression may also make effective crash cushions. The peak load for tires crushed vertically is very close to the values recorded during horizontal compression. In addition, the load would be distributed over a greater distance which would result in lower deceleration rates for an impacting vehicle. Tires did, however, deform permanently and showed significant damage when statically tested in this manner. This damage would not be expected under impact testing.

6.3 Recommendations

The environmental effects on the tire-derived blocks should be studied in detail. Impact tests should be conducted on tires in both the horizontal and vertical orientation as well as on the proposed shapes for the tire-derived materials. This would yield values for the energy required to crush each material and could be used to design a crash cushion by the principles of conservation of energy and conservation of momentum. Full-scale prototypes of the crash cushions should then be constructed and tested for compliance with the NCHRP Report 350 guidelines.

REFERENCES

American Association of State Highway and Transportation Officials, Roadside Design Guide, Washington, D.C., 1996.

Bligh, Roger P., Dean C. Alberson, and Barbara G. Butler, ?Applications of Recycled Materials in Roadside Safety Devices,? Research Report 1458-1, Texas Transportation Institute, Texas A&M University, June 1995.

Carney, John F. III and Monzer I. Faramawl, ?Reusable Impact Attenuation Devices,? Proc., American Society of Civil Engineers IV Symposium on Crash Worthiness and Occupant Protection in Transportation Systems, AMD-Vol. 210/BED-Vol. 30, pp. 161-177, 1995.

Carney, John F. III, ?Development of Maintenance-Free Highway Safety Appurtenances,? Strategic Highway Research Program, National Research Council, Washington, D.C., 1993.

Carney, John F. III, ?Reusable Truck Mounted Attenuater,? Washington State Department of Transportation, Report WA-RD 438.1, June 1997.

Carney, John F., ?Performance and Operational Experience of Crash Cushions,? NHCRP Synthesis 205, Washington, D.C.: Transportation Research Board, National Research Council, 1994.

Epps, Jon A., ?Uses of Recycled Rubber Tires in Highways,? NCHRP Synthesis 198, Transportation Research Board, National Research Council, Washington, D.C., 1994.

Fricke, Lynn B., Traffic Accident Reconstruction, Northeastern University Traffic Institute, 1990.

Griffin, Lindsay I., ?How Effective are Crash Cushions in Reducing Deaths and Injuries?? Public Roads, Vol. 47, No. 4, March 1984, pp. 132-134.

Kircher, James R., ?Impact Attenuators: A National Survey - Part I,? Public Works, Vol. 116, No. 12, December 1985, pp 34-39.

Marquis, E.L. and T.J. Hirsch, ?Development of Impact Attenuators Utilizing Waste Materials: Phase I Used-Tire Crash Cushion,? Report No. 846-1, Texas Transportation Institute, Texas A&M University, October 1973.

Marquis, E.L., T.J. Hirsch and J.F. Nixon, ?Test and Evaluation of a Tire-Sand Inertia Barrier,? Texas Transportation Institute, Texas A&M University, January 1975.

Marquis, E.L. and T.J. Hirsch, ?Full Scale Crash Tests of a Tire-Sand Inertia Barrier,? Research Report 146-12, Texas Transportation Institute, Texas A&M University, March 1975.

Michie, Jarvis D. and Maurice E. Bronstad, ?Performance and Operational Experience of Truck-Mounted Attenuators,? NCHRP Synthesis 182, Transportation Research Board, National Research Council, Washington, D.C., 1992.

Ross, H.E., D.L. Sicking, R.A. Zimmer, and J.D. Michie, ?Recommended Procedures for the Safety Performance Evaluation of Highway Features,? NCHRP Report 350, Transportation Research Board, National Research Council, Washington, D.C., 1993.

Seitz, Ronald J., Personal Communication, Topeka, Kansas, July 1998.

Sicking, Dean L., Hayes E. Ross, Jr., and Fred C. Benson, ?A Crash cushion for Narrow Objects,? Research Report 2961F, Texas Transportation Institute, Texas A&M University, September 1982.

Sicking, Dean L. and Hayes E. Ross, Jr., ?Roadside Concrete Barriers: Warrants and End Treatment,? Research Report 346-1F, Texas Transportation Institute, Texas A&M University, November 1985.

U.S. Department of Transportation, National Highway Traffic Safety Administration, ?Traffic Safety Facts 1996," Washington, D.C., 1997.

APPENDICES

APPENDIX A

MATERIALS AND TEST DATA

Table A.1 Tire Characteristics and Test Data

TIRE NO.	TYPE	SIZE	HEIGHT (in.)			WEIGHT	OUT. DIA.	IN. DIA.	AREA				
			TEST 1	TEST 2	TEST 3	(lbs)	(in.)	(in.)	(in.)	ΔY1	ΔY2	%Δ1	%Δ2
1	Firestone FR22	P195/75 R14	7.35	7.15	7.15	17.08	23.75	15.50	254.32	0.20	0.00	2.72	0.00
2	Dayton Quadra XT2	P195/75 R14	6.30	6.25	N/A	16.83	24.00	15.50	263.70	0.05	N/A	0.79	N/A
3	Cooper Lifeliner	P185/70 R14	6.92	6.60	6.55	17.50	22.50	15.50	208.92	0.32	0.05	4.62	0.76
4	Toyo 800 Plus Touring Radial	P185/70 R13	6.60	6.50	6.50	15.54	21.75	14.50	206.41	0.10	0.00	1.52	0.00
5	Ultra Supreme 770	P185/70 R14	6.50	6.35	6.35	16.17	22.50	15.50	208.92	0.15	0.00	2.31	0.00
6	Firestone FR480	P175/70 R14	6.50	6.32	6.35	14.60	22.25	15.50	200.13	0.18	-0.03	2.77	0.47
7	Classic Premium Steel Belted Radial	P175/70 R13	6.56	6.50	6.50	13.13	20.50	14.50	164.93	0.06	0.00	0.91	0.00
8	Dean Celestial Metric	P195/65 R14	7.92	7.70	7.70	16.76	21.50	15.50	174.36	0.22	0.00	2.78	0.00
9	Goodyear F32-S	P195/70 R14	7.55	7.38	7.40	14.35	22.50	15.50	208.92	0.17	-0.02	2.25	0.27
10	Supreme 700 Ultra Patriot	P185/70 R14	6.84	6.48	6.40	17.34	23.00	15.50	226.78	0.36	0.08	5.26	1.23
11	Pirelli Response	P195/60 R14	7.70	7.65	7.70	16.33	22.00	15.00	203.42	0.05	-0.05	0.65	0.65
12	Firestone FR22	P195/75 R14	7.41	7.30	7.25	16.33	24.00	15.50	263.70	0.11	0.05	1.48	0.68
13	Ultra Supreme 770 Patriot	P195/70 R14	7.50	7.05	7.05	16.75	23.00	15.50	226.78	0.45	0.00	6.00	0.00
14	Falken FK-06U	P195/60 R14	8.55	8.55	8.45	17.20	21.00	15.50	157.67	0.00	0.10	0.00	1.17
15	Goodyear Aquatread	P175/70 R13	6.65	6.45	6.45	15.22	20.50	14.50	164.93	0.20	0.00	3.01	0.00
16	Michelin X Metric	P175/70 R13	7.00	6.50	6.45	14.38	21.25	14.25	195.17	0.50	0.05	7.14	0.77
17	American Turbo Metric	P175/70 R13	6.87	6.67	6.80	12.20	20.50	14.50	164.93	0.20	-0.13	2.91	1.95
18	Goodyear Conquest	P195/70 R14	7.40	7.00	7.00	15.28	23.00	15.50	226.78	0.40	0.00	5.41	0.00
19	Michelin Radial X	P175/70 R14	6.95	6.55	6.55	14.10	22.25	15.50	200.13	0.40	0.00	5.76	0.00
20	Michelin Radial X	P175/70 R14	6.90	6.70	6.65	13.27	22.00	15.50	191.44	0.20	0.05	2.90	0.75
21	Defender HRX Radial	P205/55 R16	8.80	8.64	8.62	21.66	23.25	17.50	184.03	0.16	0.02	1.82	0.23
22	Goodyear Regatta	P205/65 R15	7.78	7.50	7.40	18.28	24.00	16.50	238.57	0.28	0.10	3.60	1.33
23	General Ameri* G45	P195/70 R14	7.64	7.26	7.28	15.64	22.75	15.50	217.80	0.38	-0.02	4.97	0.28
24	Ultra STRSport	P185/70 R14	6.92	6.75	6.75	14.38	22.25	15.50	200.13	0.17	0.00	2.46	0.00
25	General Ameri* G45	P195/70 R14	7.55	7.30	7.35	15.25	22.50	15.50	208.92	0.25	-0.05	3.31	0.68
26	Goodyear Invicta GL	P175/70 R13	6.86	6.60	6.60	13.32	21.00	14.50	181.23	0.26	0.00	3.79	0.00
27	Michelin Radial X	P175/70 R14	6.85	6.60	6.60	14.04	22.50	15.50	208.92	0.25	0.00	3.65	0.00
28	Goodyear Conquest	P195/70 R14	7.22	7.05	7.02	15.04	23.00	15.50	226.78	0.17	0.03	2.35	0.43
29	Michelin X Metric	P175/70 R13	6.85	6.60	6.60	14.24	21.25	14.25	195.17	0.25	0.00	3.65	0.00
30	Defender HRX Radial	P205/55 R16	8.80	8.65	8.65	21.76	23.00	17.50	174.95	0.15	0.00	1.70	0.00
					AVG	15.80	22.31	15.40	204.96	0.22	0.01	3.08	0.40
					ST DEV	2.186732	1.033248	0.767329	28.12808	0.1234	0.0461	1.7239	0.5167

Table A.2 Tire Static Test Results

NO.	TEST NO.	TEST TYPE	COUNTER READING	TIRE NO.	PEAK LOAD (lbs)	INIT. HT. (in.)	DISPL. (in.)	COMP. (%)
1	1-1	A	81	1	3652	7.35	5.52	75.10
2	1-2	A	82	1	3621	7.15	5.63	78.74
3	1-3	A	83	1	3636	7.15	5.64	78.88
4	1-4	A	84	1	3625	7.15	5.64	78.88
5	1-a	B	205	1	14550	7.15	5.87	82.10
6	2-1	A	85	2	2504	6.30	4.67	74.13
7	2-a	B	206	2	9710	6.25	5.77	92.32
8	3-1	A	86	3	7690	6.92	4.43	64.02
9	3-2	A	87	3	7834	6.60	4.32	65.45
10	3-3	A	88	3	7232	6.55	4.31	65.80
11	3-a	B	207	3	14960	6.55	5.08	77.56
12	4-1	A	89	4	7783	6.60	4.66	70.61
13	4-2	A	90	4	7920	6.50	4.50	69.23
14	4-3	A	91	4	7799	6.55	4.50	68.70
15	4-a	B	208	4	14300	6.55	5.13	78.32
16	5-1	A	92	5	7944	6.50	4.93	75.85
17	5-2	A	93	5	7824	6.35	4.68	73.70
18	5-3	A	94	5	7863	6.35	4.92	77.48
19	5-a	B	209	5	13960	6.35	5.16	81.26
20	6-1	A	97	6	9588	6.50	4.67	71.85
21	6-2	A	98	6	7828	6.32	4.54	71.84
22	6-3	A	99	6	7806	6.35	4.50	70.87
23	6-a	B	16162	6	13770	6.35	4.86	76.54
24	7-1	A	101	7	7827	6.56	4.92	75.00
25	7-2	A	102	7	7724	6.50	4.94	76.00
26	7-3	A	103	7	7826	6.50	4.76	73.23
27	7-a	B	16163	7	13790	6.50	5.14	79.08
28	8-1	A	104	8	13510	7.92	5.79	73.11
29	8-2	A	105	8	12590	7.70	5.57	72.34
30	8-3	A	106	8	13080	7.70	5.64	73.25
31	8-a	B	16164	8	14130	7.70	6.01	78.05
32	9-1	A	107	9	6096	7.55	5.98	79.21
33	9-2	A	108	9	6119	7.38	5.94	80.49
34	9-3	A	109	9	5622	7.40	6.07	82.03
35	9-a	B	16165	9	13680	7.40	6.35	85.81
36	10-1	A	113	10	13260	6.84	4.47	65.35
37	10-2	A	114	10	13120	6.48	4.30	66.36
38	10-3	A	115	10	11270	6.40	4.57	71.41
39	10-a	B	16166	10	13880	6.40	4.77	74.53
40	11-1	A	116	11	7873	7.70	5.57	72.34
41	11-2	A	117	11	7439	7.65	5.51	72.03
42	11-3	A	118	11	7420	7.70	5.59	72.60

Table A.2 (cont.) Tire Static Test Results

NO.	TEST NO.	TEST TYPE	COUNTER READING	TIRE NO.	PEAK LOAD (lbs)	INIT. HT. (in.)	DISPL. (in.)	COMP. (%)
43	11-a	B	269	11	19230	7.70	5.83	75.71
44	12-1	A	119	12	5839	7.41	6.00	80.97
45	12-2	A	120	12	5738	7.30	5.91	80.96
46	12-3	A	121	12	5782	7.25	5.90	81.38
47	12-a	B	270	12	16240	7.25	5.92	81.66
48	13-1	A	122	13	12890	7.50	5.44	72.53
49	13-2	A	123	13	12590	7.05	5.18	73.48
50	13-3	A	124	13	12500	7.05	5.18	73.48
51	13-a	B	271	13	16570	7.05	5.19	73.62
52	14-1	A	125	14	7920	8.56	6.16	71.96
53	14-2	A	126	14	7635	8.55	6.16	72.05
54	14-3	A	127	14	7602	8.45	6.06	71.72
55	14-a	B	272	14	17100	8.45	6.30	74.56
56	15-1	A	128	15	12260	6.65	4.79	72.03
57	15-2	A	129	15	11990	6.45	4.69	72.71
58	15-3	A	130	15	11840	6.45	4.68	72.56
59	15-a	B	273	15	16200	6.45	4.74	73.49
60	16-1	A	131	16	11050	7.00	5.06	72.29
61	16-2	A	132	16	7852	6.50	4.59	70.62
62	16-3	A	133	16	7842	6.45	4.58	71.01
63	16-a	B	274	16	15350	6.45	5.03	77.98
64	17-1	A	134	17	7904	6.87	5.34	77.73
65	17-2	A	135	17	7845	6.67	5.18	77.66
66	17-3	A	136	17	7826	6.80	5.35	78.68
67	17-a	B	275	17	14690	6.80	5.44	80.00
68	18-1	A	137	18	7852	7.40	5.69	76.89
69	18-2	A	138	18	7786	7.00	5.48	78.29
70	18-3	A	139	18	7793	7.00	5.43	77.57
71	18-a	B	16092	18	11730	7.00	5.65	80.71
72	19-1	A	140	19	12480	6.95	5.29	76.12
73	19-2	A	141	19	7834	6.55	4.81	73.44
74	19-3	A	142	19	7845	6.55	4.67	71.30
75	19-a	B	276	19	15630	6.55	5.06	77.25
76	20-1	A	143	20	7846	6.90	4.76	68.99
77	20-2	A	144	20	7792	6.70	4.97	74.18
78	20-3	A	145	20	7789	6.65	4.90	73.68
79	20-a	B	277	20	14710	6.65	5.06	76.09
80	21-1	A	146	21	10050	8.80	6.43	73.07
81	21-2	A	147	21	9584	8.64	6.25	72.34
82	21-3	A	148	21	9708	8.62	6.37	73.90
83	22-1	A	149	22	7758	7.78	6.08	78.15
84	22-2	A	150	22	7385	7.50	5.93	79.07

Table A.2 (cont.) Tire Static Test Results

NO.	TEST NO.	TEST TYPE	COUNTER READING	TIRE NO.	PEAK LOAD (lbs)	INIT. HT. (in.)	DISPL. (in.)	COMP. (%)
85	22-3	A	152	22	7380	7.40	5.58	75.41
86	22-4	A	153	22	7373	7.45	5.89	79.06
87	22-a	B	16090	22	12090	7.45	6.06	81.34
88	23-1	A	154	23	7880	7.64	5.81	76.05
89	23-2	A	155	23	7838	7.26	5.57	76.72
90	23-3	A	156	23	7856	7.28	5.51	75.69
91	23-a	B	16091	23	11730	7.28	5.88	80.77
92	24-1	A	157	24	11790	6.92	5.44	78.61
93	24-2	A	158	24	11370	6.75	5.20	77.04
94	24-3	A	159	24	11360	6.75	5.43	80.44
95	25-1	A	160	25	7792	7.55	5.78	76.56
96	25-2	A	161	25	7692	7.30	5.75	78.77
97	25-3	A	162	25	7671	7.35	5.66	77.01
98	26-1	A	163	26	7734	6.86	5.21	75.95
99	26-2	A	164	26	7669	6.60	5.14	77.88
100	26-3	A	165	26	7667	6.60	5.08	76.97
101	27-1	B	166	27	15460	6.85	5.04	73.58
102	27-2	B	167	27	14400	6.60	4.91	74.39
103	27-3	B	168	27	14350	6.60	4.99	75.61
104	28-1	B	169	28	14140	7.22	5.69	78.81
105	28-2	B	170	28	13550	7.05	5.60	79.43
106	28-3	B	171	28	13480	7.02	5.56	79.20
107	29-1	B	172	29	14670	6.85	5.33	77.81
108	29-2	B	173	29	13240	6.60	4.93	74.70
109	29-3	B	174	29	13160	6.60	5.31	80.45
110	30-1	B	175	30	19750	8.80	6.64	75.45
111	30-2	B	176	30	19490	8.65	6.48	74.91
112	30-3	B	177	30	19030	8.65	6.65	76.88
113	I-1a	C	178	27/29	2498	13.18	8.57	
114	I-1b	C	179	27/29	15690	8.60	5.91	
						13.18	10.49	79.59
115	I-2	C	180	27/29	15270	10.00	7.32	
						13.18	10.50	79.67
116	I-3	C	181	27/29	15480	10.00	7.32	
						13.18	10.50	79.67
117	I-4	C	182	27/29	15720	10.00	7.38	
						13.18	10.56	80.12
118	I-5a	C	183	27/29	1745	13.30	8.40	
119	I-5b	C	184	27/29	14770	8.40	6.10	
						13.30	11.00	82.71
120	II-1a	C	185	19/20	842	13.26	4.13	

Table A.2 (cont.) Tire Static Test Results

NO.	TEST NO.	TEST TYPE	COUNTER READING	TIRE NO.	PEAK LOAD (lbs)	INIT. HT. (in.)	DISPL. (in.)	COMP. (%)
121	II-1b	C	186	19/20	14950	9.00	6.66	
						13.26	10.92	82.35
122	II-2a	C	187	19/20	743	13.10	4.04	
123	II-2b	C	188	19/20	14290	9.00	6.48	
						13.10	10.58	80.76
124	II-3a	C	189	19/20	600	13.10	4.07	
125	II-3b	C	190	19/20	14780	9.00	6.52	
						13.10	10.62	81.07
126	III-1a	C	191	29/19/20	675	19.60	6.10	
127	III-1b	C	192	29/19/20		13.50	4.55	
128	III-1c	C	193	29/19/20	31160	9.00	5.87	
						19.60	16.47	84.03
129	III-2a	C	194	29/19/20	641	19.50	5.73	
130	III-2b	C	195	29/19/20		13.50	4.56	
131	III-2c	C	196	29/19/20	30450	9.00	5.85	
						19.50	16.35	83.85
132	III-3a	C	16082	18/22/23	970	21.50	6.29	
133	III-3b	C	16083	18/22/23		15.25	7.68	
134	III-3c	C	16084	18/22/23	25110	8.10	4.77	
						21.50	18.17	84.51
135	III-4a	C	16085	18/22/23	863	21.50	7.94	
136	III-4b	C	16086	18/22/23		13.25	6.15	
137	III-4c	C	16087	18/22/23	50550	8.10	5.27	
						21.50	18.67	86.84
138	V-1a	C	197	24/26/15/ 16/17		33.75	9.08	
139	V-1b	C	198	24/26/15/ 16/17		24.00	6.94	
140	V-1c	C	199	24/26/15/ 16/17		17.00	8.78	
141	V-1d	C	200	24/26/15/ 16/17	116500	8.30	4.97	
						33.75	30.42	90.13
142	V-2a	C	218	24/26/15/ 16/17		33.75	9.06	
143	V-2b	C	219	24/26/15/ 16/17		24.00	7.74	
144	V-2c	C	220	24/26/15/ 16/17		17.00	8.54	
145	V-2d	C	222	24/26/15/ 16/17	105100	8.30	5.06	
						33.75	30.51	90.40

Table A.2 (cont.) Tire Static Test Results

NO.	TEST NO.	TEST TYPE	COUNTER READING	TIRE NO.	PEAK LOAD (lbs)	INIT. HT. (in.)	DISPL. (in.)	COMP. (%)
146	V-2-a	C	16167	6/7/8/9/10		34.00	9.14	
147	V-2-b	C	16168	6/7/8/9/10		25.00	8.32	
148	V-2-c	C	16169	6/7/8/9/10		17.00	8.23	
149	V-2-d	C	16170	6/7/8/9/10	151400	9.00	5.66	
						34.00	30.66	90.18
150	L-1a	L	210	1		23.75	9.05	
151	L-1b	L	211	1		23.75	9.06	
152	L-1c	L	212	1	7411	23.75	4.84	
153	L-1d	L	213	1	7473	23.75	4.92	
154	L-3a	L	214	3		22.50	9.06	
155	L-3b	L	215	3		22.50	9.06	
156	L-3c	L	216	3	13400	22.50	4.00	
157	L-3d	L	217	3	13430	22.50	3.95	
158	L-11	L	278	11	15320	22.00	7.20	
159	L-15	L	279	15	15110	20.50	6.92	
160	L-16	L	280	16	14940	21.25	6.91	

Test A - 500lbs/min
Test B - 2500lbs/min
Test C - 2500lbs/min, multiple tires
Test L - 2500lbs/min, longitudinal compression

Table A.3 Tire-Derived Sample Static Test Results

NO.	TEST NO.	COUNT. READ.	LOAD RATE	SAMPLE NO.	SAMPLE TYPE	PEAK LOAD (lbs)	INIT. HT. (in.)	DISPL. (in.)	COMP. (%)
1	1-F-A	223	0.5k/min	1	FINE	19670	1.75	0.58	32.97
2	1-F-B	224	2.5k/min	1	FINE	106900	1.75	1.01	57.71
3	1-C-A	225	2.5k/min	1	COARSE	110000	2.00	1.58	79.00
4	1-CP-A	226	2.5k/min	1	COMP	110000	3.25	2.55	78.46
5	1-CP-A	227	2.5k/min	1	COMP	110000	3.25	2.51	77.23
6	2-F-A	15282	5k/min	1	FINE	150200	1.75	1.29	73.71
7	2-C-A	15283	5k/min	1	COARSE	150100	2.00	1.65	82.50
8	2-CP-A	15299	5k/min	1	COMP	150600	3.25	2.61	80.31
9	3-F-A	15300	10k/min	1	FINE	151600	1.75	1.26	72.00
10	3-C-A	15301	10k/min	1	COARSE	150800	2.00	1.63	81.50
11	3-CP-A	15302	10k/min	1	COMP	152900	3.15	2.60	82.54
12	4-F-A	15548	20k/min	1	FINE	174400	1.75	1.27	72.57
13	4-C-A	15549	20k/min	1	COARSE	173900	2.00	1.61	80.50
14	4-CP-A	15550	20k/min	1	COMP	179600	3.10	2.57	82.90
15	5-F-A	15551	40k/min	1	FINE	181400	1.75	1.22	69.71
16	5-C-A	15552	40k/min	1	COARSE	187900	2.00	1.63	81.50
17	5-CP-A	15553	40k/min	1	COMP	217700	3.10	2.76	89.03
18	6-F-A	15554	60k/min	1	FINE	205400	1.75	1.33	76.00
19	6-C-A	15555	60k/min	1	COARSE	225500	2.00	1.70	85.00
20	6-CP-A	15556	60k/min	1	COMP	244200	3.10	2.79	90.00
21	1-F-B	15557	60k/min	2	FINE	210700	1.75	1.65	94.29
22	1-F-B2	15558	60k/min	2	FINE	204500	1.75	1.29	73.71
23	1-C-B	15559	60k/min	2	COARSE	227800	2.00	1.75	87.50
24	1-CP-B	15560	60k/min	2	COMP	275800	3.10	2.81	90.65
25	1-2F-A	15561	60k/min	2/3	2 FINE	291200	3.35	3.11	92.84
26	1-2C-A	15562	60k/min	2/3	2 COARSE	250100	4.00	3.45	86.25
27	1-2CP-A	15563	60k/min	2/3	2 COMP	302800	6.30	5.85	92.86
28	7-F-A	15656	60k/min	4	FINE	203400	1.70	1.30	76.47
29	7-F-B	15657	60k/min	4	FINE	202600	1.70	1.19	70.00

Table A.3 (cont.) Tire-Derived Sample Static Test Results

NO.	TEST NO.	COUNT.	LOAD	SAMPLE	SAMPLE	PEAK LOAD	INIT. HT.	DISPL.	COMP.
30	7-F-C	15658	60k/min	4	FINE	204000	1.70	1.25	73.53
31	7-C-A	15659	60k/min	4	COARSE	214400	2.00	1.78	89.00
32	7-C-B	15660	60k/min	4	COARSE	212200	2.00	1.78	89.00
33	7-C-C	15661	60k/min	4	COARSE	214000	2.00	1.66	83.00
34	7-CP-A	15662	60k/min	4	COMP	266600	3.15	2.75	87.30
35	7-CP-B	15663	60k/min	4	COMP	250600	3.15	2.63	83.49
36	7-CP-C	15664	60k/min	4	COMP	249400	3.15	2.62	83.17
37	1-3F-A	15665	60k/min	1/2/4	3 FINE	318100	5.25	4.00	76.19
38	1-3F-B	15666	60k/min	1/2/4	3 FINE	312500	5.25	4.00	76.19
39	1-3C-A	15667	60k/min	1/2/4	3 COARSE	226100	5.90	4.88	82.71
40	1-3C-B	15668	60k/min	1/2/4	3 COARSE	219600	5.90	4.78	81.02
41	1-3CP-A	15669	60k/min	1/2/4	3 COMP	26650	N/A	N/A	N/A
42	1-3CP-A	15670	60k/min	1/2/4	3 COMP	101000	9.50	7.10	74.74
43	1-3CP-B	15671	60k/min	1/2/4	3 COMP	140600	9.50	7.33	77.16
44	1-2FC-A	15672	60k/min	2	1 FINE 1 CRSE	217900	3.65	2.87	78.63
45	1-2FC-B	15673	60k/min	2	1 FINE 1 CRSE	216600	3.65	2.83	77.53
46	1-2FCP-A	15674	60k/min	2	1 FINE 1 COMP	262200	4.75	3.83	80.63
47	1-2FCP-B	15675	60k/min	2	1 FINE 1 COMP	258600	4.75	3.77	79.37
48	1-2CCP-A	15676	60k/min	2	1 CRSE 1 CP	227100	5.05	4.15	82.18
49	1-2CCP-B	15677	60k/min	2	1 CRSE 1 CP	222300	5.05	4.19	82.97
50	1-3FCC-A	15678	60k/min	2/2/4	1 FINE 2 CRSE	244900	5.55	4.53	81.62
51	1-3FCC-B	15679	60k/min	2/2/4	1 FINE 2 CRSE	243200	5.55	4.44	80.00
52	1-3FCPCP	15680	60k/min	2/2/4	1 FINE 2 COMP	250100	8.15	6.38	78.28
53	1-3FCPCP	15681	60k/min	2/2/4	1 FINE 2 COMP	213700	8.15	6.30	77.30
54	1-1-F	16171	60k/min	4	FINE	201600	1.75	1.28	73.14
55	1-1-C	16172	60k/min	4	COARSE	216000	2.00	1.77	88.50
56	1-1-CP	16173	60k/min	4	COMP	257100	3.10	2.63	84.84
57	1-2-2F	16174	60k/min	1/4	FINE	277800	3.50	2.65	75.71
58	1-2-2C	16175	60k/min	1/4	COARSE	248600	4.00	3.28	82.00
59	1-2-2CP	16176	60k/min	1/4	COMP	303100	6.25	5.25	84.00

Table A.4 Dynamic Tire Test Results

TEST NO.	TIRE NO.	FREQ	NOM LD (lbs)	ACT LD (lbs)	DEF (in.)	AREA (cm^2)		WORK (ft-lbs)		R/C RATIO
						Crush	Rebound	Crush	Rebound	
1	20	1	1000	979	1.53	135.0	54.2	68.1	27.3	0.40
2	20	1	2500	2572	2.97	118.6	54.7	320.0	147.6	0.46
3	20	1	5000	5000	4.07	90.0	41.5	603.4	278.2	0.46
4	20	2	1000	950	1.48	128.8	55.2	65.0	27.8	0.43
5	20	2	2500	2497	3.02	118.8	54.8	320.6	147.9	0.46
6	20	2	5000	4887	3.18	74.8	35.0	501.5	234.6	0.47
7	6	1	1000	986	0.93	78.6	37.3	39.7	18.8	0.47
8	6	1	2500	2587	2.23	89.7	41.5	242.0	112.0	0.46
9	6	1	5000	5075	3.14	81.9	32.7	549.1	219.2	0.40
10	6	2	1000	1014	0.97	75.4	40.0	38.0	20.2	0.53
11	6	2	2500	2542	2.25	92.2	43.7	248.8	117.9	0.47
12	6	2	5000	4962	3.10	79.8	33.0	535.0	221.2	0.41
13	23	1	1000	979	1.41	112.8	53.6	56.9	27.0	0.48
14	23	1	2500	2527	4.07	172.7	76.9	466.0	207.5	0.45
15	23	1	5000	4850	4.90	94.0	43.7	630.2	293.0	0.46
16	23	2	1000	950	1.63	129.9	63.4	65.5	32.0	0.49
17	23	2	2500	2572	4.54	179.6	82.4	484.6	222.3	0.46
18	23	2	5000	5000	4.99	93.3	43.6	625.5	292.3	0.47
19	17	1	1000	943	2.21	207.8	92.6	104.8	46.7	0.45
20	17	1	2500	2466	4.07	130.6	62.4	352.4	168.4	0.48
21	17	1	5000	4887	4.64	71.6	37.2	480.0	249.4	0.52
22	17	2	1000	950	2.14	156.1	115.4	78.7	58.2	0.74
23	17	2	2500	2542	4.24	130.8	61.3	352.9	165.4	0.47
24	17	2	5000	5075	4.45	78.1	35.7	523.6	239.3	0.46
25	4	1	1000	993	0.97	75.8	43.3	38.2	21.8	0.57
26	4	1	2500	2602	2.25	87.7	39.8	236.6	107.4	0.45
27	4	1	5000	5000	3.55	94.2	44.6	631.5	299.0	0.47
28	4	2	1000	979	1.06	83.3	45.2	42.0	22.8	0.54
29	4	2	2500	2527	2.33	84.6	35.2	228.3	95.0	0.42
30	4	2	5000	4812	3.42	90.3	40.3	605.4	270.2	0.45
31	19	1	1000	979	1.06	84.6	40.9	42.7	20.6	0.48
32	19	1	2500	2572	2.87	118.0	57.2	318.4	154.3	0.48
33	19	1	5000	5038	3.81	90.7	45.6	608.1	305.7	0.50
34	19	2	1000	1021	1.22	99.5	45.3	50.2	22.9	0.46
35	19	2	2500	2572	2.65	97.1	45.7	262.0	123.3	0.47
36	19	2	5000	5038	3.94	92.6	47.0	620.8	315.1	0.51
37	18	1	1000	950	2.27	185.5	85.6	93.6	43.2	0.46
38	18	1	2500	2633	4.47	152.5	78.9	411.5	212.9	0.52
39	18	1	5000	5038	4.24	71.1	35.4	476.7	237.3	0.50
40	18	2	1000	1000	2.17	173.5	80.8	87.5	40.8	0.47
41	18	2	2500	2739	3.66	138.2	56.8	372.9	153.3	0.41
42	18	2	5000	5113	4.32	81.8	40.1	548.4	268.8	0.49

Table A.4 (cont.) Dynamic Tire Test Results

TEST NO.	TIRE NO.	FREQ	NOM LD (lbs)	ACT LD (lbs)	DEF (in.)	AREA (cm^2)		WORK (ft-lbs)		R/C RATIO
						Crush	Rebound	Crush	Rebound	
43	5	1	1000	964	1.03	78.4	40.3	39.6	20.3	0.51
44	5	1	2500	2542	2.29	81.5	30.6	219.9	82.6	0.38
45	5	1	5000	5038	3.89	108.6	40.5	728.1	271.5	0.37
46	5	2	1000	957	1.16	96.9	44.3	48.9	22.3	0.46
47	5	2	2500	2527	2.57	95.2	44.1	256.9	119.0	0.46
48	5	2	5000	5038	3.94	110.1	43.7	738.1	293.0	0.40
49	10	1	1000	979	0.96	82.9	42.5	41.8	21.4	0.51
50	10	1	2500	2542	2.08	78.8	37.8	212.6	102.0	0.48
51	10	1	5000	5038	3.00	78.0	37.6	522.9	252.1	0.48
52	10	2	1000	964	0.90	73.3	36.4	37.0	18.4	0.50
53	10	2	2500	2602	2.03	76.5	37.8	206.4	102.0	0.49
54	10	2	5000	5038	2.91	74.6	37.5	500.1	251.4	0.50
55	7	1	1000	993	1.55	118.0	54.5	59.5	27.5	0.46
56	7	1	2500	2572	3.06	111.7	56.7	301.4	153.0	0.51
57	7	1	5000	5075	4.15	89.1	44.7	597.4	299.7	0.50
58	7	2	1000	986	1.38	103.6	52.0	52.3	26.2	0.50
59	7	2	2500	2572	3.17	124.7	63.0	336.5	170.0	0.51
60	7	2	5000	5075	3.98	85.5	44.5	559.8	291.4	0.52

Frequency 1 - 0.1 Hz
Frequency 2 - 0.08 Hz

Table A.5 Dynamic Tire-Derived Sample Test Results

TEST NO.	SAMP TYPE	FREQ	NOM LD (lbs)	ACT LD (lbs)	DEF (in.)	AREA (cm^2)		WORK (ft-lbs)		R/C RATIO
						Crush	Rebound	Crush	Rebound	
1	FINE	1	1000	1000	0.08	5.0	2.8	2.5	1.4	0.56
2	FINE	1	2500	2618	0.14	11.6	7.0	12.4	7.5	0.60
3	FINE	1	5000	5038	0.28	18.6	11.7	49.4	31.1	0.63
4	FINE	2	1000	1000	0.08	4.9	2.8	2.5	1.4	0.57
5	FINE	2	2500	2618	0.14	11.2	7.1	12.0	7.6	0.63
6	FINE	2	5000	5038	0.26	16.9	10.4	44.9	27.6	0.62
7	CRSE	1	1000	1000	0.22	18.6	9.0	9.4	4.5	0.48
8	CRSE	1	2500	2587	0.47	47.7	25.8	51.0	27.6	0.54
9	CRSE	1	5000	5038	0.70	44.5	27.0	118.1	71.7	0.61
10	CRSE	2	1000	1007	0.25	21.0	12.1	10.6	6.1	0.58
11	CRSE	2	2500	2618	0.50	47.4	28.3	50.7	30.2	0.60
12	CRSE	2	5000	5038	0.70	44.4	25.8	117.9	68.5	0.58
13	CMP	1	1000	993	0.44	39.6	21.6	20.0	10.9	0.55
14	CMP	1	2500	2618	0.87	84.9	44.8	90.7	47.9	0.53
15	CMP	1	5000	5038	1.24	72.7	39.5	193.0	104.9	0.54
16	CMP	2	1000	993	0.47	43.5	21.6	21.9	10.9	0.50
17	CMP	2	2500	2633	0.97	81.5	46.7	87.1	49.9	0.57
18	CMP	2	5000	5038	1.22	71.1	41.2	188.8	109.4	0.58

Frequency 1 - 0.1 Hz
Frequency 2 - 0.08 Hz

APPENDIX B

SAMPLE OUTPUT FROM TESTS

TEST NUMBER 15-a

Test Compression Test
Procedure TIRES 1

Test Date	07-10-1997	Tested By	LARRY CHEEK
Test Time	02:50:07 PM	Test Counter	00000273
Elapsed Time	00:05:00	Area	238.76 In²
Peak Load	16200 Lbs	Compr Strgth	67.830 PSI
Modulus	29.480 PSI		

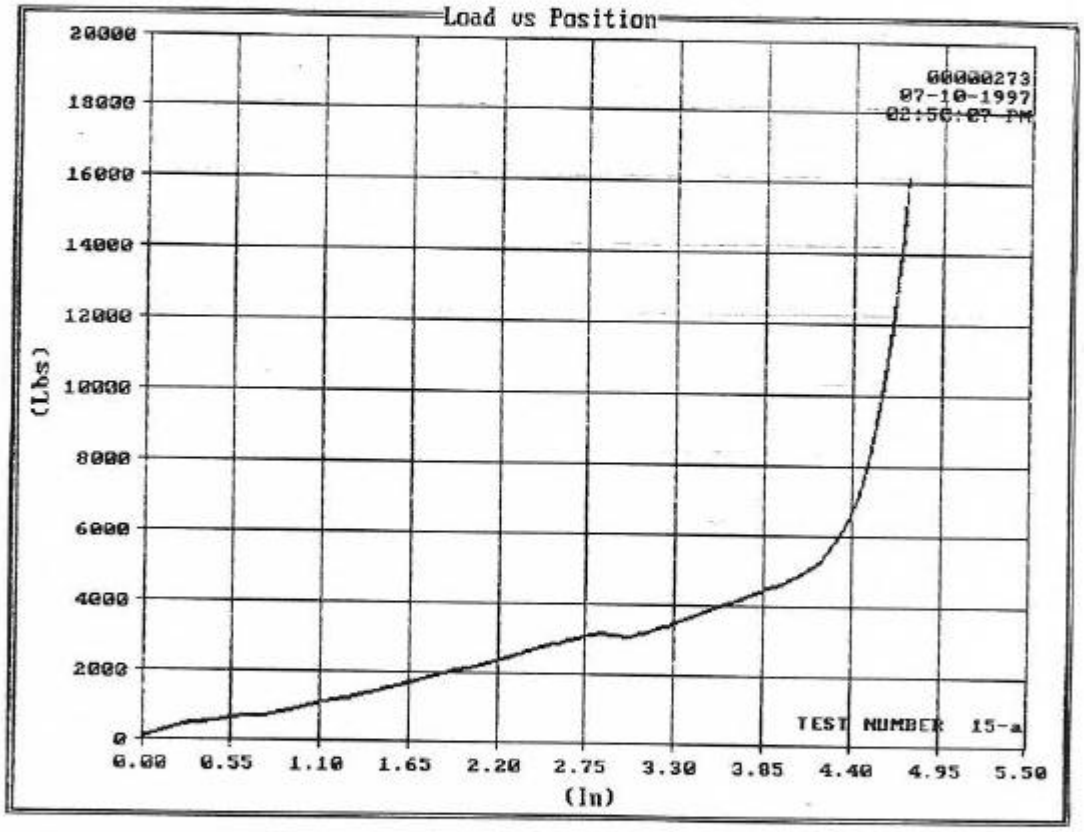

TEST NUMBER I-4

Test Procedure: Compression Test TIRES 1

Test Date	03-06-1997	Tested By	LARRY CHEEN
Test Time	02:06:23 PM	Test Counter	000001E2
Elapsed Time	00:05:01	Area	250.35 in²
Peak Load	15720 Lbs	Compr Strgth	62.780 PSI
Modulus	4.902 PSI		

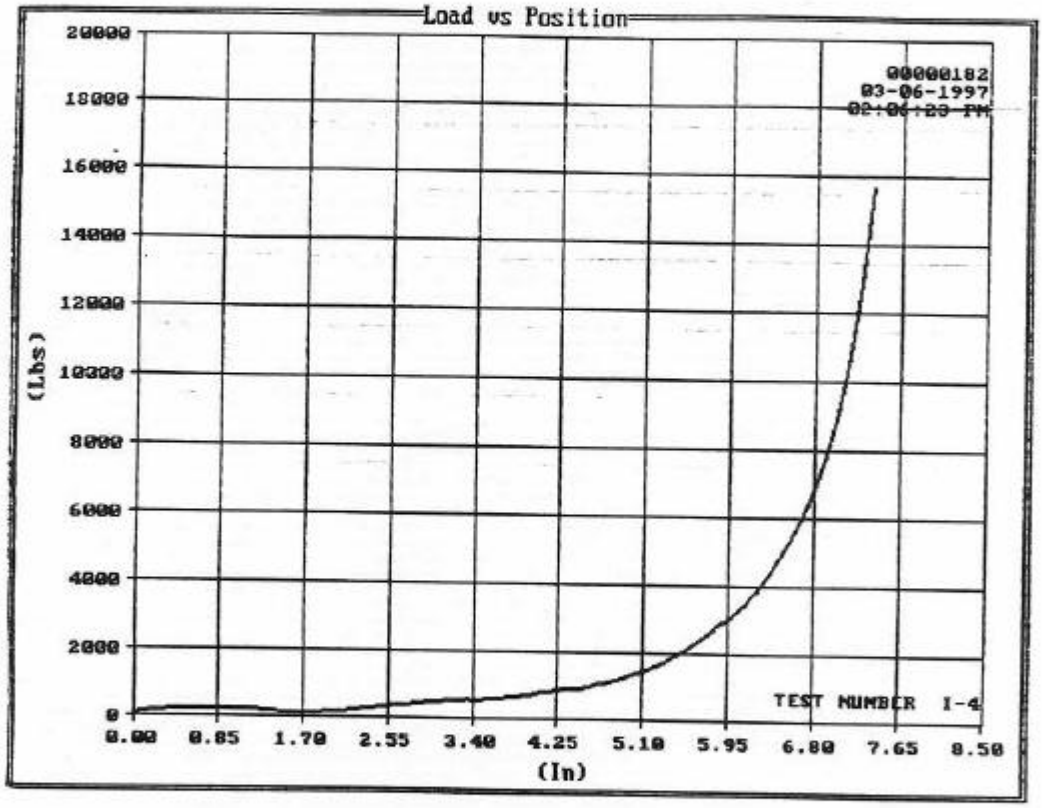

TEST NO III-4c

Test Compression Test
Procedure TIRES 1

Test Date	06-20-1997	Tested By	LARRY CHEEK
Test Time	02:41:06 PM	Test Counter	00016087
Elapsed Time	00:20:00	Area	226.78 In)
Peak Load	50550 Lbs	Compr Strgth	222.90 PSI
Modulus	33.80 PSI		

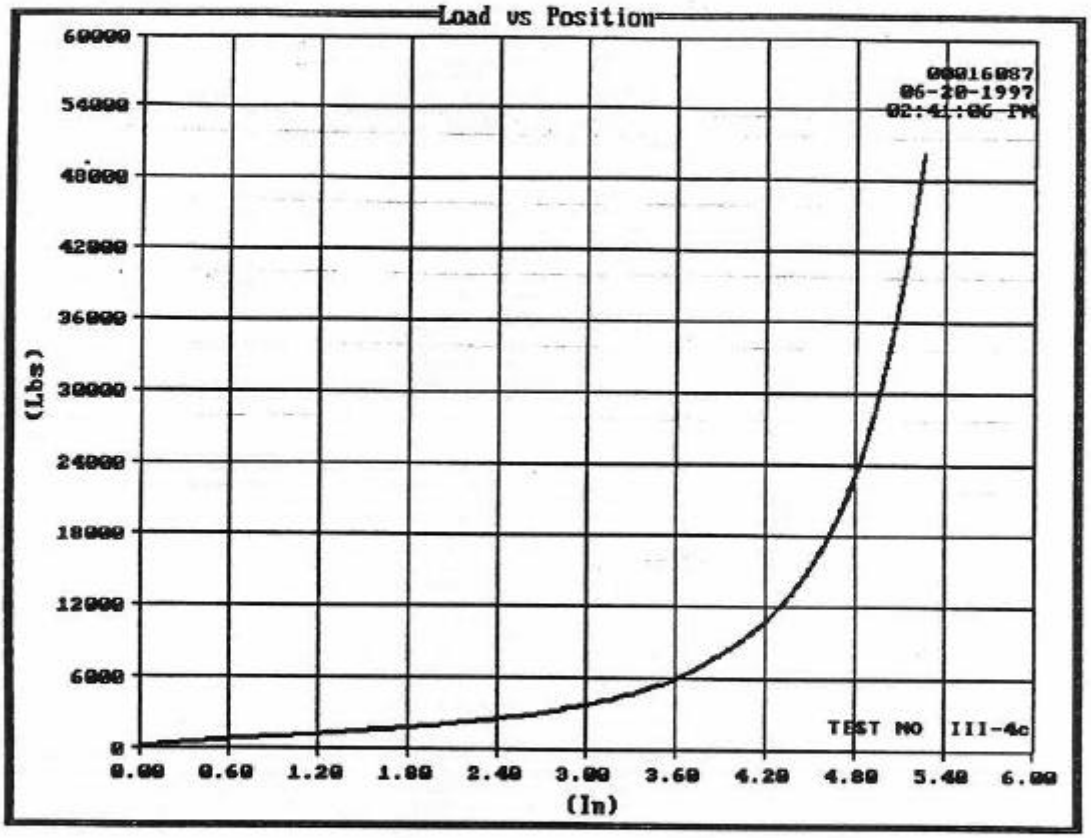

TEST NUMBER L-15

Test Procedure: Compression Test TIRES 1

Test Date	07-10-1997	Tested By	LARRY CHEEK
Test Time	03:58:34 PM	Test Counter	00000279
Elapsed Time	00:05:00	Area	6.2832 In²
Peak Load	15110 Lbs	Compr Strgth	2406.0 PSI
Modulus	430.9 PSI		

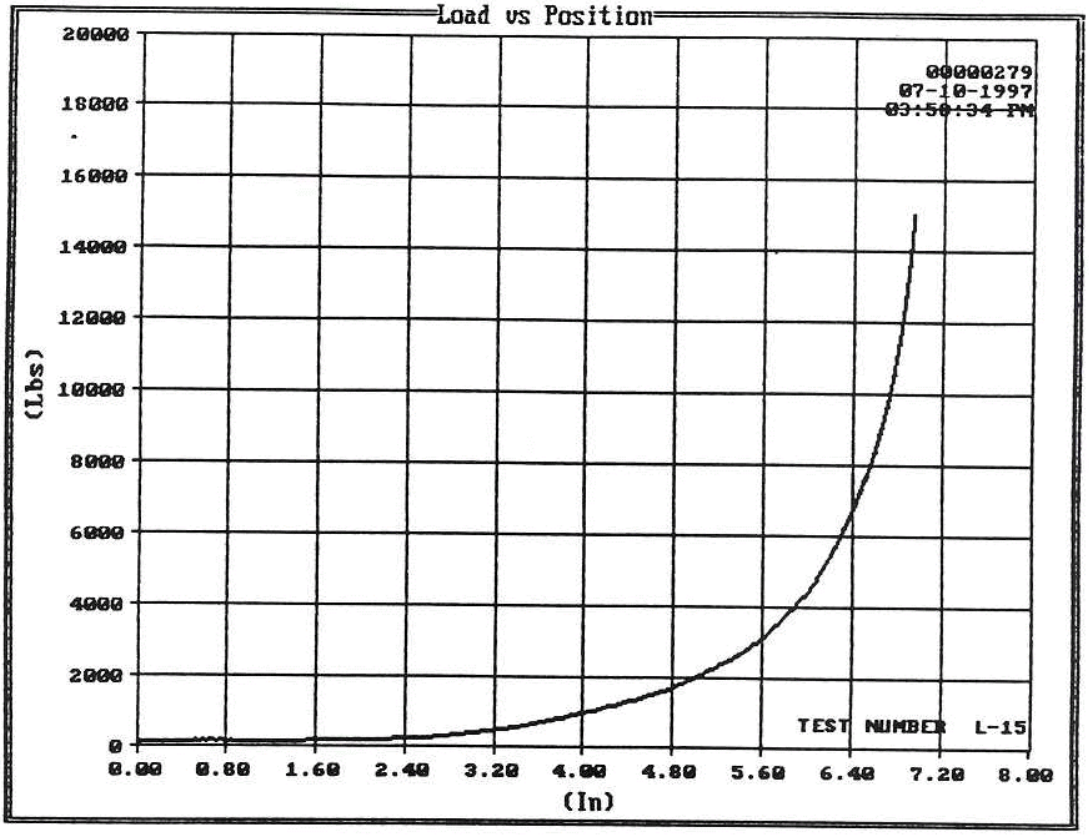

TEST NO		1-F-B (2)	
PAD DESCRIPTION		FINE	
MFG		DODGE REGUPOL	
PAD HT		1.75	
FINAL HT		1.70	
Test	Compression Test		
Procedure 12 x 12 PAD			
Test Date	05-22-1997	Tested By	LARRY CHEEK
Test Time	01:20:49 PM	Test Counter	00015558
Elapsed Time	00:03:00	Area	144.00 In)
Peak Load	204500 Lbs	Compr Strgth	1420.00 PSI
Strgth at Fail	1416.00 PSI	Load at Fail	203900 Lbs
Modulus			

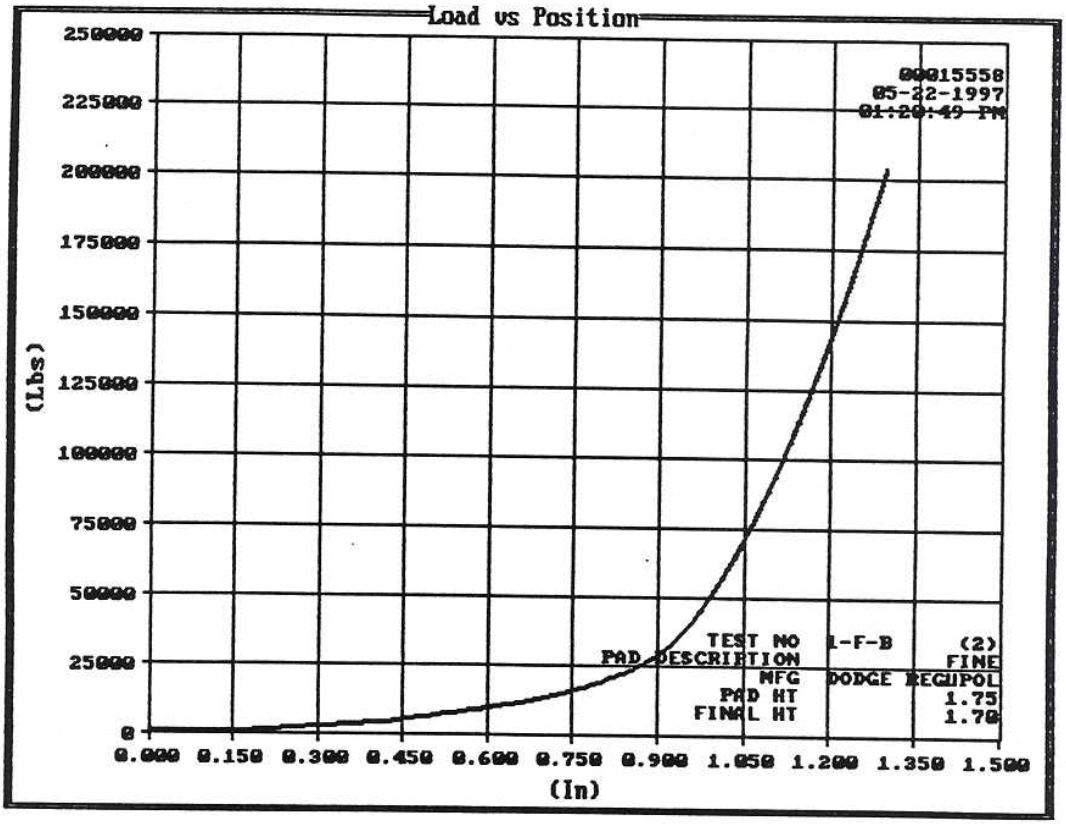

TEST NO	1-2F-A
PAD DESCRIPTION	TWO FINE 2,3
MFG	DODGE REGUPOL
PAD HT	3.35
FINAL HT	3.35

Test Compression Test
Procedure 12 x 12 PAD

Test Date	05-22-1997	Tested By	LARRY CHEEK
Test Time	01:44:18 PM	Test Counter	00015561
Elapsed Time	00:03:00	Area	144.00 In)
Peak Load	291200 Lbs	Compr Strgth	2022.00 PSI
Strgth at Fail	2017.00 PSI	Load at Fail	290400 Lbs
Modulus			

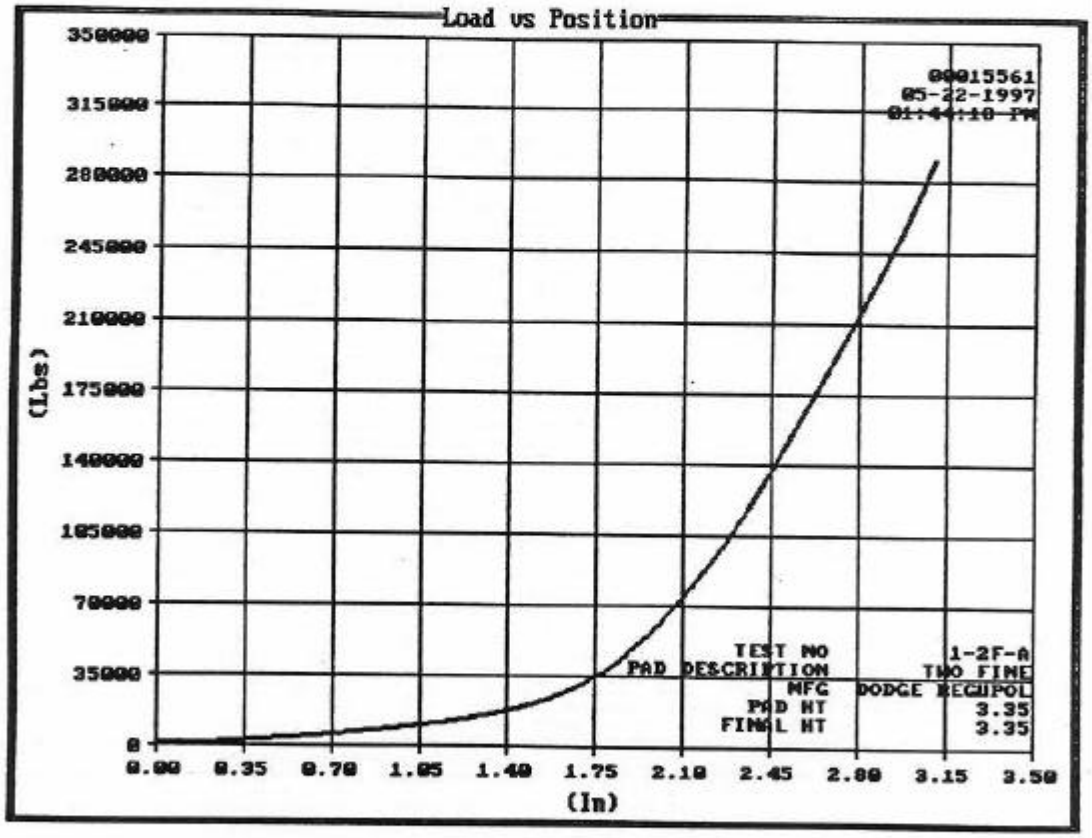

TEST NO	7-CP-A
PAD DESCRIPTION	COMPOSITE
MFG	DODGE REGUPOL
PAD HT	3.00
FINAL HT	3.15

Test Compression Test
Procedure 12 x 12 PAD

Test Date	05-29-1997	Tested By	LARRY CHEEK
Test Time	12:56:26 PM	Test Counter	00015662
Elapsed Time	00:03:00	Area	144.00 In²
Peak Load	266600 Lbs	Compr Strgth	1852.00 PSI
Strgth at Fail	1846.00 PSI	Load at Fail	265800 Lbs
Modulus			

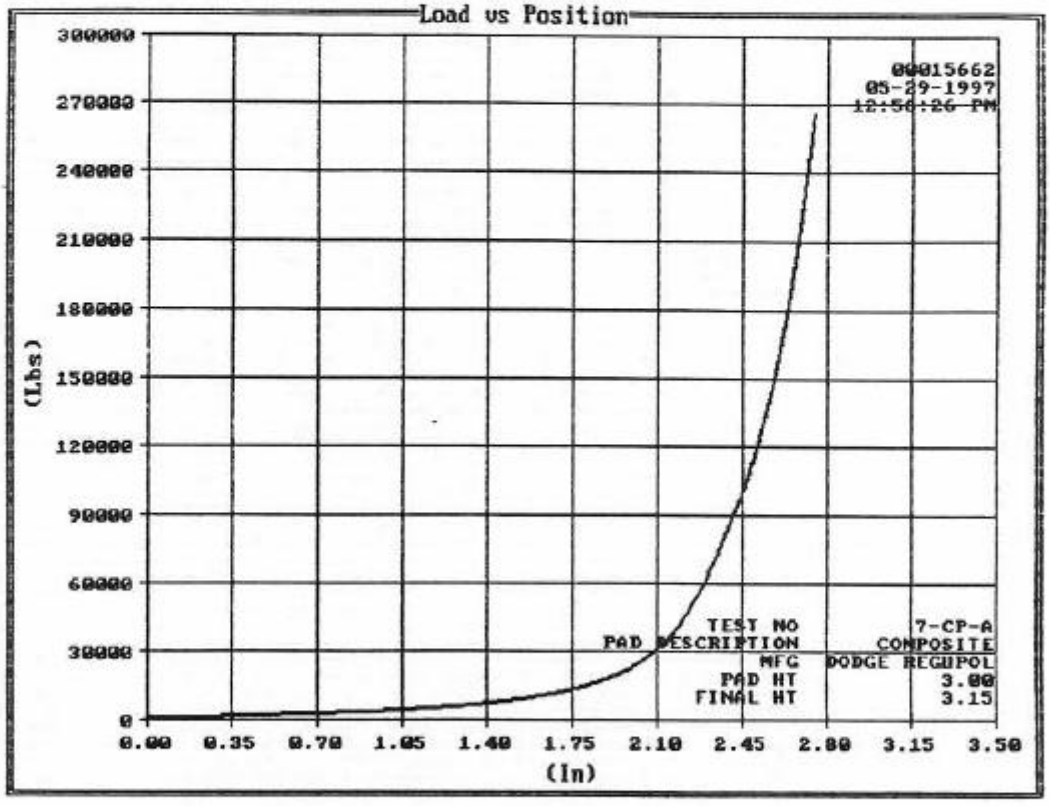

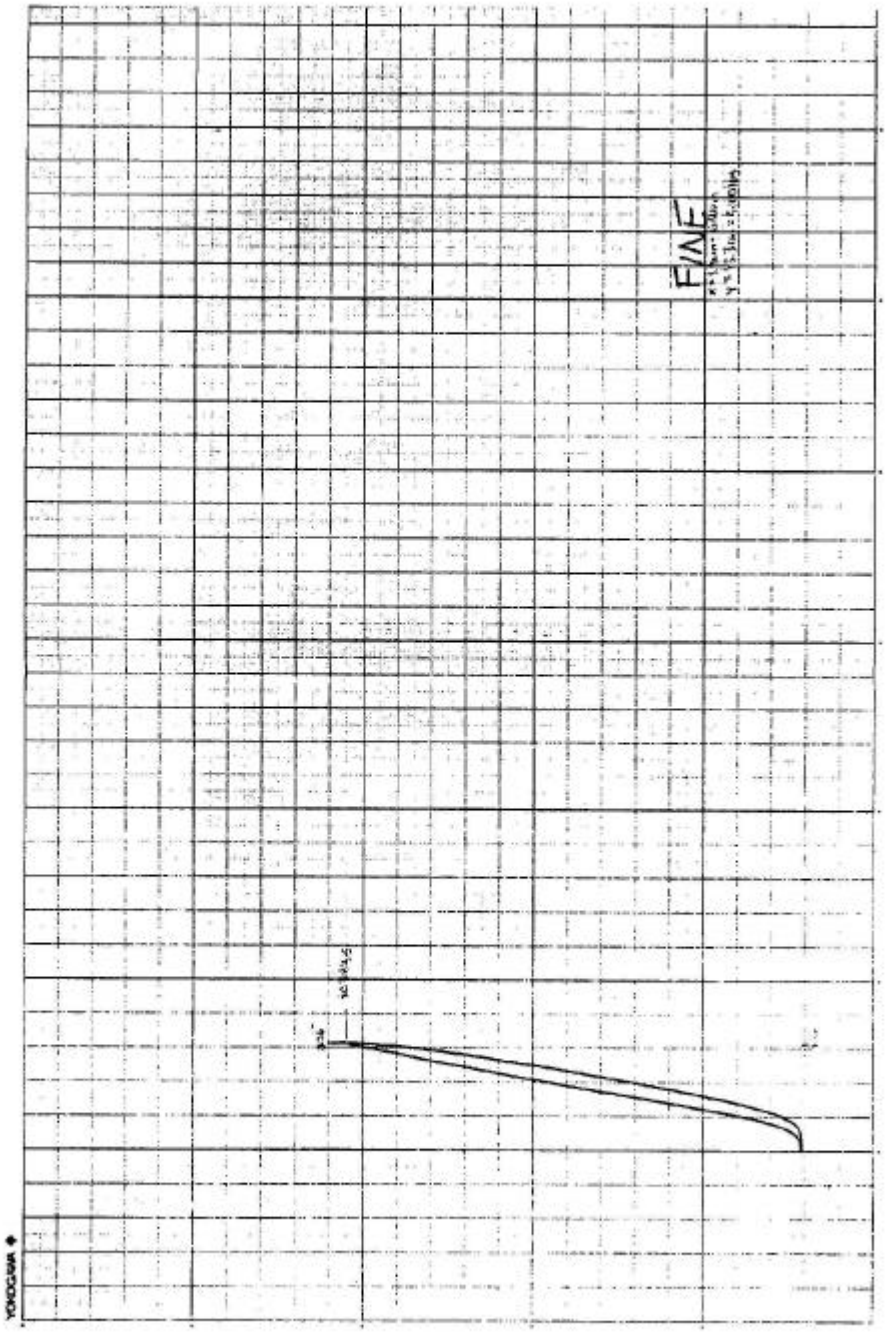
F/ΔE

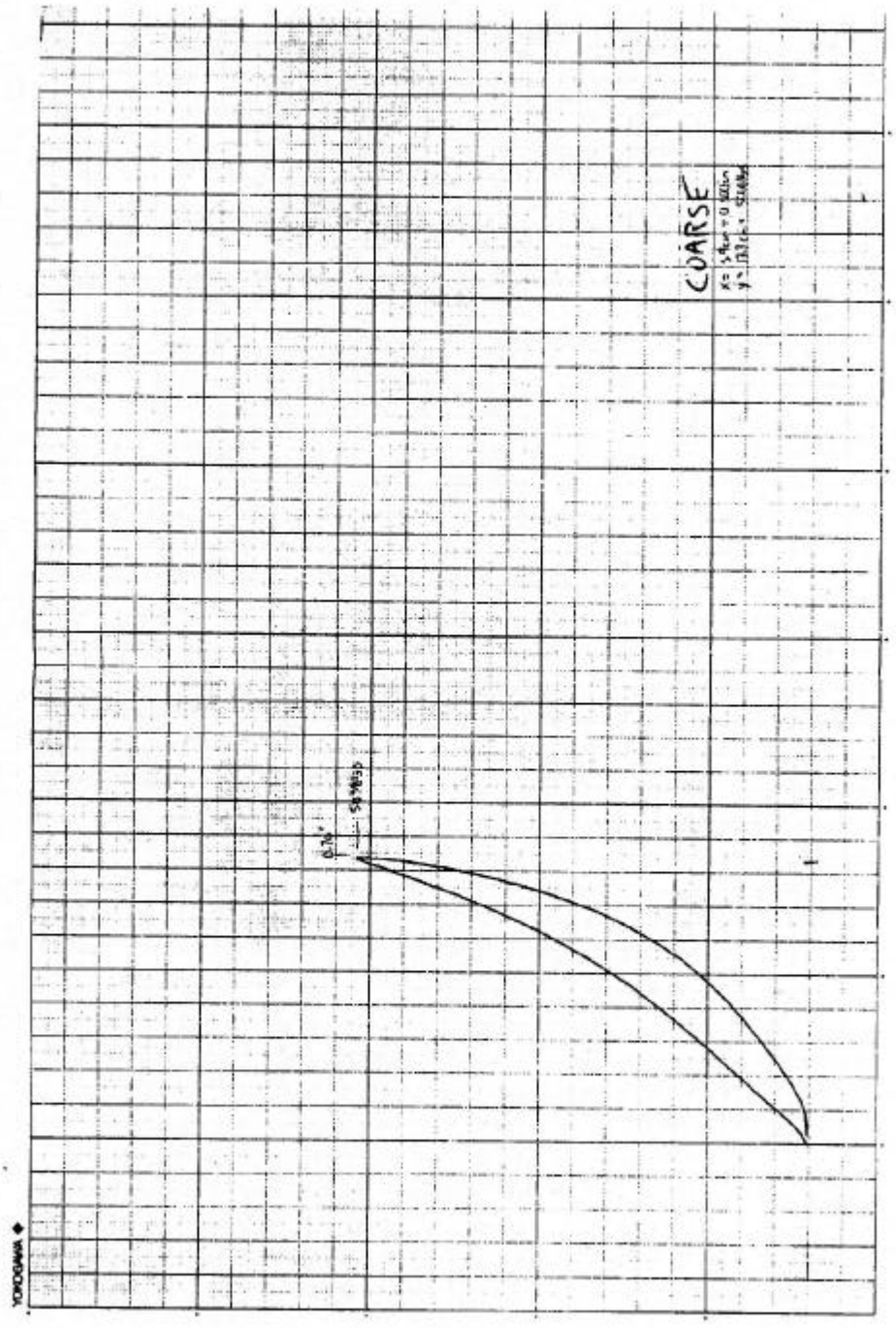
COARSE

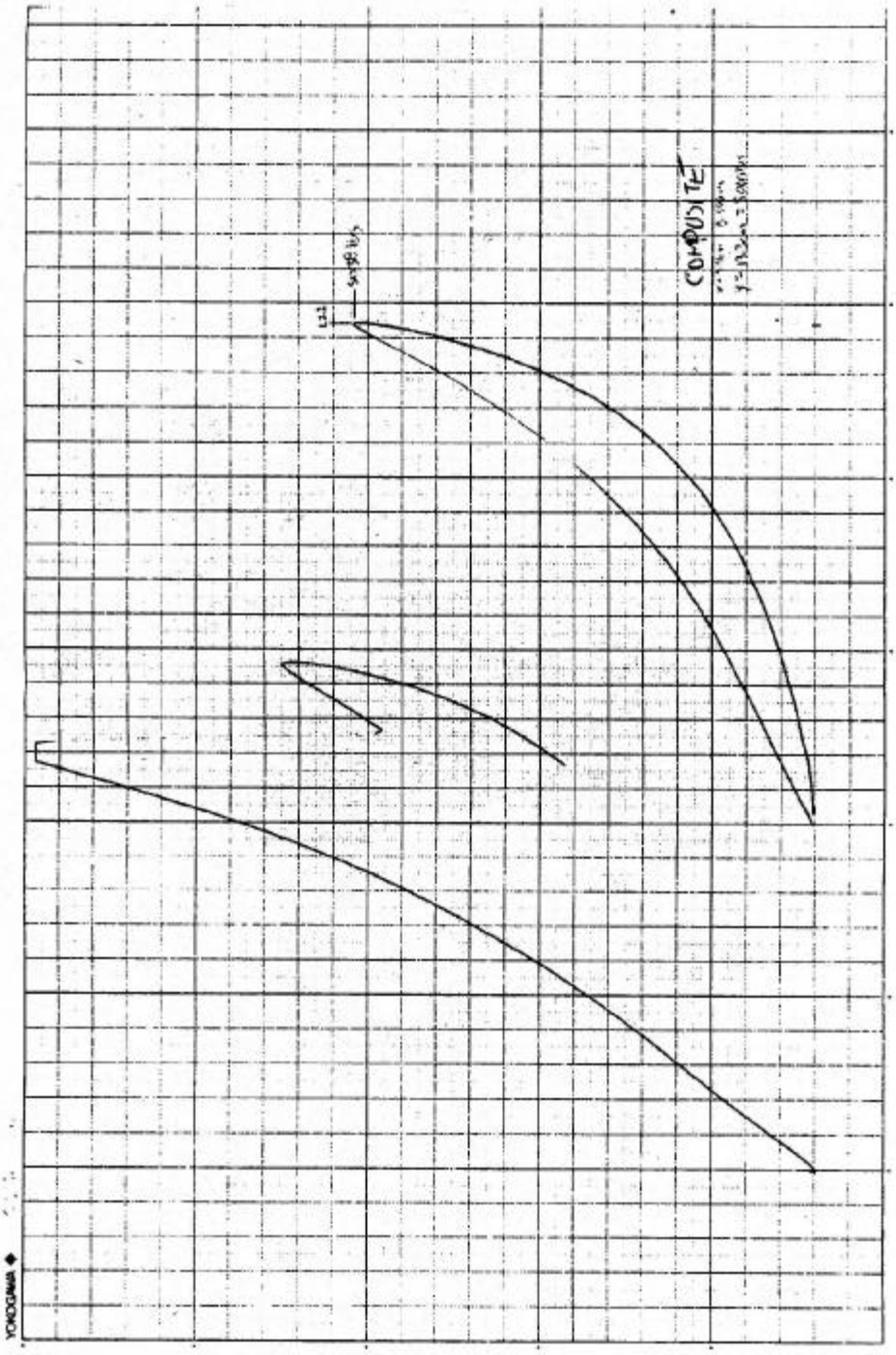

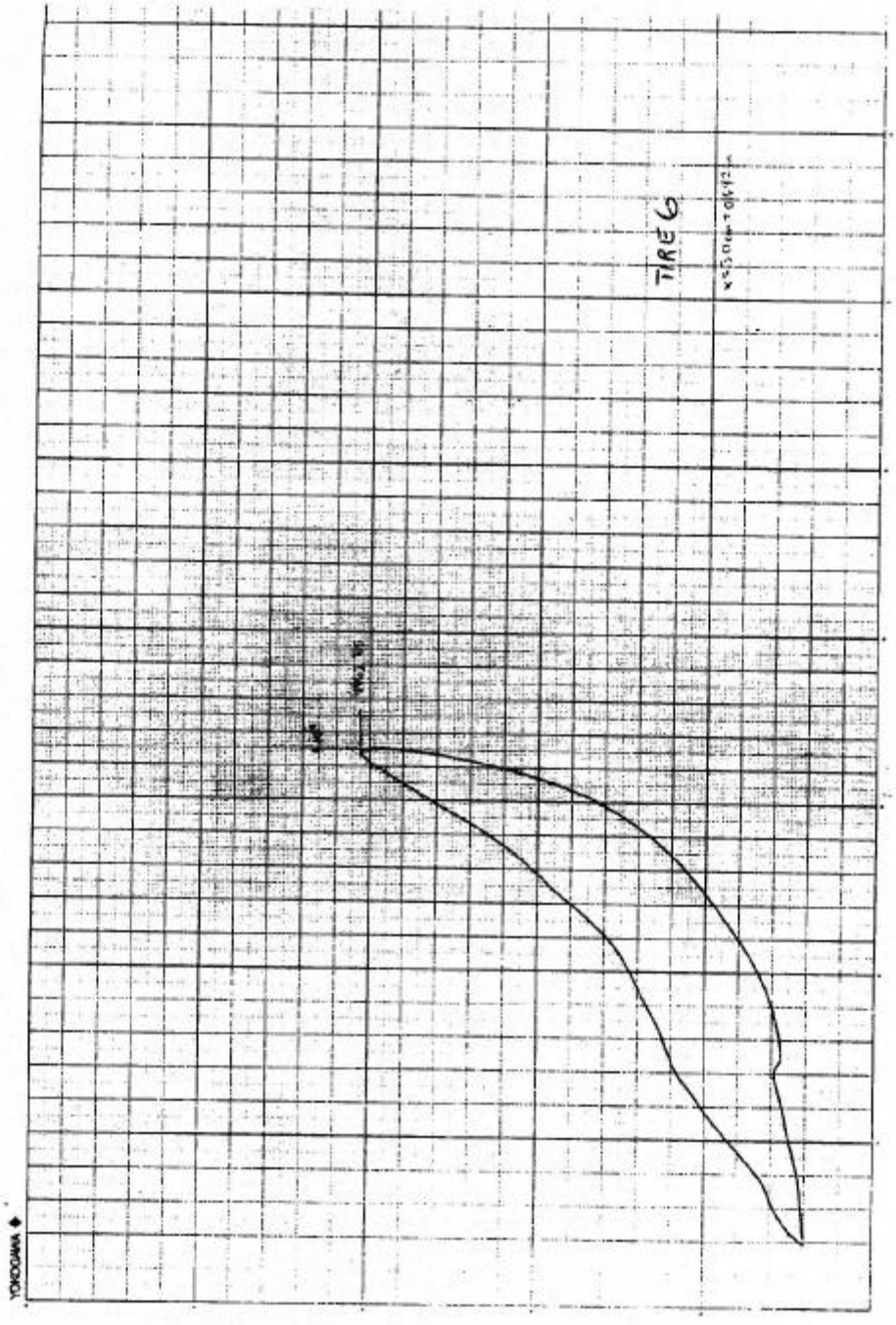
TIRE 6
YOKOGAWA

APPENDIX C

SAMPLE SAS OUTPUT

The SAS System 1
22:39 Friday, April 3, 1998

Correlation Analysis

3 'VAR' Variables: DEF LOAD DEF3

Simple Statistics

Variable	N	Mean	Std Dev	Sum	Minimum	Maximum
DEF	46	35.45783	78.19463	1631	4.74000	360.00000
LOAD	40	24603	30051	984130	9710	151400
DEF3	46	2073278	8077682	95370806	06.49642	46656000

Pearson Correlation Coefficients / Prob > |R| under Ho: Rho=0
/ Number of Observations

	DEF	LOAD	DEF3
DEF	1.00000	0.91768	0.91845
	0.0	0.0001	0.0001
	46	40	46
LOAD	0.91768	1.00000	0.98006
	0.0001	0.0	0.0001
	40	40	40
DEF3	0.91845	0.98006	1.00000
	0.0001	0.0001	0.0
	46	40	46

The SAS System 2
22:39 Friday, April 3, 1998

Model: MODEL1
Dependent Variable: LOAD

Analysis of Variance

Source	DF	Sum of Squares	Mean Square	F Value	Prob>F
Model	1	33828669234	33828669234	924.573	0.0001
Error	38	1390359443.8	36588406.417		
C Total	39	35219028678			

Root MSE	6048.83513	R-square	0.9605
Dep Mean	24603.25000	Adj R-sq	0.9595
C.V.	24.58551		

Parameter Estimates

Variable	DF	Parameter Estimate	Standard Error	T for H0: Parameter=0	Prob > |T|
INTERCEP	1	13333	1025.7099956	12.999	0.0001
DEF3	1	3.926567	0.12913449	30.407	0.0001

The SAS System 3
22:39 Friday, April 3, 1998

Obs	Dep Var LOAD	Predict Value	Std Err Predict	Lower95% Mean	Upper95% Mean	Lower95% Predict	Upper95% Predict
1	14550.0	14127.6	1016.564	12069.7	16185.5	1710.6	26544.5
2	9710.0	14087.7	1017.009	12028.9	16146.5	1670.6	26504.8
3	14960.0	13848.2	1019.715	11783.9	15912.5	1430.2	26266.2
4	14300.0	13863.5	1019.540	11799.6	15927.5	1445.6	26281.5
5	13960.0	13872.9	1019.433	11809.1	15936.6	1455.0	26290.8
6	13770.0	13784.1	1020.447	11718.4	15849.9	1365.9	26202.4
7	13790.0	13866.6	1019.505	11802.7	15930.5	1448.7	26284.6
8	14130.0	14185.8	1015.917	12129.2	16242.4	1769.1	26602.5
9	13680.0	14338.8	1014.231	12285.6	16392.0	1922.6	26755.0
10	13880.0	13759.6	1020.729	11693.2	15825.9	1341.2	26177.9
11	19230.0	14111.5	1016.744	12053.2	16169.8	1694.5	26528.5
12	16240.0	14148.1	1016.336	12090.6	16205.5	1731.2	26564.9
13	16570.0	13882.3	1019.326	11818.8	15945.8	1464.5	26300.2
14	17100.0	14315.2	1014.489	12261.5	16369.0	1899.0	26731.5
15	16200.0	13751.6	1020.821	11685.0	15818.1	1333.2	26170.0
16	15350.0	13833.1	1019.887	11768.5	15897.8	1415.0	26251.2
17	14690.0	13965.5	1018.382	11903.9	16027.1	1548.0	26383.1
18	11730.0	14041.6	1017.526	11981.7	16101.5	1624.3	26458.9
19	15630.0	13842.1	1019.784	11777.7	15906.6	1424.1	26260.1
20	14710.0	13842.1	1019.784	11777.7	15906.6	1424.1	26260.1
21	12090.0	14207.2	1015.679	12151.1	16263.4	1790.6	26623.9
22	11730.0	14131.7	1016.518	12073.8	16189.5	1714.7	26548.6
23	14350.0	13821.3	1020.022	11756.4	15886.2	1403.2	26239.4
24	13480.0	14008.3	1017.900	11947.7	16068.9	1590.9	26425.7
25	13160.0	13921.3	1018.883	11858.7	15983.9	1503.6	26339.0
26	19030.0	14488.1	1012.607	12438.2	16538.0	2072.5	26903.8
27	15690.0	17865.9	981.736	15878.5	19853.3	5460.5	30271.4
28	15270.0	17878.9	981.639	15891.7	19866.1	5473.5	30284.3
29	15480.0	17878.9	981.639	15891.7	19866.1	5473.5	30284.3
30	15720.0	17957.3	981.062	15971.2	19943.3	5552.0	30362.5
31	14770.0	18559.7	976.839	16582.2	20537.2	6155.8	30963.5
32	14950.0	18446.5	977.603	16467.4	20425.5	6042.3	30850.6
33	14290.0	17983.6	980.869	15997.9	19969.3	5578.4	30388.8
34	14780.0	18036.5	980.484	16051.6	20021.4	5631.5	30441.6
35	31160.0	30876.0	978.400	28895.3	32856.7	18471.6	43280.4
36	30450.0	30495.3	975.838	28519.9	32470.8	18091.8	42898.9
37	50550.0	38886.6	1065.537	6729.6	41043.7	26452.9	51320.4
38	116500	123866	3401.710	116980	130752	109817	137915
39	105100	124850	3432.777	117901	131799	110770	138930
40	151400	126503	3485.016	119448	133558	112371	140635
41	.	861472	27539.03	805722	917222	804393	918551
42	.	6798441	222775.8	6347455	7249427	6347288	7249593

The SAS System 1
22:37 Friday, April 3, 1998

Correlation Analysis

3 'VAR' Variables: TIRE_NO LOAD T3

Simple Statistics

Variable	N	Mean	Std Dev	Sum	Minimum	Maximum
TIRE_NO	50	6.06000	11.04612	303.00000	1.00000	50.00000
LOAD	40	24603	30051	984130	9710	151400
T3	50	5760	20677	287997	1.00000	125000

Model: MODEL1
Dependent Variable: LOAD

Analysis of Variance

Source	DF	Sum of Squares	Mean Square	F Value	Prob>F
Model	1	33482059533	33482059533	732.493	0.0001
Error	38	1736969144.7	45709714.334		
C Total	39	35219028678			

Root MSE	6760.89597	R-square	0.9507
Dep Mean	24603.25000	Adj R-sq	0.9494
C.V.	27.47969		

Parameter Estimates

Variable	DF	Parameter Estimate	Standard Error	T for H0: Parameter=0	Prob > |T|
INTERCEP	1	12437	1159.6615220	10.725	0.0001
T3	1	891.296566	32.93217426	27.065	0.0001

The SAS System 3
22:37 Friday, April 3, 1998

Obs	Dep Var LOAD	Predict Value	Std Err Predict	Lower95% Mean	Upper95% Mean	Lower95% Predict	Upper95% Predict
1	14550.0	13328.3	1147.298	11005.8	15650.9	-554.0	27210.7
2	9710.0	13328.3	1147.298	11005.8	15650.9	-554.0	27210.7
3	14960.0	13328.3	1147.298	11005.8	15650.9	-554.0	27210.7
4	14300.0	13328.3	1147.298	11005.8	15650.9	-554.0	27210.7
5	13960.0	13328.3	1147.298	11005.8	15650.9	-554.0	27210.7
6	13770.0	13328.3	1147.298	11005.8	15650.9	-554.0	27210.7
7	13790.0	13328.3	1147.298	11005.8	15650.9	-554.0	27210.7
8	14130.0	13328.3	1147.298	11005.8	15650.9	-554.0	27210.7
9	13680.0	13328.3	1147.298	11005.8	15650.9	-554.0	27210.7
10	13880.0	13328.3	1147.298	11005.8	15650.9	-554.0	27210.7
11	19230.0	13328.3	1147.298	11005.8	15650.9	-554.0	27210.7
12	16240.0	13328.3	1147.298	11005.8	15650.9	-554.0	27210.7
13	16570.0	13328.3	1147.298	11005.8	15650.9	-554.0	27210.7
14	17100.0	13328.3	1147.298	11005.8	15650.9	-554.0	27210.7
15	16200.0	13328.3	1147.298	11005.8	15650.9	-554.0	27210.7
16	15350.0	13328.3	1147.298	11005.8	15650.9	-554.0	27210.7
17	14690.0	13328.3	1147.298	11005.8	15650.9	-554.0	27210.7
18	11730.0	13328.3	1147.298	11005.8	15650.9	-554.0	27210.7
19	15630.0	13328.3	1147.298	11005.8	15650.9	-554.0	27210.7
20	14710.0	13328.3	1147.298	11005.8	15650.9	-554.0	27210.7
21	12090.0	13328.3	1147.298	11005.8	15650.9	-554.0	27210.7
22	11730.0	13328.3	1147.298	11005.8	15650.9	-554.0	27210.7
23	14350.0	13328.3	1147.298	11005.8	15650.9	-554.0	27210.7
24	13480.0	13328.3	1147.298	11005.8	15650.9	-554.0	27210.7
25	13160.0	13328.3	1147.298	11005.8	15650.9	-554.0	27210.7
26	19030.0	13328.3	1147.298	11005.8	15650.9	-554.0	27210.7
27	15690.0	19567.4	1085.064	17370.8	21764.0	5705.6	33429.3
28	15270.0	19567.4	1085.064	17370.8	21764.0	5705.6	33429.3
29	15480.0	19567.4	1085.064	17370.8	21764.0	5705.6	33429.3
30	15720.0	19567.4	1085.064	17370.8	21764.0	5705.6	33429.3
31	14770.0	19567.4	1085.064	17370.8	21764.0	5705.6	33429.3
32	14950.0	19567.4	1085.064	17370.8	21764.0	5705.6	33429.3
33	14290.0	19567.4	1085.064	17370.8	21764.0	5705.6	33429.3
34	14780.0	19567.4	1085.064	17370.8	21764.0	5705.6	33429.3
35	31160.0	36502.1	1155.868	34162.1	38842.0	22616.8	50387.4
36	30450.0	36502.1	1155.868	34162.1	38842.0	22616.8	50387.4
37	50550.0	36502.1	1155.868	34162.1	38842.0	22616.8	50387.4
38	.	69480.0	1972.854	65486.2	73473.9	55222.5	83737.6
39	116500	123849	3819.635	116117	131582	108129	139569
40	105100	123849	3819.635	116117	131582	108129	139569
41	151400	123849	3819.635	116117	131582	108129	139569
42	.	468781	16446.53	435487	502075	432783	504779

43	.	903734	32500.24	837940	969527	836532	970935
44	.	3020563	110701.7	2796459	3244667	2796041	3245084
45	.	7142810	263010.0	6610374	7675246	6610198	7675421
46	.	13938946	514116.8	12898171	14979721	12898081	14979811
47	.	24077444	888719.8	22278325	25876564	22278273	25876616
48	.	38226777	1411518	35369309	41084246	35369276	41084279
49	.	57055417	2107210	52789594	61321241	52789572	61321263
50	.	1.1142E8	4116072	1.0309E8	1.1976E8	1.0309E8	1.1976E8

The SAS System 1
01:25 Monday, March 16, 1998

General Linear Models Procedure
Class Level Information

Class	Levels	Values
NO	10	1 2 3 4 5 6 7 8 9 10
FREQ	2	1 2
LOAD	3	1000 2500 5000

Number of observations in data set = 60

General Linear Models Procedure

Dependent Variable: DEF

Source	DF	Sum of Squares	Mean Square	F Value	Pr > F
Model	14	84.23339000	6.01667071	61.38	0.0001
Error	45	4.41089500	0.09801989		
Corrected Total	59	88.64428500			

R-Square	C.V.	Root MSE	DEF Mean
0.950241	11.28424	0.3130813	2.7745000

Source	DF	Type I SS	Mean Square	F Value	Pr > F
NO	9	20.55393500	2.28377056	23.30	0.0001
FREQ	1	0.01261500	0.01261500	0.13	0.7215
LOAD	2	63.60987000	31.80493500	324.47	0.0001
FREQ*LOAD	2	0.05697000	0.02848500	0.29	0.7492

Source	DF	Type III SS	Mean Square	F Value	Pr > F
NO	9	20.55393500	2.28377056	23.30	0.0001
FREQ	1	0.01261500	0.01261500	0.13	0.7215
LOAD	2	63.60987000	31.80493500	324.47	0.0001
FREQ*LOAD	2	0.05697000	0.02848500	0.29	0.7492

The SAS System 1
10:51 Wednesday, March 18, 1998

---------- TYPE=1 ----------

Model: MODEL1
Dependent Variable: LOAD

Analysis of Variance

Source	DF	Sum of Squares	Mean Square	F Value	Prob>F
Model	1	1862030769.2	1862030769.2	51.132	0.0056
Error	3	109249230.77	36416410.256		
C Total	4	1971280000			

Root MSE	6034.60109	R-square	0.9446
Dep Mean	172200.00000	Adj R-sq	0.9261
C.V.	3.50441		

Parameter Estimates

Variable	DF	Parameter Estimate	Standard Error	T for H0: Parameter=0	Prob > |T|
INTERCEP	1	146654	4477.3355392	32.755	0.0001
RATE	1	946.153846	132.31738188	7.151	0.0056

The SAS System 2
10:51 Wednesday, March 18, 1998

---------- TYPE=2 ----------

Model: MODEL1
Dependent Variable: LOAD

Analysis of Variance

Source	DF	Sum of Squares	Mean Square	F Value	Prob>F
Model	1	2850120692.3	2850120692.3	114.574	0.0017
Error	3	74627307.692	24875769.231		
C Total	4	2924748000			

Root MSE	4987.56145	R-square	0.9745
Dep Mean	175420.00000	Adj R-sq	0.9660
C.V.	2.84321		

Parameter Estimates

Variable	DF	Parameter Estimate	Standard Error	T for H0: Parameter=0	Prob > |T|
INTERCEP	1	143814	3700.4908568	38.864	0.0001
RATE	1	1170.576923	109.35951919	10.704	0.0017

The SAS System 3
10:51 Wednesday, March 18, 1998

---------- TYPE=3 ----------

Model: MODEL1
Dependent Variable: LOAD

Analysis of Variance

Source	DF	Sum of Squares	Mean Square	F Value	Prob>F
Model	1	9555551557.7	9555551557.7	514.879	0.0002
Error	3	55676442.308	18558814.103		
C Total	4	9611228000			

Root MSE	4307.99421	R-square	0.9942
Dep Mean	193480.00000	Adj R-sq	0.9923
C.V.	2.22658		

Parameter Estimates

Variable	DF	Parameter Estimate	Standard Error	T for H0: Parameter=0	Prob > |T|
INTERCEP	1	135609	3196.2900781	42.427	0.0001
RATE	1	2143.365385	94.45902170	22.691	0.0002